UNIVERSITÀ DEGLI STUDI DI TRIESTE, ISTITUTO NAZIONALE DI OCEANOGRAFIA E GEOFISICA SPERIMENTALE (OGS)

XVIII CICLO DEL DOTTORATO DI RICERCA IN BIOLOGIA AMBIENTALE

MODELLING MEDITERRANEAN CORALS AND CORALLIGENOUS HABITATS

Settore scientifico-disciplinare: **BIO/07**

DOTTORANDO
GIOVANNI GALLI

COORDINATORE
PROF. SERENA FONDA UMANI

SUPERVISORE DI TESI
PROF. COSIMO SOLIDORO
PROF. ANNALISA FALACE

ANNO ACCADEMICO 2014 / 2015

Table of contents

"Tornando quest'oggi a dir qualche cosa de' polipi di questa cellularia, osservo che ad onta del rinnovamento dell'acqua in molti piedi non vengono più fora"

"Coming back today to say something about the polyps of this cellularia, I observe that, despite renewing the water, from many bases they don't come out anymore"

Lazzaro Spallanzani, 1784

Overview

Abstract

This thesis is constituted of five different studies revolving around the themes of Mediterranean corals and coralligenous reefs, organism and communities ecology and physiology, and all of this is focused from the point of view of numerical simulations and quantitative approaches. The scales in space and time of the studies presented vary widely, ranging from basin-wide multidecadal projections to physiological level processes. Also the applications that are presented pertain to different frameworks: mechanistic models, empirical models, and statistical analyses.

The first chapter represents a brief introduction and a literature review on how different modelling frameworks can be used to describe coral growth; the second chapter is a case study application of many of the concepts developed in chapter one to the Mediterranean red coral (*Corallium rubrum*). The third chapter looks into the physiological details of the process of calcification in symbiotic corals in order to elucidate the action mechanisms of different stressors. The fourth chapter is a basin-wide assessment of heat-waves related risk for red coral and other related species. Finally chapter five treats a problem of habitat classification, relation to environmental variability and mapping, applied to a submerged archipelago of rocky outcrops in the Northern Adriatic Sea.

Quantitative approaches to the fields of biology and ecology are not new, though the existing studies about marine calcifiers in general, and Mediterranean species in particular, are surprisingly scarce. This thesis wants to exemplify how such applications are powerful tools to understand the processes that shape unique marine habitats such as the Mediterranean coralligenous reefs.

1. What this thesis is about

Today's oceans are faced with a novel variety of pressures often related to the increase of human population. Land use severely alters thousands of kilometers of coastal environments worldwide, the resulting polluting activities, especially waste water discharge, have in the sea their ultimate sink. The unsustainable harvesting of fish stocks not just hinders our ability to effectively exploit resources, but also triggers changes in marine ecosystems structure. At the same time the Earth's climate is changing due to anthropogenic greenhouse gasses emissions; this has consequences for the marine environment also: the world's oceans are expected to become warmer on average; episodic extreme events such as heat waves and intense weather phenomena are expected to become more frequent and severe; the dissolution of atmospheric carbon dioxide decreases seawater pH, a process named ocean acidification. All of these issues bear consequences for marine life forms which, being adapted to different conditions, may not be able to efficiently cope with change. This is especially true if such changes, as it is the case, are brought about over very short time periods, compared to geological time scales, which rules out the possibility of evolutionary adaptation for most organisms.

Science is engaged in developing tools that allow to evaluate and quantify future impacts, either in the hope of reverting current trends, or to be prepared for the inevitable. This is clearly no easy task as it implies disentangling the many relations that underlie world climate, biological organisms and ecosystems and human societies, all of which are, undoubtedly, complex and not fully understood items.

This thesis is intended to address some of these issues, in particular some aspects regarding a certain type of organisms (marine calcifiers) from a specific ecosystem (Mediterranean coralligenous habitats) and concerning certain issues related to the interactions among organisms and their environment (ecology). To understand this it is sometimes needed to go back to the basics, that is the ways that living things or any of their parts function (physiology). All of this will be focused from the point of view of numerical analyses, simulations and theory and integrated in computer-based applications (models). This thesis, the works that compose it, is also a collection of points of view on the same topic from different perspectives

and distances (scales), from basin-scale projections to physiological level processes.

Biological organisms and ecosystems are complex entities whose dynamics and states are continuously set through a full range of processes acting at widely different scales in both time and space. The Marine realm is in no way an exception to such statement, but also owns a peculiar feature that bears two-sided consequences: as the hydrosphere is not mankind's biome, aquatic ecosystems are hardly accessible and hardly subdued, so that, whereas on land nature has been bent in many ways for farming and livestock purposes, marine and freshwater ecosystems are usually exploited as such, not so much unlike hunter gatherer societies did with pre-historic lands. Though if in the Paleolithic sustainable resources management was not people's concern, it is now; and whereas technology provides several means for increasing land productivity and buffering the effects of climatic variability, this is barely possible with the aquatic environment. Whoever means to exploit water-based resources has to deal with their intrinsic variability.

Perhaps for these reasons, quantitative approaches to traditionally softer sciences like biology and ecology (which are a central topic of this thesis) have been, and still are, largely focused on the aquatic environment since the seminal works of Ludwig von Bertalanffy (1938) and Vito Volterra (1926). The latter of the two conceived his eponymous equations, that describe ecosystem dynamics in terms of predator-prey interactions, by looking at the composition of fish landings before and after World War I (during which industrial fisheries did not operate) in the Northern Adriatic Sea. Curiously enough Volterra devised the piece of science that now serves as the archetype for mostly any trophic network model, by looking at such a marginal sub-basin, the Northern Adriatic, in an enclosed little sea, the Mediterranean.

All of this thesis case studies are about the Mediterranean Sea (Fig. 1) and the Northern Adriatic is featured as well (in chapter 5) as it hosts the *trezze*, a unique kind of reef-like habitat. The Mediterannean Sea is indeed a special place within the world ocean; Bethoux et al. (1999) described it as a miniature ocean as it features many of the characteristics of larger water bodies (dense waters formation, thermohaline circulation in relation to climate) on a smaller scale. It is an enclosed basin, located in a temperate climate and, due to its segregation, it hosts endemic species and unique

habitats; among these the coralligenous reefs, which are the subject of this thesis, deserve a special mention.

Fig. 1 The Mediterranean Sea.

2. Mediterranean Coralligenous reefs

Coralligenous habitats (see Ballesteros 2006 for a review) are reef-like calcareous bioconstructions unique to the Mediterranean, but, unlike their famous tropical counterparts, are not found in shallow waters; instead they develop in somewhat deep waters, in the mesophotic zone, usually below the summer thermocline, around 20-30 meters, and up to around 100 meters deep. Mostly for this very reason, and despite their appeal, they remain little known to the general public. The other major feature that differentiate Mediterranean coralligenous from tropical reefs is that the former do not involve corals as main engineering species but instead coralline algae (*Lithophyllum sp.*, *Mesophyllum sp.*, *Neogoniolithon sp.*, Ballesteros 2006) whose calcareous thalli are laid down and grow on each other resulting in massive outcrops (Fig. 2).

Besides calcareous algae, the coralligenous habitats host a great deal of biodiversity both in sessile species like scleractinians and gorgonian corals, bryozoans, sponges, etc. and motile species, such as crustaceans, mollusks and fishes, that take advantage of the complex tridimensional environment provided by engineering species, for sheltering purposes and for which the coralligenous are also important nursery grounds. With a provisional species count of 1666 (Ballesteros 2006), coralligenous habitats are considered the second biodiversity hotspot of the Mediterranean after Posidonia meadows.

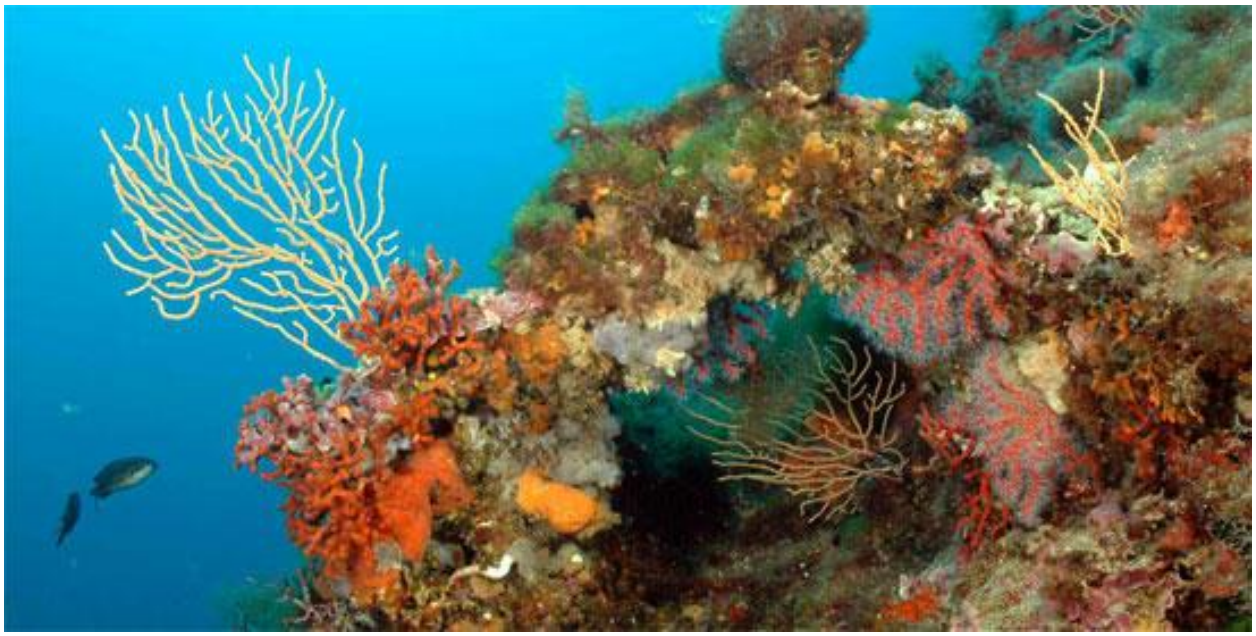

Fig. 2 Coralligenous reef from Marseille, France.

The reason why such similar kinds of bioconstructions, coralligenous and tropical coral reefs, develop under such different environmental conditions, the mesophotic zone, in relatively cold waters vs. surface warm and oligotrophic waters, in the Mediterranean vs. in the tropics was investigated by Zabala and Ballesteros (1989); these authors ascribe it to the temperate climatology and pronounced seasonality of the surface waters in the Mediterranean that results in shallow hard substrates being mostly colonized by fast growing generalist species like turf and erect algae and sponges that are able to out-compete slow growing calcifiers, like those that characterize the coralligenous, in an highly variable environment. On the contrary the temperature conditions below the summer thermocline are relatively stable all year round and the little light is not sufficient for fast growing algae to be competitive. In such conditions slow growing species

with frugal food requirements and resistant to grazing (i.e. calcareous species) can thrive and develop complex ecosystems. The drawback to it is that coralligenous species are specialists; they are adapted to narrow temperature ranges (between 10 and 23°C Ballesteros 2006), do not tolerate high sedimentation rates, and, as calcifiers, are potentially sensitive to ocean acidification. On top of that, the sessile nature of coralligenous building species implies that, whenever their environment changes, they have limited or no ability to relocate to more suitable places. The coralligenous are indeed vulnerable environments.

These unique biomes are also little understood from the ecological point of view. Despite in recent years a substantial deal of research effort has been spent in the study of coralligenous reefs, the scientific community has, at present, only a partial understanding of the ecological processes that happen within them and that ultimately result in the observed variability and spatial distribution of the coralligenous along environmental gradients within the Mediterranean. Coralligenous reefs across the Mediterranean are in fact not homogeneous biocenoses, but rather they differ from region to region, as a patchwork of local variants on the theme of mesophotic calcareous bioconstructions. This variability is not yet entirely classified.

The investigation of coralligenous habitats also inevitably implies dealing with certain ecological and physiological aspects that are not yet completely understood (also like any other research activity) and that are characteristic to coralligenous species, such as symbioses, modular and colonial growth forms and biocalcification. All of these processes are of vital importance for many coralligenous species and, often, also of interest as phenomena directly affected by climate change related pressures; as it will be shown in this thesis, a modelling perspective is amenable to capture their essence and numerical applications are convenient tools to understand such processes.

3. Numerical modelling of biological systems

All of this thesis is also about mathematical models of biological systems. The introduction of numerical simulation approaches in the fields of biology

and ecology is not recent, as exemplified before, though it remains somewhat of a niche specialization among biologists and ecologists. The main reasons for it (by educated guess) are that the unparalleled complexity of life makes it challenging to formulate general laws with high predictive power (as it happens for instance in the field of physics), and, on the other hand, that living organisms and ecosystems states are very often difficult to measure, making it difficult to see the big picture that is needed to formulate general laws. In this context, models are regarded as useful tools for testing ecological hypotheses and understanding observed patterns, and are the prime means for predicting how living beings and ecosystems will respond to change.

In the present work a collection of different modelling approaches is presented. Such approaches can be coarsely divided in two main groups: data driven models (in chapters 4, 5) and process based models (in chapters 1, 2, 3).

Data driven applications make use of techniques, usually statistical, that allow the recognition of patterns in, typically large, ecological data sets without requiring detailed knowledge of the processes involved. Such applications usually rely on numerical regressions, often quite sophisticated, and are clearly data-demanding, on the other hand they allow to account for most of the possibly available information (multivariate statistics) without the strict need for a conceptual understanding of the object of the study. The studies presented in chapters 4 and 5 pertain to this class of models.

Instead process based models are that class of applications where the system that is object of study is in the first place reduced to a conceptual scheme, that is a simplified version of reality, where all the variables and processes that are considered relevant are defined and linked together. These models typically rely on a physical background, i.e. the application of basic physical laws to biological organization. Process based models are usually less data-demanding than statistical approaches, yet the amount of information needed to adequately constrain a model is often not negligible and poor data can result in useless outcomes; on the other hand they can provide a mechanistic understanding of the object of the study, allow for generality to emerge and are more suitable tools for predictive purposes. The works presented in chapters 1, 2 and 3 pertain to such class of models.

Biological processes that happen at organism level, can be understood in terms of organism energetics. This is done by recognizing that a biological entity can be conceptualized as an open system that maintains an high level of internal organization at the expenses of a continuous flux of energy in and out of it (see chapter 1). An organism has hence a budget of usable energy to allocate to the components of its biological machinery, like growth, standard metabolism, activity, skeleton deposition, etc. (Fig 3) Some of this energy will be retained within the organism as newly formed biomass, the rest will be dissipated to the outside. How the available energy is allocated to the various processes depends on how the metabolic components are organized and connected with each other.

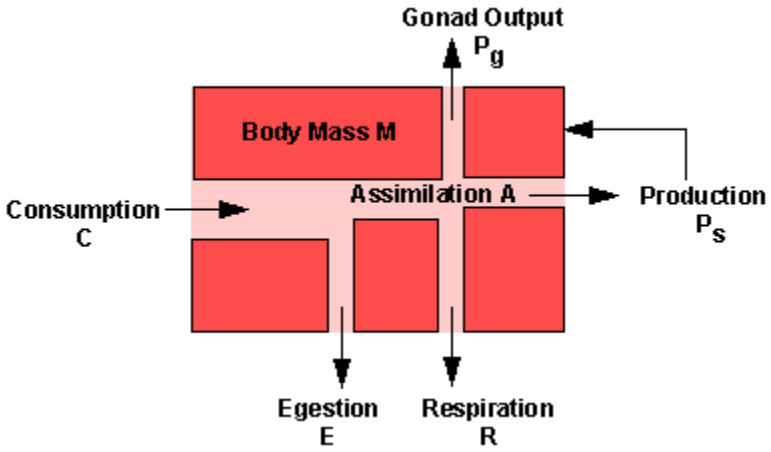

Fig. 3 One possible scheme for an organism energy budget from Brey 2001.

The cornerstone of this paradigm is very easy: to apply thermodynamics principles (mass/energy local conservation) to biological systems. The tricky part is to identify organism components and processes (e.g. polyps gemmation, symbioses, reproduction, calcification...) and to find out where they may fit from the point of view of metabolic organization.

During the course of this work it appeared necessary to devise novel approaches within well established modelling frameworks meant at including relevant processes that happen at organism level, such as colonial growth (chapter 1 and 2), biocalcification (chapter 1, 2, 3) and coral symbioses (chapter 3), that were overlooked in traditional models. Such applications are here used as tools to understand the functioning of organisms and ecosystems in relation to their environment.

4. Ecological and physiological aspects of coralligenous species from a modelling perspective

Biocalcification

Biologically mediated deposition of carbonates (biocalcification), is the key process that allows the formation of skeletons, shells, and reef habitats. Ocean acidification is expected to have impacts on marine calcifying organisms because it will negatively affect the saturation state of carbonates in seawater, which is in turn related to precipitation and dissolution rates. But, whereas the chemistry of carbonate species in seawater, including calcium carbonate deposition and dissolution phenomena, is rather well known, living organisms are no rocks. A key feature of biological organization is to sustain conditions within the organism that are far from the thermodynamic equilibrium of the surrounding environment; although seemingly trivial, only recently this concept has been recognized to be important also in the field of biocalcification. Coral skeleton indeed is not in direct contact with seawater and recent studies (Al-Horani et al. 2003; Venn et al. 2011) demonstrated that corals actively regulate the chemical properties of the internal calcifying medium from which the skeleton is secreted, clearly an energy-requiring activity; this ability is however limited and negative effects of acidified seawater on calcification are beyond doubt for many species from widely different taxa (not just corals) and habitats. Despite the huge research effort seen in recent years, the effects of seawater chemistry on marine calcifiers remains an elusive topic, as stated by Allemand et al. (2011) in an extensive review on coral calcification; that review opens with two quotes, written almost one century apart by scientists engaged with coral calcification:

A question which has common interest both for zoologist and paleontologist is the relation of the soft parts of the polyp to the hard calcareous or horny skeleton produced in most corals. (Ogilvie 1896)

The poor understanding of calcification mechanisms in corals results from a lack of information on tissue / skeleton interactions and temporal / spatial patterns in skeleton morphogenesis. (Brown et al. 1983)

Both these authors recognize that the key to understand biocalcification lies in the interactions between the living parts of the coral and the skeleton, an aspect that is currently often overlooked in many research studies. The contributions that will be presented in chapter 1, 2, 3, attempt to approach the problem from this very perspective, by considering biocalcification as one of the energy requiring processes that are integrated in organism metabolism.

Coral Symbiosis and light enhanced calcification

The symbiotic relationship between coral host and dinoflagellate symbiont, that is vital in many species, is known to be disrupted by prolonged exposure to high temperature (heat wave), resulting in the condition known as coral bleaching (coral expells his symbionts) that, if prolonged, causes the death of the coral. Despite coral bleaching events having become sadly common in tropical reefs worldwide, still little is known about the physiological machinery which holds corals and their symbionts together and about the causes that make it fail.

Symbiotic corals also display a tight link between zooxanthellae photosynthesis and skeleton deposition: higher calcification rates (3x on average, Gattuso et al. 1999) are consistently observed during daytime, when photosynthesis is performed; this phenomenon is called light-enhanced calcification. The mechanisms that have been proposed for light-enhanced calcification are very diverse and range from inorganic chemistry to biological control (Allemand et al. 2011). Nonetheless, whatever the cause of this phenomenon, a clear understanding of the physiology of coral-zooxanthellae symbiosis is required to assess the influence of photosynthesis on vital rates in general, including calcification.

Syntrophic symbioses, like the one that happens in many corals, can be conveniently understood in the light of host and symbiont energetics, combined with evolutionary reasoning: symbiosis must be beneficial, in terms of fitness, for both the host and the symbiont whilst the two actors

must retain selfish behavior (sensu Dawkins 1976). These concepts have been incorporated in the syntrophic symbiosis model developed by Muller & Nisbet (2014). In this model zooxanthellae produce an excess of photosyntate that is translocated to the coral host and it thus represents additional energy available for whatever metabolic purpose must be fulfilled, whilst the coral supplies its symbionts with waste material (nutrients) that serve as substrate for algal photosynthesis. The interesting outcome of this setup is that, although the regulation mechanism is entirely passive, it suffices to obtain a stable relationship; furthermore this relationship shifts from mutualism to parasitism as environmental conditions change, thus providing a candidate trigger for bleaching events.

As most of the coralligenous coral species do not bear symbionts, concern for bleaching incidence is better spent on tropical reefs than on Mediterranean coralligenous; However the topics of symbioses and light enhanced calcification are both treated in this thesis, in chapter 3, where Muller and Nisbet reasoning is incorporated in a calcification model for the Mediterranean scleratinian coral *Cladocora caespitosa*.

Modular growth

Modular architecture is a development mode of living organisms where body accretion is performed by the iteration of identically planned modules, if such modules also are potentially autonomous organisms (like coral polyps), the whole is considered a colony. Modular and colonial architectures are generally typical of sessile species. Corals, bryozoans seaweeds and terrestrial plants, being forced for life in the same place, evolved highly adaptive body plans in order to exploit at best the surrounding environment. Modular growth also have consequences from the organism development point of view: whereas solitary organisms usually display asymptotic growth and a maximal attainable size (for reasons that will be treated in chapters 1 two 2), growth by module iteration would be free from such constraints, resulting in the so-called indeterminate growth. Such an unlimited growth would in theory follow an exponential law, eventually resulting in very fast growth rates for colonies, which is clearly negated by many slow growing, relatively little colonial and modular species. It has been proposed that the single modules within a colony are subject to intra-colonial competition for available resources, such as food

and/or light, that effectively limits their scope for growth as the number of modules increases.

To date very little is known about growth patterns in coral or other coralligenous species also. This is due to many reasons: the slow growth and long life span of many species makes it very unpractical to compile size at age data sets and some measures can be taken just in destructive ways; furthermore the *size* parameter is not as clearly defined as it is in other species; in animals with a well defined body plan, metrics like length or height bear clear relationships with other measures, such as body weight and surface area, that are tightly linked to metabolism and vital rates in general. As an example von Beralanffy growth equation parameters estimates, that are based on such kind of information, are available for most commercial fish species, this isn't true for corals (and not just because von Bertalanffy growth equation doesn't fit coral growth). In modular and colonial species parameters such as height, diameter, total branches length, weight, etc. are not so tightly related because of variable growth forms; and whereas the weight of the polyps, as a proxy for the share of an organism that is metabolically active, would be an informative measure, weight inclusive of the skeleton (that is metabolically inactive) is more often measured.

The topic of modular and colonial growth will be addressed in this thesis (chapters 1, 2) from the perspectives of organism energetics and populations dynamics; in particular it will be analyzed how per capita food availability in a population of polyps, that composes a colony, depends on the density of the population and how this changes as the population of polyps increases in number. Results show that these processes are influenced by colony morphology and may, or may not, result in trophic shading and growth determinacy.

5. Chapters outline

Modelling coral growth

The first chapter is theory oriented and serves as an introduction to chapters 2 and 3. It was originally conceived as a contribution to the marine animal forest handbook (Rossi et al. eds. 2017) where it serves the purpose of introducing the basics of organism growth modelling as well as treating some peculiarities of coral growth (clonality, biocalcification) that are traditionally overlooked in traditional models; also some state of the art applications in the field of coral growth modelling are discussed. In this thesis this chapter is useful as it introduces the class of process-based models that are developed in the following chapters where, on the other hand, basic explanation is kept at minimum.

The chapter treats mainly the basics of the application of general systems theory to biological organisms. In such framework a living being is conceptualized as an open system that exchanges energy and matter with the environment in order to staying alive. Since energy and matter are conservative quantities (they obey a local conservation law according to the first principle of thermodynamics) the amount of each that is retained within the organism equals incoming minus outgoing fluxes. This is an holistic perspective: the complexity of the biological machinery is extremely reduced, to a single state variable (usually biomass or energy content) or a small set of them when different compartments in the organism are identified (e.g. living tissue and calcified skeleton).

In fact it is important to recognize that any model does not mimic reality but rather small subsets of reality's properties, often macroscopic properties, that are believed to be good enough proxies for the salient traits of the modelled system. For instance the weight of an organism and its evolution over time may be the goal and also may be modelled without including any explicit information on organism anatomy and behavior, let alone the single cells and sub-cellular items.

Such models are defined by systems of differential equations, that is the rate of change, over time, of the system properties (state variables) is described instead of the properties themselves. The state of the system (the

values of its state variables) at a given time is the result of the rates of change of the state variables over time and of the initial and boundary conditions. This kind of models do have indeed a very strong and general rationale, thermodynamics, and in fact similarly formulated compartmental models are widespread across different disciplines, from earth systems science to engineering, hence the label general systems theory.

From such simple principles, much interestingly, substantial complexity and order can emerge; compartmental models, based on mass and energy balance, can effectively mimic seemingly purposeful phenomena by relying just on passive control mechanisms; possible examples are the harmonious growth of different body parts or the balance of biodiversity components that is observed in natural ecosystems. Also the same system may exhibit widely different responses (periodic oscillations, chaotic oscillations, stability) just by varying some external conditions.

Because of these aspects, and also because complex emerging behaviors are often unexpected, i.e. they may be difficult to foresee before they are simulated, the quote the *whole is more than the sum of its parts* (originally from Aristotle) rose as some kind of motto for general systems theory. The whole is in fact very often some complex, non-linear, function of its parts.

Modelling red coral (Corallium rubrum) growth in response to temperature and nutrition.

In chapter 2 a bioenergetic growth model especially developed for the Mediterranean coral *Corallium rubrum*, (Red coral, Fig. 4) is presented.

Until recently studies about coral ecology and physiology have mostly neglected the energetic aspect or kept it to minimal complexity (Dubinsky & Jokiel 1994; Anthony et al. 2002). It is however important to understand how corals allocate energy to the components of their biological machinery as the partitioning of a limited resource implies constraints for the organism and can result in evolutionary trade-offs between organism goals (e.g. growth, survival, reproduction). Living beings devise optimal strategies for energy allocation through evolution, though such strategies are environment-dependent and may become maladaptive as external conditions are altered by, e.g. climate change.

Modelling coral growth though presents a number of issues to overcome; those arise from the incomplete understanding of coral physiology and ecology and from the fact that corals are substantially different from the species for which growth models have been traditionally developed (e.g. fish): they are sessile, colonial, a large part of their weight is in calcified skeleton and sometimes they host photosynthetic symbionts.

According to Krogh's principle, due to the substantial number of existing species, *for such a large number of problems there will be some animal of choice, or a few such animals, on which it can be most conveniently studied*. Red coral is in fact an excellent case study for disentangling so many aspects of coral ecology and physiology (not symbioses though); because of its relatively small size whole colonies can be sampled, measured and incubated making it possible to acquire fundamental information on organism functioning that are difficult to obtain for, say, large reef building species; for instance size at age data sets that are necessary to infer the characteristics of colony development are available (Santangelo et al. 2007; Priori et al. 2013); It is possible to measure whole colony vital rates (respiration, food intake, reproductive output, calcification...), thus avoiding the artifacts that may arise from data obtained from fragments. Not lastly, Red coral is an highly valued species (it is used for jewelry), so that red coral research is more likely to get founded than for other, perhaps more ecologically important, species from the same habitats, and this reflects into the amount of available information.

In this model several concepts introduced in the previous chapter are developed: Modular architecture is treated by coupling a single polyp growth module with a module for the population dynamics of the polyps within the colony. A resource acquisition module is developed (see also chapter 1), based on solid theoretical reasoning, in which the competition for food among the colony's polyps results in an inverse relation between food intake per polyp and polyps number (trophic shading). This module, together with polyps population dynamics, effectively sets a limit for colony size in a system that would otherwise grow indefinitely. This is an important result and an improvement over previous studies because trophic shading and size limits arise not because they were assumed a priori in the model formulation, but rather as a consequence of coral development mode.

Fig. 4 Small red coral colony.

One other major focus of the model are the energetic aspects of skeleton formation. Red coral skeleton is composed of Mg-rich calcite and organic matter, the two fractions are incorporated in the skeleton at asynchronous rates during the yearly cycle, generating growth bandings similar to the ones found in trees. Calcareous parts formation process has been traditionally neglected in bioenergetic models, even in those for species that secrete a substantial amount of it (e.g. bivalves). Though calcifying organisms often exhibits dynamics, such as the asynchronous growth of soft tissue and calcified structures, that are indicative of a dedicated metabolic pathway. Until recently, and much surprisingly, no study addressed this issue. This model builds on a recently developed theory of energy allocation to calcareous parts (Kooijman 2009; Pecquerie et al. 2012). The results are promising as observed patterns are faithfully reproduced and they may help setting an unexplored path for future research in the nowadays hot topic of biocalcification.

Biologically mediated and abiotic mechanisms for light enhanced calcification (LEC) and the cost of carbonates deposition in corals.

The model developed in chapter 3 represents a close look into the physiological mechanisms that control calcification in zooxanthellate corals.

Symbiotic corals are known to increase calcification rates under the light. This phenomenon, called light-enhanced calcification (LEC), is believed to be mediated by photosynthetic activity (Gattuso et al. 1999). This phenomenon is highly debated with hypotheses coarsely divided between abiotic and biologically mediated mechanisms. At the same time evidence is building up that calcification in corals relies on active ion transport to deliver the skeleton building blocks into the calcifying medium, hence it is a costly activity. Corals, trough their metabolism, allocate some part of the energy budget they obtain from food and photosynthesis to calcification (Dubinsky & Jokiel 1994), and convert it to calcium carbonate.

Besides Light, temperature and water chemistry (ocean acidification) are also known to affect calcification rates.

To understand how much of the variability in calcification that is observed under different external conditions is due to biologically mediated and abiotic mechanisms, it is necessary to understand how the calcification machinery works.

The description of the processes and compartments that come into play during coral calcification (McConnaughey & Whelan 1997; Allemand et al. 2011; Fig 5), together with the recent discovery that corals exert control over calcifying medium chemical properties (Al-Horani et al. 2003; Venn et al. 2011) opened the doors to a deeper understanding of physiological and environmental control of the process of calcification in corals.

Seawater is separated from the calcification site by at least a couple of layers of bodily tissues: the coelenteron and the calicoblastic epitelium (Tambutté et al. 1996). Carbon dioxide, carbonate ions and calcium ions move across these layers both trough passive and active mechanisms. Active mechanism are responsible for transporting chemical species against concentration gradients and they do this at the expenses of a metabolic energy investment.

The processes of transport and reaction of chemical species, from seawater up to the incorporation into the skeleton are amenable to be simulated with box models not dissimilar from those presented in chapters 1 and 2. Such models though have a different approach than the holistic one found in bioenergetic modelling, their philosophy being instead reductionist: they look into the fine scale details of the biological machinery, like anatomical organization, CO_2 permeation of cell layers and trans membrane transport proteins; Clearly, resolving such fine scale details requires a substantial amount of data.

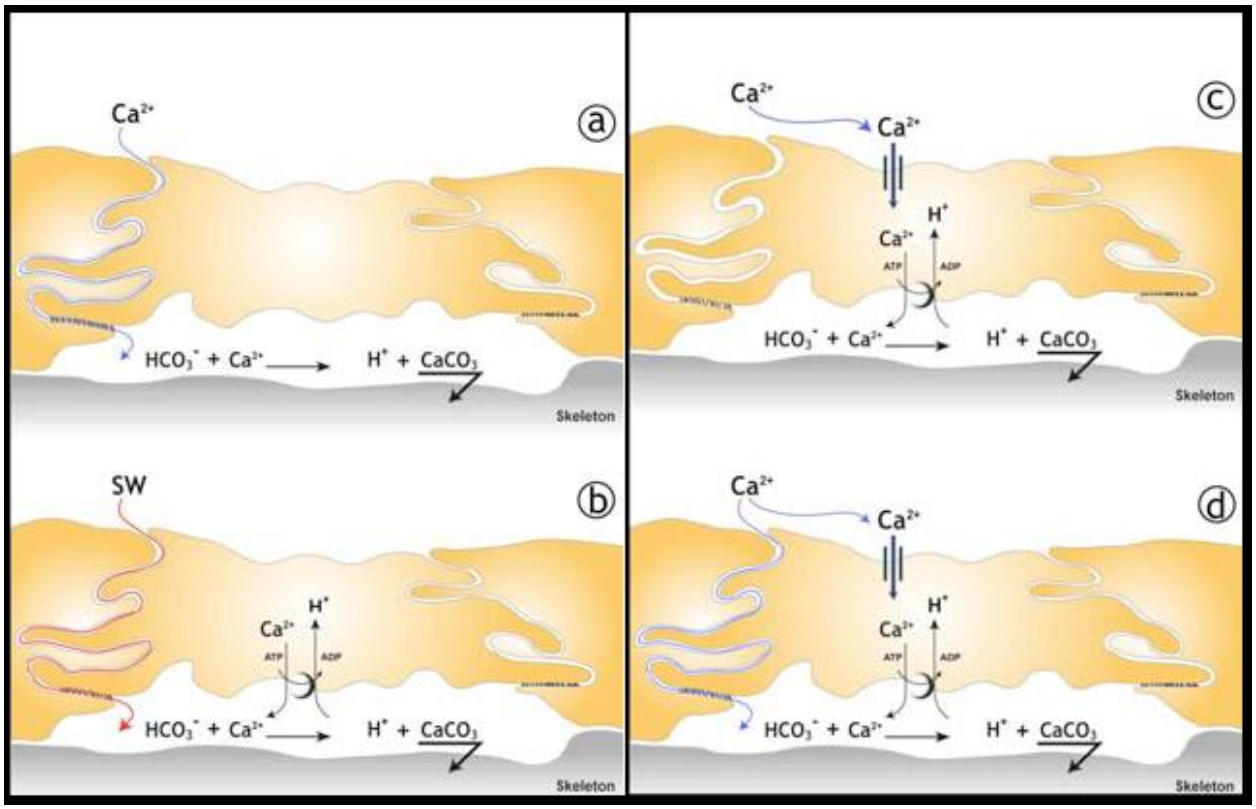

Fig. 5 Four hypothesized schematizations of the calcification machinery from Allemand et al. 2011. a) ions provided by passive transport pathway only, b) Passive seawater diffusion and active protons removal. c) Active ions transport only d) ions provided by both active and passive pathways.

Hohn & Merico (2012; 2015) compared different conceptual models of coral calcification to determine which one produced the better agreement with experimental observations. The authors found the model that performed better was the one that incorporated all three of the proposed metabolic pathways (active transport, paracellular diffusion, transcellular diffusion) involved in calcification.

(Nakamura et al. 2013) used a similar model to test the plausibility of the oxygen hypothesis (Allemand et al. 2011) for light enhanced calcification (LEC), concluding that Oxygen-boosted respiration may be responsible for the increase in calcification during daytime.

In chapter 3 we developed a calcification model, based on generally accepted schematizations of the physiology of calcification and of coral-zooxanthellae symbiosis, and test it on a dataset for the Mediterranean coral *Cladocora caespitosa* (Rodolfo-metalpa et al. 2010, Fig 6). This model is used to test how much of the simulated variability in calcification rates under different conditions is due to biologically mediated or abiotic mechanisms. We tested the effects of metabolic rates (gross photosynthesis, respiration), temperature and seawater chemistry (DIC, TA) and concluded that the largest part of the observed effects are due to biologically mediated mechanisms, in particular with the energy supply to the active transport pathway. Abiotic effects are also present but are about one order of magnitude lower than the biologically mediated ones.

Fig. 6 *Cladocora caespitosa* colony.

Metabolic activities, and calcification is no exception to that, are indeed energy demanding, because building and maintaining the components of a living being involves chemical transformations that would not happen spontaneously under common environmental conditions. Living organisms must allocate the limited amount of resources they are able to fetch among

different activities, each one of which serves different purposes and contributes differently to organism fitness. This is believed to result in trade-offs among different activities that are resolved, trough evolutionary mechanisms, with optimal allocation strategies. Such strategies though are environment-dependent and may become maladaptive as external conditions change.

Increasing frequency of heat waves will cause the extinction of red coral shallow banks

The contribution in chapter 4 is motivated by recent mortality outbreaks in Mediterranean hard substrate communities (including coralligenous) that affected several species of invertebrates and occurred jointly with summery heat waves (Garrabou et al. 2009. Fig. 7). Not unlike tropical corals during harmful bleaching events, also Mediterranean species prove to have little tolerance to thermal extremes, although no bleaching is involved; in fact several taxa were affected, including asymbiotic corals and non corals. The asymbiotic gorgonian *Corallium rubrum*, red coral, which is also a major case study in this thesis (see also chapters 1 and 2), was among the most affected species. Various hypotheses have been formulated about the causes of the mortalities, these include a mismatch between energy supply and demand due to high temperatures (increased metabolic rates) and low food (typical of Mediterranean climatology in late summer) and harmful pathogens outbreak. Though, instead of addressing the mechanisms leading to mortality, the contribution in chapter 4 attempts to answer a perhaps more sensible question: are the conditions that determined the outbreaks likely to appear more frequently in the future, and what are the expected consequences for red coral populations in the Mediterranean.

Temperature exposure thresholds were determined for red coral by Torrents et al. (2008) with laboratory incubations and quantified as number of consecutive days at a given temperature that are necessary for lethal or sub-lethal (partial mortality of the colony) effects to appear. This valuable information was combined with the results of a state of the art simulation of Mediterranean thermal regimes under current and future conditions (Oddo et al. 2009). For any point in the Mediterranean mortality risk criteria were considered met if exposure thresholds were exceeded at least once in each reference period (present and future).

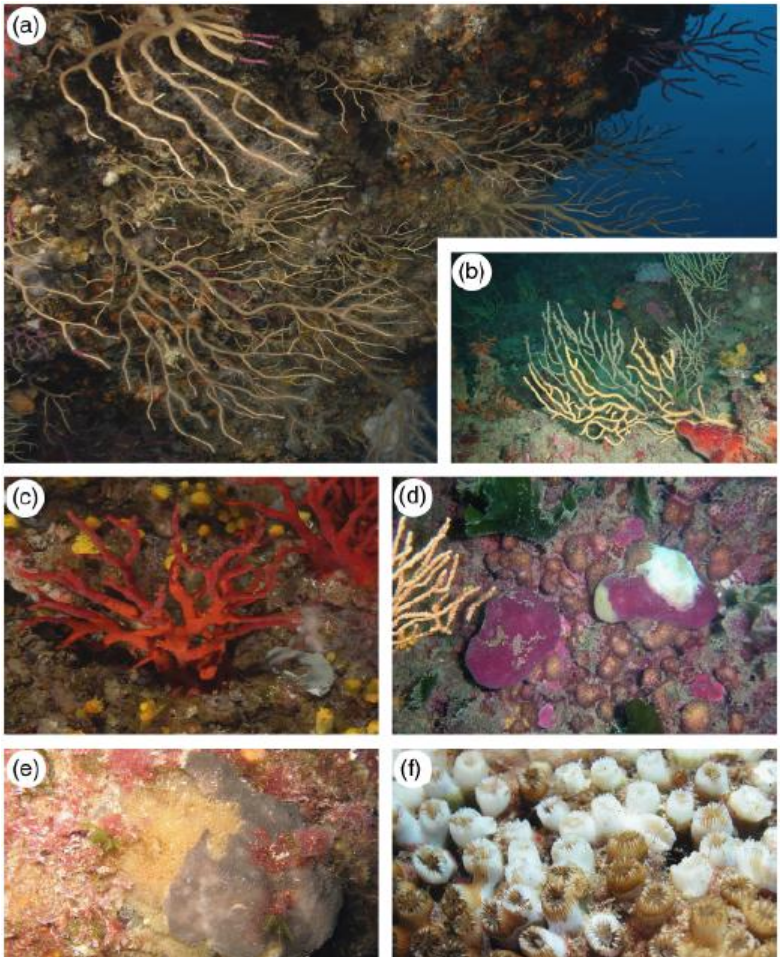

Fig. 7 Effects of the 2003 mass mortality event on coralligenous species. (a) Paramuricea clavata colonies with almost completely denuded axis. (b) Eunicella cavolinii showing signs of partial mortality. (c) Red coral colony with signs of partial mortality. (d) The sponge Petrosia ficiformis with signs of partial mortality (white area). (e) Spongia officinalis with signs of partial mortality. (f) Cladocora caespitosa, detail of polyps suffering tissue necrosis. image from Garrabou et al. 2009.

According to the simulation results, heat waves frequency and intensity will substantially rise through all of Mediterranean shallow waters in the near future and conditions similar or worse to those that triggered the observed mortalities may become commonplace threatening the existence of red coral shallow banks. The results also allow to infer future risk not just for red coral but also for many other sessile species both from coralligenous habitats and not. In fact, as several species were affected by mortality under the same conditions, it's easy to conclude they will exhibit similar thermotolerance thresholds.

The rationale behind this method is indeed very simple and the amount of assumptions minimal. This work stands as an example of data-driven model of empirical, rather than statistical, nature, with minimal data requirements and yet great predictive power as it is deeply rooted in observation. Also the presented risk assessment methodology is easily portable to different case studies as the only requirements are temperature forecasts, that are generally available from model simulations, and thermotolerance thresholds that can be assessed in the lab or even deduced from real life mortality events.

Calcareous Bio-Concretions in the Northern Adriatic Sea: Habitat Types, Environmental Factors that Influence Habitat Distributions, and Predictive Modelling

The last work presented is about Northern Adriatic Trezze and the relationships between biological communities spatial distribution and environmental parameters. In the economy of this thesis it serves as a case study for statistical data-driven modelling, both because different techniques were employed and integrated, and to exemplify the insight into spatial ecology that such methods provide.

The Trezze are rocky outcrops that are found on the otherwise invariantly sandy/muddy bottom of the Northern Adriatic. The geological origin of such peculiar features is traced to methane seepage, cementation and lithification processes (Gordini et al. 2004). The ecological importance of these outcrops is paramount as they represent almost the only hard substrates in the western part of Northern Adriatic. Some of them host rich communities of sessile invertebrates and coralline algae that are akin to coralligenous communities (Casellato & Stefanon 2008, Fig 8), and serve as nursery grounds for various species of fish and invertebrates. The Trezze are also little studied biocenoses and only recently their ecological importance has been recognized. To date there is no complete mapping of the outcrops and only some them were sampled. Substantial variability in communities composition is known to exist but was never sorted out and links to environmental variability remain putative.

Fig. 8 detail of *Nordalti*, one calcareous outcrop from the Northern Adriatic.

These issues were addressed by matching biological data (species abundance on 33 outcrops) with oceanographic physical and chemical data in three hierarchical layers of analysis: Habitats classification, identification of environmental variables influence on habitats and predictive habitats distribution modelling.

Habitat classification is performed by means of clustering analysis (fuzzy k-means method), a class of statistical methods capable of grouping the items in a dataset based on their similarity. This method identifies an optimal number of clusters among which the items in a dataset (species distribution on each outcrop) can be grouped and assigns to each data point a membership grade value for each cluster. The final classification provides important insight into the typologies of Mediterranean hard substrate habitats and their succession: Three classes of biocenoses are identified, ranging from the less valuable turf algae dominated outcrops, to filter

feeders (mainly sponges), to calcareous algae dominated outcrops that are closely related to coralligenous but lack upright gorgonians (a fourth stage of fully developed coralligenous that is not present in the sampled area).

Secondly the question of how the environment contributes to shape the spatial distribution of habitats is addressed. To do this the clusters membership grades were confronted with a spatial set of nine meaningful environmental variables by means of direct gradient analysis (redundancy analysis, RDA). Benthic habitats distribution clearly follows environmental gradients, this is utterly clear when looking at the depth zonation of biocenoses; it is however hard to tell which environmental factors contribute (temperature, nutrients, water movement...) as most of them tend to co-vary with depth. Here the factors that bear statistically significant relations with biocenoses distribution are identified with an objective procedure, this allows to formulate ecological hypotheses and can serve for predictive purposes.

In fact in the third layer of analysis, clusters membership grades were predicted for a large area in the Northern Adriatic where no biological sampling is available, based on environmental variables and regression coefficients obtained from the RDA analysis. As the knowledge of the distribution of outcrops is to date only partial, such predictive model could be useful for identifying sites that may host valuable communities for future sampling and marine protected areas spatial planning purposes.

6. References

Al-Horani, F. a, Al-Moghrabi, S.M. & De Beer, D., 2003. The mechanism of calcification and its relation to photosynthesis and respiration in the scleractinian coral Galaxea fascicularis. *Marine Biology*, 142(3), pp.419–426.

Allemand, D. et al., 2011. Coral calcification, cells to reefs. In Z. Dubinsky & N. Stambler, eds. *Coral Reefs: An Ecosystem in Transition*. Dordrecht: Springer Netherlands, pp. 119–150.

Anthony, K.R.N., Connolly, S.R. & Willis, B.L., 2002. Comparative analysis of energy allocation to tissue and skeletal growth in corals. *Limnology and Oceanography*, 47(5), pp.1417–1429.

Ballesteros, E., 2006. Mediterranean coralligenous assemblages: a synthesis of present knowledge. *Oceanography and Marine Biology: An Annual Review*, 44, pp.123–195.

von Bertalanffy, L., 1938. A QUANTITATIVE THEORY OF ORGANIC GROWTH (INQUIRIES ON GROWTH LAWS. II). *Human Biology*, 10(2), pp.181–213.

Bethoux, J.P. et al., 1999. The Mediterranean Sea: A miniature ocean for climatic and environmental studies and a key for the climatic functioning of the North Atlantic. *Progress in Oceanography*, 44(1-3), pp.131–146.

Brey, T., 2001. Population dynamics in benthic invertebrates. A virtual handbook. Version 01.2. Available at: http://www.thomas-brey.de/science/virtualhandbook.

Brown, B.E., Hewit, R. & Le Tissier, M.D., 1983. The nature and construction of skeletal spines in Pocillopora damicornis (Linnaeus). *Coral Reefs: Journal of the International Society for Reef Studies*, 2(2), pp.81–89.

Casellato, S. & Stefanon, A., 2008. Coralligenous habitat in the northern Adriatic Sea: An overview. *Marine Ecology*, 29(3), pp.321–341.

Dawkins, R., 1976. the Selfish Gene. *30th Anniversary Edition--with a new Introduction by the Author*, pp.1–13.

Dubinsky, Z. & Jokiel, P.L., 1994. Ratio of energy and nutrient fluxes regulates symbiosis between zooxanthellae and corals. *Pacific Science*, 48(3), pp.313–324.

Garrabou, J. et al., 2009. Mass mortality in Northwestern Mediterranean rocky benthic communities: Effects of the 2003 heat wave. *Global Change Biology*, 15(5), pp.1090–1103.

Gattuso, J.P., Allemand, D. & Frankignoulle, M., 1999. Photosynthesis and calcification at cellular, organismal and community levels in coral reefs: A review on interactions and control by carbonate chemistry. *Am. Zool.*, 39(1), pp.160–183.

Gordini, E. et al., 2004. The cemented deposits of the Trieste Gulf (Northern Adriatic Sea): aereal distribution, geomorphologic characteristics and high resolution seismic survey. *Journal of Quaternary Science*, 17, pp.555–563.

Hohn, S. & Merico, A., 2012. Modelling coral polyp calcification in relation to ocean acidification. *Biogeosciences*, 9(11), pp.4441–4454.

Hohn, S. & Merico, A., 2015. Quantifying the relative importance of transcellular and paracellular ion transports to coral polyp calcification . *Frontiers in Earth Science*, 2(January), p.37.

Kooijman, S.A.L.M., 2009. *Dynamic energy budget theory for metabolic organisation, third edition* 3rd ed., Cambridge University Press.

McConnaughey, T.A. & Whelan, J.F., 1997. Calcification generates protons for nutrient and bicarbonate uptake. *Earth-Science Reviews*, 42(1-2), pp.95–117.

Muller, E.B. & Nisbet, R.M., 2014. Dynamic energy budget modeling reveals the potential of future growth and calcification for the coccolithophore Emiliania huxleyi in an acidified ocean. *Global Change Biology*, 20(6), pp.2031–2038.

Nakamura, T., Nadaoka, K. & Watanabe, A., 2013. A coral polyp model of photosynthesis, respiration and calcification incorporating a transcellular ion transport mechanism. *Coral Reefs*, 32(3), pp.779–794.

Oddo, P. et al., 2009. A nested Atlantic-Mediterranean Sea general circulation model for operational forecasting. *Ocean Science*, 5(4), pp.461–473.

Ogilvie, M.M., 1896. Microscopic and Systematic Study of Madreporarian Types of Corals. *Philosophical Transactions of the Royal Society of London B: Biological Sciences*, 187, pp.83–345.

Pecquerie, L. et al., 2012. Reconstructing individual food and growth histories from biogenic carbonates. *Marine Ecology Progress Series*, 447, pp.151–164.

Priori, C. et al., 2013. Demography of deep-dwelling red coral populations: Age and reproductive structure of a highly valued marine species. *Estuarine, Coastal and Shelf Science*, 118(January), pp.43–49.

Rodolfo-Metalpa, R. et al., 2010. Response of the temperate coral Cladocora caespitosa to mid- and long-term exposure to p CO 2 and temperature levels projected for the year 2100 AD. *Biogeosciences*, 7,

pp.289–300.

Rossi, S. et al. eds., 2017. Growth patterns in long-lived benthic suspension feeders. In *Marine Animal Forest, The Ecology of Benthic Biodiversity Hotspots*. Springer International Publishing Switzerland.

Santangelo, G., Bramanti, L. & Iannelli, M., 2007. Population dynamics and conservation biology of the over-exploited Mediterranean red coral. *Journal of Theoretical Biology*, 244(3), pp.416–423.

Tambutté, É. et al., 1996. A compartmental approach to the mechanism of calcification in hermatypic corals. *The Journal of experimental biology*, 199, pp.1029–41.

Torrents, O. et al., 2008. Upper thermal thresholds of shallow vs. deep populations of the precious Mediterranean red coral Corallium rubrum (L.): Assessing the potential effects of warming in the NW Mediterranean. *Journal of Experimental Marine Biology and Ecology*, 357(1), pp.7–19.

Venn, A. et al., 2011. Live tissue imaging shows reef corals elevate pH under their calcifying tissue relative to seawater. *PLoS ONE*, 6(5).

Volterra, V., 1926. Variazioni e fluttuazioni del numero d'individui in specie animali conviventi. *Memorie della R. Accademia dei Lincei*, 6(2), pp.31–113.

Zabala, M.E. & Ballesteros, E., 1989. Surface-dependent strategies and energy flux in benthic marine communities or, why corals do not exist in the Mediterranean. *Sci.Mar.*, 53(1), pp.3–17.

1. Modelling coral growth

One of the big challenges in the study of animal forests species is to provide reliable estimates of their ecological response under current and future anthropogenic pressures, such as climate change and the introduction of invasive species.

Growth rate, form, and size are proxies to evaluate the species at the organism level, and as such, they provide metrics to assess species performance under different environmental conditions. However, in the case of corals, colony development can take decades, making most of the potential experimental approaches almost impossible to implement. At the same time routinely measured vital parameters such as growth rates are usually not constant over the entire lifespan, frequently changing with organism size and/or age. Consequently, the extrapolation of growth rates, experimentally obtained on colony fragments, to whole colonies, or even reefs must be carefully considered.

Numerical simulation techniques provide diverse frameworks for addressing these issues. Application scales vary widely, ranging from small scale physiological processes (e.g. ion transport across tissues, see chapter 3) to whole ecosystem dynamics. The choice of the appropriate scale is a matter of the study aims and knowledge available for the targeted species. Even though, for conservation purposes, population and ecosystem approaches need to be considered, in some cases it is convenient to study simpler and smaller scale systems in order to understand their basic functioning and scale up to higher, more complex levels. Coral growth lends itself particularly well to this approach, as colonies, which are characterized by their modular architecture, are a good example of a whole organism that results from the iteration of a single, potentially autonomous and relatively invariant unit, the polyp.

In this section we will outline the basics of some modelling applications that we believe are relevant for the studies dealing with coral growth, as well as present some examples of related literature and own contributions. Emphasis will be made on published studies that have already provided knowledge on growth processes, as well as, on existing gaps and promising research perspectives.

1.1 Organism and population growth models

From a modelling perspective, a living organism (either a coral or another living being) can be considered an open system that maintains high levels of internal organization by a continuous flux of energy through its boundary. Classical growth models are the so called bioenergetic models whose history dates back to the first half of the XXth century (von Bertalanffy 1938, see Kooijman 2009 for an extensive treatise). Such class of models describes growth as the evolution of a quantity (usually energy, biomass, or mass of a specific compound) over time through the balance of input and output fluxes, through the system boundary and between compartments within the system.

The simplest possible formulation (as a differential equation) of a bioenergetic growth model considers one single compartment for biomass (or energy), one input, and one output flux that depends on the system biomass/energy according to power laws (also termed allometric laws, see Glazier 2005 for a review):

$$\frac{dY}{dt} = IN - OUT = aY^{\alpha} - bY^{\beta} \tag{1.1}$$

Where Y is mass or energy, t is time, a and b are specific rates of Y flow (e.g. per unit mass or surface), and α, β are the allometric scaling coefficients (typically ≤ 1).

Positive growth can continue only if the inputs exceed the outputs, therefore, if $\beta > \alpha$, eventually a value of Y is reached at which the two terms on the right hand side are equal, stopping growth. This explains growth patterns observed in the majority of known species, including fast growth early in life and the existence of a maximal size (Fig. 1.1).

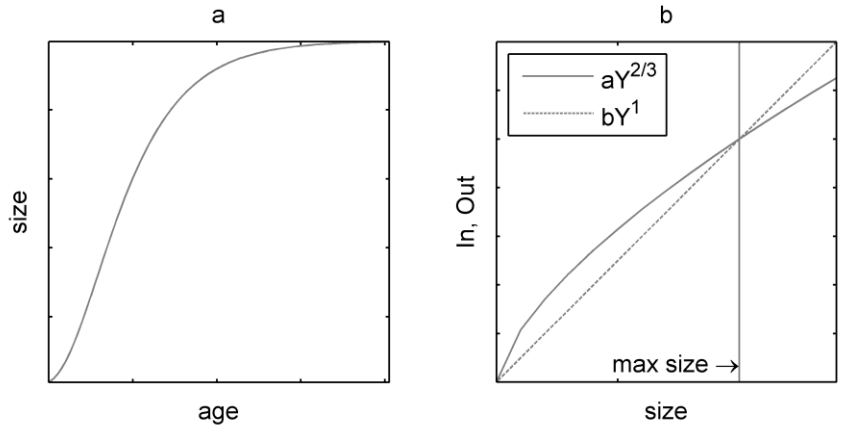

Fig. 1.1 a. Growth curve resulting from eq. 1.1, characterized by the existence of an asymptotic maximal size. b. *IN* and *OUT* fluxes from eq. 1.1 as a function of organism size with *Y*: organism size, *a*, *b*: constant coefficients.

Bioenergetic models are particularly interesting because they are based on first principles (mass/energy conservation) and can be applied to any species (of course with species-specific formulations), offering a wide array of applications. Whilst the bioenergetic modelling framework has been successfully applied to a variety of species, both terrestrial and marine, colonial and modular architectures(as found in corals, sponges, and seaweeds) entail some issues that must be properly addressed. For instance, the values of allometric scaling coefficients (in eq. 1.1) that are typically observed in solitary organisms may not be valid for colonies (Sebens 1987), possibly resulting in indeterminate growth.

When modelling the growth of a modular organism, it must be considered whether the colony will be described as a single organism or as a result of the co-existence of single modules. If a colony is described as a "population" of polyps, colony growth, measured as the increment of polyp number (*N)* over time, results from the two processes of (1) new polyps being originated by division ("births"), and (if applicable) (2) polyps death. The population's birth and death rates are usually considered to be dependent on population size. As an example, the famous Verhulst equation describing self-limiting growth of a population can be written as:

$$\frac{dN}{dt} = Births - Deaths = rN - \frac{r}{K}N^2 \qquad (1.2)$$

Where r is the population's specific growth rate, K is the environment's carrying capacity, and the term $(r/K)N$ represents the specific mortality rate (assumed to depend linearly on population size N). Population dynamics may then be coupled with a single polyp growth model (of the kind described in eq. 1.1) by making population growth and mortality rates functions of polyp biomass. Polyps indeed seem to undergo fission only if some threshold size is attained (Sebens 1980; Kooijman 2009), and they will arguably die if their biomass falls below a minimal value. The available information on these matters is however surprisingly scarce.

1.2 Growth indeterminacy, trophic shading and bioenergetic implications of shape

One of the properties generally attributed to modular organisms is growth indeterminacy. For example, colonies may escape the constraints that limit maximal size of the single module if colony resource acquisition were to scale linearly with the number of modules (Sebens 1980; 1987). At present, it is unclear whether modular architecture ensures growth indeterminacy; in fact alternative theories have been proposed. It may seem trivial to infer if an organism does or does not display a maximal attainable size (size being defined as metabolically active biomass); though in corals the parameter size is elusive compared to other individual animals whose total mass is mostly metabolically active (instead of mostly calcium carbonate) and that can be readily weighted or their weight inferred from parameters like length or height (e.g. fish). Whereas coenosarc weight would qualify as an informative measure of metabolically active biomass, the skeleton, that is metabolically inactive, is more often measured. Also, as corals do not have defined body plans, parameters such as length, height or diameter, are usually scarcely informative for corals.

Models offer a valid alternative to test existing hypotheses. Kim & Lasker (1998) investigated the potential limits of modular growth with a bioenergetic model where colony resource acquisition does not scale linearly with the number of modules. The cornerstone of their reasoning was that polyps in a coral colony compete for resource acquisition, therefore, as the number of modules increase, the availability of food per module decreases. This process is known as *trophic shading* (analogous to *self-shading* in trees), and the authors demonstrated that it may effectively limit the maximal size of a colony that would otherwise exhibit indeterminate growth.

A simple process-based model of resource acquisition incorporating the phenomenon of trophic shading can be constructed as follows. Let us consider a colony surrounded by a conveniently chosen control volume, V, of water that is considered, for the sake of simplicity, well mixed. Polyp specific consumption rate (assumed to be a non-photosynthesizing organism) is assumed to have a Michaelis-Menten type of dependence on food concentration, F, in the control volume. This kind of functional response is generally considered realistic, and in fact, is extensively found in literature, however different kinds of relations (e.g. linear, Holling type III) do not change the results substantially.

Assuming that colony resource acquisition, A, scales linearly with colony surface, S, then it can be written as:

$$A = a_{max} \frac{F}{k_F + F} S \tag{1.3}$$

Where a_{max} is the maximum resource acquisition rate per unit of surface and k_F is the semi-saturation constant. If Q is the water flow through the control volume and F_b the bulk food concentration, then the variation of the mass of food, M, in the control volume over time is:

$$\frac{dM}{dt} = QF_b - QF - a_{max} \frac{F}{k_F + F} S \tag{1.4}$$

Assuming stationary conditions (the right side of the equation equals zero) and solving for F, gives a second order polynomial in F:

$$F^2 + F\left(k_F - F_b + \frac{a_{max}\,S}{Q}\right) - k_F F_b = 0 \qquad (1.5)$$

This admits just one positive solution dependent on the values of S and Q.

This formalization is rather general and can be used to study the variation of F, (hence of resource acquisition), with colony size once the relationship between flow and colony surface is established. It is possible to further specify the value of Q if we let the control volume V be cubic so that the area of a side is $A_S = V^{2/3}$, and let the flow be oriented normally to two faces so that, $Q = v \cdot A_S = v \cdot V^{2/3}$, where v is flow speed.

We distinguish now two ideal cases, one in which the colony is spherical, the other in which it grows according to a space-filling pattern so that the surface area contained per unit of volume is constant at all sizes. The second case approximates branching and fractal geometries typical of many marine sessile species. In the spherical geometry case we have $S = \pi \cdot V^{2/3}$, whilst for space-filling growth the relation reads, $S = k \cdot V$, with k constant. By substituting the relations for S and Q in eq. 1.5 we obtain,

$$F^2 + F \cdot \left(k_F - F_b + \frac{a_{max} \cdot \pi}{v}\right) - k_F \cdot F_b = 0 \qquad (1.6)$$

and,

$$F^2 + F \cdot \left(k_F - F_b + \frac{a_{max} \cdot k \cdot V^{1/3}}{v}\right) - k_F \cdot F_b = 0 \qquad (1.7)$$

for spherical and space-filling geometries, respectively. It is readily noted that the value of F for the spherical case is constant and independent on colony size, whilst in the space-filling case, the result is related to the size

of the control volume, therefore, the size of the colony is to the power of 1/3. By plotting the solutions of eq. 1.6 and 1.7 with respect to a measure of colony size (Fig. 1.2), it is evident that space-filling growth specific resource acquisition diminishes with colony size, whilst this doesn't happen in the spherical case.

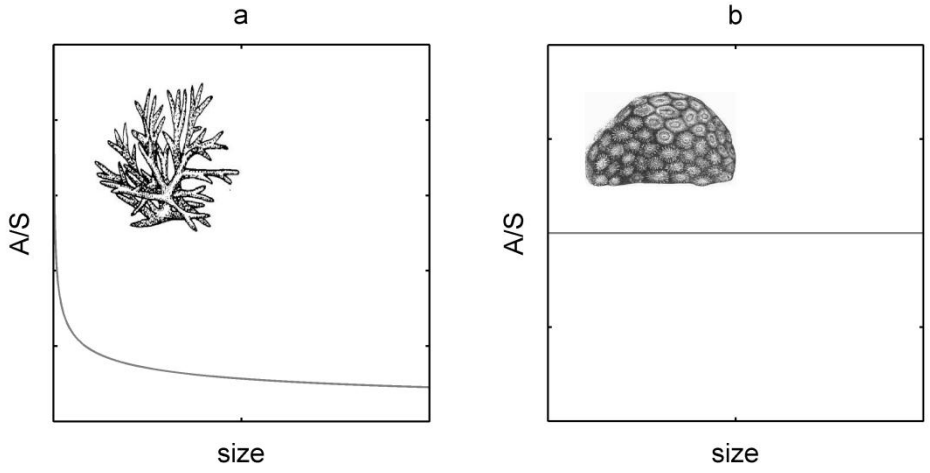

Fig. 1.2 Model of the specific resource acquisition rate (per unit surface area) according to the size of the control volume for space-filling (a) and spherical (b) colony shape.

The presented model uses a number of simplifications, above all the assumption of a well mixed volume of water around the coral and ideal geometries. Nonetheless, the results indicate that the process of trophic shading is mediated by the geometry of resource acquisition. This has consequences also for the size of the polyps: in branching forms the polyps will be less and less fed as the colony grows bigger, as a consequence they will lose weight, resulting in an inverse relationship between colony size and polyp size (Kim and Lasker 1998, see also chapter 2). On the other hand massive forms, for which food availability doesn't depend on colony size, would be characterized by polyps of relatively invariant size; massive forms would also generally feature larger polyps than branching forms. Furthermore, if we accept that polyps division rate is mediated by polyp size (i.e. only large enough polyps can undergo fission, Sebens 1980), polyps in branching forms will eventually get too thin to undergo fission and colony growth will stop, i.e. trophic shading may effectively limit polyps number, hence maximal colony size. Spherical forms on the other hand would be characterized by indeterminate growth (see later in this chapter for a case study application). These conclusions are derived for idealized

geometries, however, it is reasonable to predict that actual growth forms will fall somewhere between the two extremes.

1.3 Growth of calcified structures and skeletal rings formation

In classical bioenergetic models, the distinction between living biomass and skeleton is usually neglected, however, this is an important issue to deal with when attempting to describe the growth of organisms that are in high proportion calcium carbonate. A general quantitative theory linking biogenic carbonates formation to organism metabolism is currently lacking (Allemand et al. 2011). In particular, it is unclear which part of coral energy budgets are devoted to skeleton formation (but see Anthony et al. 2002), how much $CaCO_3$ is yielded per amount of energy invested (Palmer 1992; Anthony et al. 2002), and how those quantities are affected by the external environment and organism status.

Some calcification models exploit the rather well known inorganic chemistry of carbonates and calcium carbonates in seawater. Hohn & Merico (2012; 2015) developed a model of single coral polyp calcification based on the trans-calcification concept that describes the path of the chemical species relevant for inorganic $CaCO_3$ deposition from seawater to the calcification site. Nakamura et al. (2013) further expanded this model by incorporating a link between active ion transport and the rate of zooxanthellae photosynthesis. The aim of these models is to provide a mechanistic understanding of the physiological scale processes that are involved in the deposition of the skeleton. Colony growth is not resolved, however, a general framework is developed that could be fruitfully scaled up to describe whole organism accretion. Anthony et al. (2002) dealt with the comparative analysis of energy allocation to tissue and skeletal growth in corals by using a bioenergetic growth model based on colony/branch geometry (branching or hemispherical). Results were consistent with the observed weak correlation between calcified and organic tissue growth across environmental conditions, suggesting that tissue properties (e.g. biomass, energetic content), rather than skeletal growth, are a better proxy for health or stress in corals. Furthermore, the authors found the existence

of threshold dimensions (quantified as the radius of the colony/branch) below which energy investment is tissue dominated and above which most of the organism's budget is devoted to the skeleton. Since these threshold radii are small (on the order of centimeters), the authors conclude that the energy investment of most branching corals is tissue dominated, whilst massive forms are skeleton dominated for most of their life history.

Skeleton deposition and accretion ring patterns can be linked to organism metabolism and environmental conditions (modeled in a bioenergetic framework) as demonstrated in Fablet et al. 2011 and Pecquerie et al. 2012 for fish otoliths. The authors recognized that carbonates deposition is decoupled from living tissue growth as the two processes originate from separate metabolic pathways; also, two distinct pathways are identified accounting for the organic and inorganic fractions of the skeleton. As such pathways are differently affected by the organism's status and external variables (temperature, food, etc.), the ratio between $CaCO_3$ and organic matter flow follows a seasonal cycle. Such studies demonstrate how it is possible to infer one of the three variables: ring appearance, thermal history, and feeding history, if two of them are known.

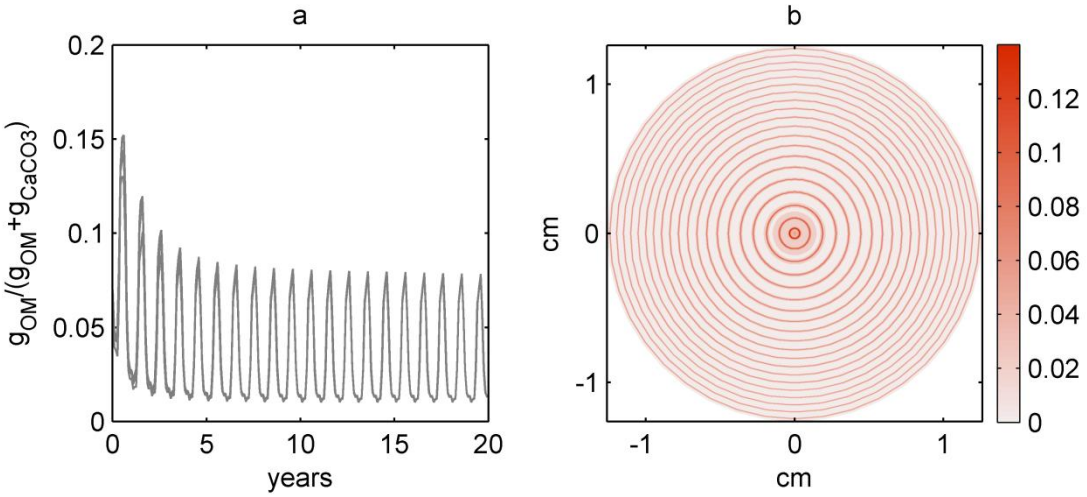

Fig. 1.3 a. Model of the time dynamics of skeleton chemical composition expressed as mass of organic matter over total skeleton mass; b. Same data as in panel a, but with a different graphic representation that makes seasonal accretion bands apparent; color bar values are organic matter mass over total skeletal mass as in a.

This kind of reasoning is not species specific and can be applied to corals as well. In the next chapter it is presented a model for the Mediterranean octocoral *Corallium rubrum* where the growth of the organic component is an energetic cost linked to food assimilation, and influenced by seasonality in food availability and temperature, whereas the growth of the inorganic component, is an energetic cost which does not depend directly on food (rather depending on past feeding history), but does vary with temperature, although with a different kinetic. The differences between organic and inorganic component dynamics give rise to accretion rings (Fig. 1.3) whose aspect and timing matches already published observations. For example Marschal et al. 2004 showed that yearly patterns observed for *C. rubrum* consists of thin rings rich in organic matter, which alternate with thick rings with low organic matter (OM) content. The thickness of rings is related to high or low inorganic matter deposition. Thick rings are laid down during summer when temperatures are relatively high and food levels are low, whilst thin rings are deposited in winter when temperatures are low and food availability is high.

1.4 An application of a growth model to the case study of *Corallium rubrum*

Possible applications for some of the concepts described above, are featured in a recently developed model for *Corallium rubrum* (see chapter 2) and are reported here. The model consists of two coupled modules: one accounting for single polyp growth dynamics, including both soft tissue and calcified structures, and the other for population dynamics of polyps within the colony, considering the polyps as individuals and the colony as a population. Trophic shading is implemented as described above for the space-filling case, as *C. rubrum* is characterized by a branching morphology. Polyp division rate is assumed to depend on polyp biomass according to a sigmoid function, no mortality term was considered because there is no conclusive evidence for polyps dying before the colony for this species (but see Vielzeuf et al. 2008). Skeletal growth is described above in the accretion ring formation section. The model uses monthly total organic carbon (TOC) concentrations from the NW Mediterranean (Rossi & Gili

2005) and uses it as a proxy for food concentration. In order to fit the model, colony weight, polyp number and age were considered (Santangelo et al. 2003; Priori et al. 2013). As no clear correlation has been found between polyp number and age, nor between colony weight and age, we tested the model's performance against both weight and polyp number at the same time. This resulted in a 3D space (weight, polyp number, and age) in which, instead of a growth curve, we have a growth surface representing all possible combinations of weight, polyp number, and age. Growth surface is generated in the model by multiple growth trajectories obtained by varying the sole water flow speed parameter in the trophic shading module. This choice is intended to mimic the high variability in local hydrodynamic conditions that colonies experience and that are dictated by small scale patch morphology and water flow.

In Fig. 1.4, some results of the model are displayed. Model results show good adherence with the experimental sets from Santangelo et al. (2003) and Priori et al. (2013). The trophic shading module has the effect of limiting maximal polyp number (Fig. 1.4a) and total polyp mass (Fig. 1.4d), effectively resulting in determinate growth of soft tissue and polyps population. These effects arise because polyp size diminishes with polyp number (Fig. 1.4c). $CaCO_3$ mass (Fig. 1.4b) on the other hand shows unlimited growth due to the absence of maintenance costs for the skeleton.

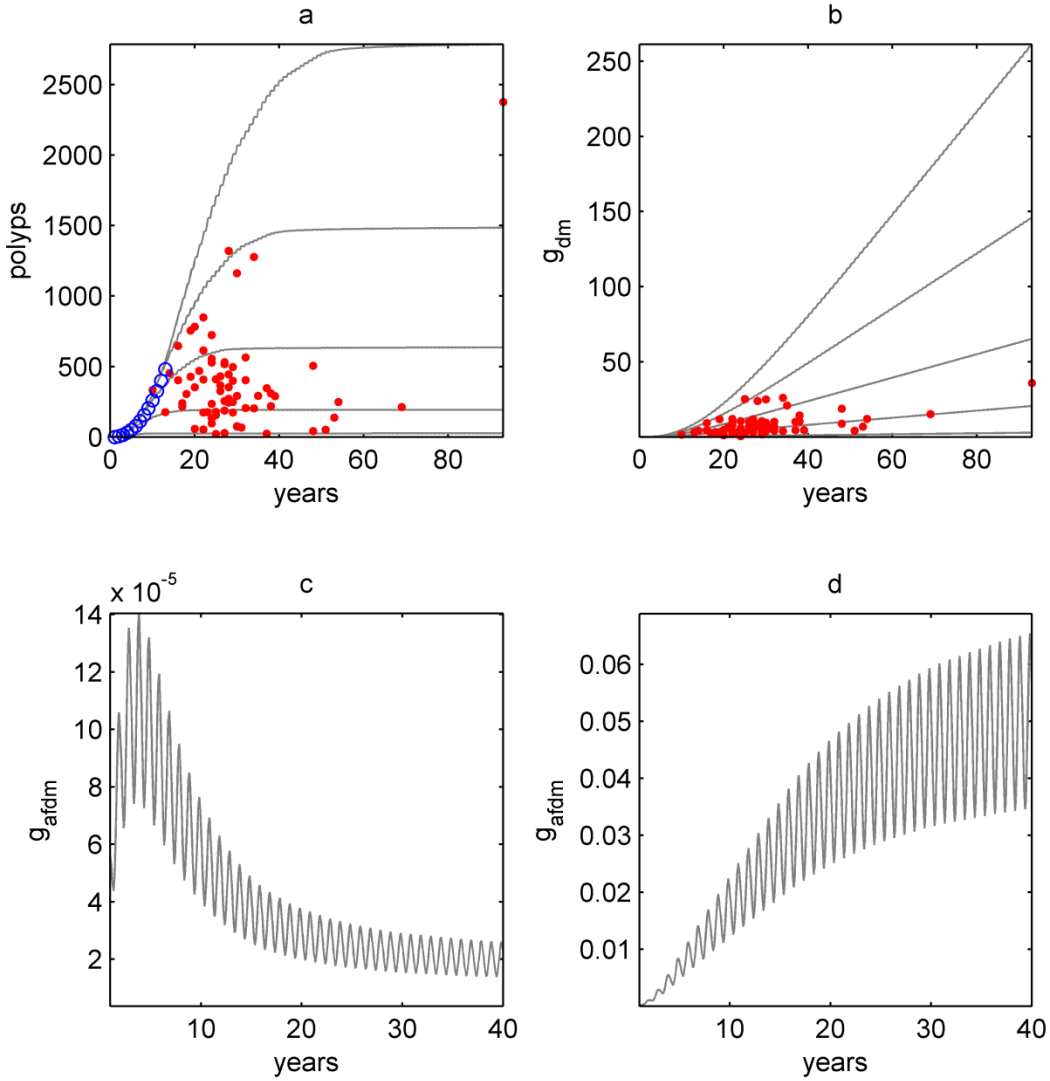

Fig. 1.4 a. Model of the polyp number over time under different flow rates and experimental data points; b. Total colony mass under different flow rates and experimental data points, c., d. Single polyp mass (ash free dry weight) and total polyp mass (ash free dry weight) over time at a single flow regime. In plots a, b, solid lines are simulated growth trajectories under different flow regimes, filled dots in all plots are data included in Priori et al. (2013), empty dots are results included in Santangelo et al. (2003).

1.5 Morphogenesis models

The modelling applications that have been mentioned so far describe growth as a zero-dimensional process (i.e. spatial dimensions are only implicitly considered or not at all). Whereas, coral polyps are relatively similar among different species (at least from a body plan perspective), and coral growth forms (branching, encrusting, massive...) are widely different among species and even within the same species.

Morphological plasticity is interpreted as an adaptation of sessile growth that allows an organism to exploit, at best, the micro environment of the patch where it once settled, and from where it is very unlikely to ever move (Bradshaw 1965). Although some part of morphological variability is arguably mediated by genetics, a considerable part of it is believed to be determined by environmental conditions.

As mentioned before, at small scales trophic and, in photosynthesizing species, light shading affect each module differently. Exposed modules, such as those in apical branches, have more scope for growth and reproduction than sheltered ones. This in turn determines differential growth rates for different portions of the colony and, ultimately, growth form (Kaandorp 1999).

Based on these premises, tridimensional coral morphogenesis models were developed by Kaandorp and co-workers (see Kaandorp 1999; 2013 for an introduction). Such models work by coupling polyp-oriented models of coral growth with hydrodynamic simulations. Colony growth forms are not known a priori nor defined by the user, but rather emerge from the interplay between flow regime and processes of resource acquisition and shading among modules. Simulations show that under high flow conditions, the diffusive boundary layer around the coral surface is thin with short residence times; hence the variability in food particles concentration is relatively small among different portions of the colony. This determines similar growth potential for all polyps that in turn results in massive growth forms. On the other hand, branching forms, which are characterized by high surface to volume ratio and a thick boundary layer, arise in low flow conditions with high diffusive boundary layer residence times. These effects increase the variability of resource allocation for different portions of

the colony, producing unequal growth and the emergence of branching patterns. It is important to note that these results are strictly valid only within the same species (same vital parameters) and with all environmental conditions (different from flow speed) being equal; the terms 'branching' and 'massive' are thus to be interpreted relative to the range of growth forms in a species.

The growth forms that can be obtained by these means bear striking similarity with their real life counterparts. Moreover the models are developed with a remarkably low number of species-specific parameters and, due to the ubiquity of the processes involved, can be applied to a wide variety of species including sponges and seaweeds.

1.6 References

Allemand, D. & Bénazet-Tambutté, S. (1996). Dynamics of calcification in the mediterranean red coral, Corallium rubrum (Linnaeus) (Cnidaria, Octocorallia). *Journal of Experimental Zoology*. 276 (4). p.pp. 270–278.

Allemand, D., Tambutté, É., Zoccola, D. & Tambutté, S. (2011). Coral calcification, cells to reefs. In: Z. Dubinsky & N. Stambler (eds.). *Coral Reefs: An Ecosystem in Transition*. Dordrecht: Springer Netherlands, pp. 119–150.

Anthony, K.R.N., Connolly, S.R. & Willis, B.L. (2002). Comparative analysis of energy allocation to tissue and skeletal growth in corals. *Limnology and Oceanography*. 47 (5). p.pp. 1417–1429.

Ballesteros, E. (2006). Mediterranean coralligenous assemblages: a synthesis of present knowledge. *Oceanography and Marine Biology: An Annual Review*. 44. p.pp. 123–195.

von Bertalanffy, L. (1938). A QUANTITATIVE THEORY OF ORGANIC GROWTH (INQUIRIES ON GROWTH LAWS. II). *Human Biology*. 10 (2). p.pp. 181–213.

Bramanti, L., Iannelli, M. & Santangelo, G. (2009). Mathematical modelling for conservation and management of gorgonians corals: youngs and olds, could they coexist? *Ecological Modelling*. 220 (21). p.pp. 2851–2856.

Bramanti, L., Magagnini, G., De Maio, L. & Santangelo, G. (2005). Recruitment, early survival and growth of the Mediterranean red coral Corallium rubrum (L 1758), a 4-year study. *Journal of Experimental Marine Biology and Ecology*. 314 (1). p.pp. 69–78.

Bramanti, L., Movilla, J., Guron, M., Calvo, E., Gori, A., Dominguez-Carri, C., Griny, J., Lopez-Sanz, A., Martinez-Quintana, A., Pelejero, C., Ziveri, P. & Rossi, S. (2013). Detrimental effects of ocean acidification on the economically important Mediterranean red coral (Corallium rubrum). *Global Change Biology*. 19 (6). p.pp. 1897–1908.

Bramanti, L., Vielmini, I., Rossi, S., Tsounis, G., Iannelli, M., Cattaneo-Vietti, R., Priori, C. & Santangelo, G. (2014). Demographic parameters of two populations of red coral (Corallium rubrum L. 1758) in the North Western Mediterranean. *Marine Biology*. 161 (5). p.pp. 1015–1026.

Brey, T. (2001). *Population dynamics in benthic invertebrates. A virtual handbook. Version 01.2.* [Online]. 2001. Available from: http://www.thomas-brey.de/science/virtualhandbook.

Cebrian, J., Duarte, C.M. & Pascual, J. (1996). Marine climate on th Costa Brava (northwest Mediterranean) littoral. *Publ. Espec. Inst. Esp. Oceanogr.* 22. p.pp. 9–21.

Cerrano, C., Cardini, U., Bianchelli, S., Corinaldesi, C., Pusceddu, A. & Danovaro, R. (2013). Red coral extinction risk enhanced by ocean acidification. *Scientific Reports*. 3. p.p. 1457.

Coma, R., Ribes, M., Gili, J.M. & Zabala, M. (1998). An energetic approach to the study of life-history traits of two modular colonial benthic invertebrates. *Marine Ecology Progress Series*. 162 (1). p.pp. 89–103.

Coma, R., Ribes, M., Serrano, E., Jiménez, E., Salat, J. & Pascual, J. (2009). Global warming-enhanced stratification and mass mortality events in the Mediterranean. *Proceedings of the National Academy of Sciences of the United States of America*. 106 (15). p.pp. 6176–81.

Cupido, R., Cocito, S., Manno, V., Ferrando, S., Peirano, A., Iannelli, M., Bramanti, L. & Santangelo, G. (2012). Sexual structure of a highly reproductive, recovering gorgonian population: Quantifying reproductive output. *Marine Ecology Progress Series*. 469. p.pp. 25–36.

Fablet, R., Pecquerie, L., de Pontual, H., Høie, H., Millner, R., Mosegaard, H. & Kooijman, S.A.L.M. (2011). Shedding Light on Fish Otolith Biomineralization Using a Bioenergetic Approach. *PLoS ONE*. 6 (11).

Garrabou, J., Coma, R., Bensoussan, N., Bally, M., Chevaldonn??, P., Cigliano, M., Diaz, D., Harmelin, J.G., Gambi, M.C., Kersting, D.K., Ledoux, J.B., Lejeusne, C., Linares, C., Marschal, C., P??rez, T., Ribes, M., Romano, J.C., Serrano, E., Teixido, N., Torrents, O., Zabala, M., Zuberer, F. & Cerrano, C. (2009). Mass mortality in Northwestern Mediterranean rocky benthic communities: Effects of the 2003 heat wave. *Global Change Biology*. 15 (5). p.pp. 1090–1103.

Garrabou, J. & Harmelin, J.G. (2002). A 20-year study on life-history traits of a“nharvested long-lived temperate coral in the NW Mediterranean: insights“ninto conservation and management needs. *Journal of Animal Ecology*. 71 (6). p.pp. 966–978.

Garrabou, J., Perez, T., Sartoretto, S. & Harmelin, J.G. (2001). Mass mortality event in red coral Corallium rubrum populations in the Provence region (France, NW Mediterranean). *Marine Ecology Progress Series*. 217. p.pp. 263–272.

Gnaiger, E. (1983). Calculation of energetic and biochemical equivalents of respiratory oxygen consumption. In: *Polarographic Oxygen Sensors. Aquatic and Physiological Applications.* pp. 337–345.

Guan, Y., Hohn, S. & Merico, A. (2015). Suitable Environmental Ranges

for Potential Coral Reef Habitats in the Tropical Ocean. *Plos One*. 10 (6). p.p. e0128831.

Heitzer, A., Kohler, H.P.E., Reichert, P. & Hamer, G. (1991). Utility of phenomenological models for describing temperature dependence of bacterial growth. *Applied and Environmental Microbiology*. 57 (9). p.pp. 2656–2665.

Hilbish, T.J. (1986). Growth trajectories of shell and soft tissue in bivalves: Seasonal variation in Mytilus edulis L. *Journal of Experimental Marine Biology and Ecology*. 96 (2). p.pp. 103–113.

Hohn, S. & Merico, A. (2012). Modelling coral polyp calcification in relation to ocean acidification. *Biogeosciences*. 9 (11). p.pp. 4441–4454.

Hohn, S. & Merico, A. (2015). Quantifying the relative importance of transcellular and paracellular ion transports to coral polyp calcification . *Frontiers in Earth Science*. 2 (January). p.p. 37.

Hoogenboom, M.O. & Connolly, S.R. (2009). Defining fundamental niche dimensions of corals: Synergistic effects of colony size, light, and flow. *Ecology*. 90 (3). p.pp. 767–780.

Jokiel, P.L. (2011). Ocean acidification and control of reef coral calcification by boundary layer limitation of proton flux. *Bulletin of Marine science*. 87 (3). p.pp. 639–657.

Kim, K. & Lasker, H.R. (1998). Allometry of resource capture in colonial cnidarians and constraints on modular growth. *Functional Ecology*. 12. p.pp. 646–654.

Kruszyński, K.J., Kaandorp, J.A. & Van Liere, R. (2007). A computational method for quantifying morphological variation in scleractinian corals. *Coral Reefs*. 26 (4). p.pp. 831–840.

Maltby, L. (1999). Studying stress: The importance of organism-level responses. *Ecological Applications*. 9 (2). p.pp. 431–440.

Marschal, C., Garrabou, J., Harmelin, J.G. & Pichon, M. (2004). A new method for measuring growth and age in the precious red coral Corallium rubrum (L .). *Coral Reefs*. 23. p.pp. 423–432.

Martin, Y., Bonnefont, J.L. & Chancerelle, L. (2002). Gorgonians mass mortality during the 1999 late summer in French Mediterranean coastal waters: The bacterial hypothesis. *Water Research*. 36 (3). p.pp. 779–782.

McCulloch, M., Falter, J., Trotter, J. & Montagna, P. (2012). Coral resilience to ocean acidification and global warming through pH up-regulation. *Nature Climate Change*. 2 (8). p.pp. 623–627.

Nakamura, T., Nadaoka, K. & Watanabe, A. (2013). A coral polyp model

of photosynthesis, respiration and calcification incorporating a transcellular ion transport mechanism. *Coral Reefs*. 32 (3). p.pp. 779–794.

Neat, F.C., Wright, P.J. & Fryer, R.J. (2008). Temperature effects on otolith pattern formation in Atlantic cod Gadus morhua. *Journal of Fish Biology*. 73 (10). p.pp. 2527–2541.

Palmer, A.R. (1992). Calcification in marine molluscs: how costly is it? *Proceedings of the National Academy of Sciences of the United States of America*. 89 (4). p.pp. 1379–1382.

Pecquerie, L., Fablet, R., De Pontual, H., Bonhommeau, S., Alunno-Bruscia, M., Petitgas, P. & Kooijman, S.A.L.M. (2012). Reconstructing individual food and growth histories from biogenic carbonates. *Marine Ecology Progress Series*. 447. p.pp. 151–164.

Picciano, M. & Ferrier-Pagès, C. (2007). Ingestion of pico- and nanoplankton by the Mediterranean red coral Corallium rubrum. *Marine Biology*. 150 (5). p.pp. 773–782.

Porter, J.W. (1976). Autotrophy, heterotrophy, and resource partitioning in Caribbean reef-building corals. *American Naturalist*. 110. p.pp. 731–742.

Pörtner, H.-O. (2008). Ecosystem effects of ocean acidification in times of ocean warming: a physiologist's view. *Marine Ecology Progress Series*. 373. p.pp. 203–217.

Previati, M., Scinto, A., Cerrano, C. & Osinga, R. (2010). Oxygen consumption in Mediterranean octocorals under different temperatures. *Journal of Experimental Marine Biology and Ecology*. 390 (1). p.pp. 39–48.

Priori, C., Mastascusa, V., Erra, F., Angiolillo, M., Canese, S. & Santangelo, G. (2013). Demography of deep-dwelling red coral populations: Age and reproductive structure of a highly valued marine species. *Estuarine, Coastal and Shelf Science*. 118 (January). p.pp. 43–49.

Rodolfo-Metalpa, R., Martin, S., Ferrier-Pages, C. & Gattuso, J.-P. (2010). Response of the temperate coral Cladocora caespitosa to mid- and long-term exposure to pCO2 and temperature levels projected for the year 2100 AD. *Biogeosciences*. 7. p.pp. 289–300.

Rossi, S. & Gili, J. (2005). Composition and temporal variation of the near-bottom seston in a Mediterranean coastal area. *Estuarine, Coastal and Shelf Science*. 65. p.pp. 385–395.

Rossi, S., Gili, J.M., Coma, R., Linares, C., Gori, A. & Vert, N. (2006). Temporal variation in protein, carbohydrate, and lipid concentrations in Paramuricea clavata (Anthozoa, Octocorallia): Evidence for summer-

autumn feeding constraints. *Marine Biology*. 149 (3). p.pp. 643–651.

Rossi, S. & Tsounis, G. (2007). Temporal and spatial variation in protein, carbohydrate, and lipid levels in Corallium rubrum (Anthozoa, Octocorallia). *Marine Biology*. 152 (2). p.pp. 429–439.

Rossi, S., Tsounis, G., Orejas, C., Padrón, T., Gili, J.M., Bramanti, L., Teixidó, N. & Gutt, J. (2008). Survey of deep-dwelling red coral (Corallium rubrum) populations at Cap de Creus (NW Mediterranean). *Marine Biology*. 154 (3). p.pp. 533–545.

Santangelo, G. & Abbiati, M. (2001). Red coral: Conservation and management of an over-exploited Mediterranean species. In: *Aquatic Conservation: Marine and Freshwater Ecosystems*. 2001, pp. 253–259.

Santangelo, G. & Bramanti, L. (2010). Quantifying the decline in Corallium rubrum populations. *Marine Ecology Progress Series*. 418. p.pp. 295–297.

Santangelo, G., Bramanti, L. & Iannelli, M. (2007). Population dynamics and conservation biology of the over-exploited Mediterranean red coral. *Journal of Theoretical Biology*. 244 (3). p.pp. 416–423.

Santangelo, G., Carletti, E., Maggi, E. & Bramanti, L. (2003). Reproduction and population sexual structure of the overexploited Mediterranean red coral Corallium rubrum. *Marine Ecology Progress Series*. 248. p.pp. 99–108.

Santangelo, G., Cupido, R., Cocito, S., Bramanti, L., Tsounis, G. & Iannelli, M. (2012). Demography of long-lived octocorals: survival and local extinction. *Proceedings of the 12th International Coral Reef Symposium*. (July). p.pp. 9–13.

Sebens, K.P. (2002). Energetic constraints, size gradients, and size limits in benthic marine invertebrates. *Integrative and comparative biology*. 42 (4). p.pp. 853–861.

Sebens, K.P. (1987). The ecology of indeterminate growth in animals. *Annual Reviews of Ecological Systems*. 18. p.pp. 371–407.

Sebens, K.P. (1980). The regulation of asexual reproduction and indeterminate body size in the sea anemone Anthopleura elegantissima (Brandt). *Biological Bulletin*. 158. p.pp. 370–382.

Solidoro, C., Melaku Canu, D. & Rossi, R. (2003). Ecological and economic considerations on fishing and rearing of Tapes phillipinarum in the lagoon of Venice. *Ecological Modelling*. 170 (2-3). p.pp. 303–318.

Solidoro, C., Pastres, R., Melaku Canu, D., Pellizzato, M. & Rossi, R. (2000). Modeling the growth of Tapes philippinarum in Northern Adriatic lagoons. *Marine Ecology Progress Series*. 199. p.pp. 137–148.

Tambutté, S., Tambutté, E., Zoccola, D. & Allemand, D. (2008). Organic Matrix and Biomineralization of Scleractinian Corals. In: *Handbook of Biomineralization: Biological Aspects and Structure Formation*. pp. 243–259.

Torrents, O., Tambutté, E., Caminiti, N. & Garrabou, J. (2008). Upper thermal thresholds of shallow vs. deep populations of the precious Mediterranean red coral Corallium rubrum (L.): Assessing the potential effects of warming in the NW Mediterranean. *Journal of Experimental Marine Biology and Ecology*. 357 (1). p.pp. 7–19.

Tsounis, G., Rossi, S., Aranguren, M., Gili, J.M. & Arntz, W. (2006a). Effects of spatial variability and colony size on the reproductive output and gonadal development cycle of the Mediterranean red coral (Corallium rubrum L.). *Marine Biology*. 148 (3). p.pp. 513–527.

Tsounis, G., Rossi, S., Bramanti, L. & Santangelo, G. (2013). Management hurdles for sustainable harvesting of Corallium rubrum. *Marine Policy*. 39 (1). p.pp. 361–364.

Tsounis, G., Rossi, S., Grigg, R., Santangelo, G., Bramanti, L. & Gili, J. (2010). The exploitation and conservation of precious corals. *Oceanography and Marine ….* 48. p.pp. 161–212.

Tsounis, G., Rossi, S., Laudien, J., Bramanti, L., Fernández, N., Gili, J.M. & Arntz, W. (2006b). Diet and seasonal prey capture rates in the Mediterranean red coral (Corallium rubrum L.). *Marine Biology*. 149 (2). p.pp. 313–325.

Vielzeuf, D., Garrabou, J., Baronnet, A., Grauby, O. & Marschal, C. (2008). Nano to macroscale biomineral architecture of red coral (Corallium rubrum). *American Mineralogist*. 93. p.pp. 1799–1815.

Weinbauer, M.G., Brandstätter, F. & Velimirov, B. (2000). On the potential use of magnesium and strontium concentrations as ecological indicators in the calcite skeleton of the red coral (Corallium rubrum). *Marine Biology*. 137 (5-6). p.pp. 801–809.

2. Modelling red coral (*Corallium rubrum*) growth in response to temperature and nutrition.

Abstract

Corals are marine modular organisms and are important from both ecological and economical points of view. Here we developed and applied a numerical model for describing the growth of Red Coral (*Corallium rubrum*), This species is a stony octocoral endemic of the Mediterranean Sea, where it has been exploited for jewelry for centuries. Red coral does not host photosynthetic symbiotic organisms, and therefore is not subject to bleaching. Nevertheless, red coral growth and survival do depend on sea water temperature, as well as on trophic conditions and other physico-chemical parameters. The model follows a bioenergetic approach to describes the growth of a colony (polyps number, polyps and gametes biomass, skeletal $CaCO_3$ and skeletal organic matter) as a function of food availability and seawater temperature. The model is calibrated vs available experimental observations. Model results highlight that red coral suitability decreases for increasing temperature, larger colonies are more sensitive to high temperature and actual limits of corals ecological niche also depend on food availability as influenced by seston concentration in water, hydrodynamic condition and coral morphology. Bioenergetic considerations also support the conclusion that, tough modular, red coral exhibits constrained growth because of the competition for available food among the colony's polyps. The model can be used also to map red coral suitability along the Mediterranean Sea, so highlighting vulnerability hot spots.

2.1 Introduction

Corals are charismatic marine organisms and are important from both economic and ecological perspectives. They are composed of a number of small polyps attached to a calcium carbonate skeleton (in hard corals); the skeletons often present complex morphologies and serve as a refuge for a number of other species; this enhances marine biodiversity and contributes to shape marine environments which are beautiful and very attractive to divers. Also the skeleton of some species is harvested to produce jewels.

The octocoral *Corallium rubrum*, or red coral, is a stony gorgonian coral endemic of the Mediterranean. Is commonly found on hard substrates, on steep walls and overhangs, below 20 m deep and up to >100 m and it probably is the most charismatic among Mediterreann corals, which are key components of hard substrate benthic ecosystems of prime ecological importance, such as the coralligenous reefs (Ballesteros, 2006). Red coral is a slow growth, long lived species (Bramanti et al., 2005); it doesn't host photosynthetic symbiotic organisms and therefore is not subject to bleaching (heat-triggered expulsion of symbionts, often with lethal consequences), however, its growth and survival do depend on seawater temperature (Torrents et al., 2008), as well as on trophic conditions and other physico-chemical parameters. In fact, colonies acquire the energy they need to live by filtering particulate matter in the water though the polyps. Furthermore, both filtering activity and respiration depend on temperature (Previati et al., 2010). Red coral has been exploited by the jewelry industry since ancient times for its glossy red skeleton and is currently considered over-harvested (Santangelo & Abbiati 2001; Tsounis et al. 2010; 2013).

Besides fishing, shallow red coral populations have been subject in recent years (1999, 2003, Garrabou et al. 2001; Garrabou et al. 2009; Bramanti et al. 2005) to mass mortalities that occurred jointly with positive summer temperature anomalies. A cause and effect relationship is advocated in which mortalities are triggered by a combination of increased metabolic demands, due to high temperature, and summery food shortage (Rossi et al., 2006; Rossi & Tsounis, 2007; Coma et al., 2009), this condition may also have been exacerbated by pathogens outbreaks (Martin et al., 2002). In fact Red coral is believed to be subject to seasonal feeding constraints, with the winter/spring period being more favorable than summer/autumn

period (Rossi & Tsounis, 2007). This might be related to the seasonal change in Mediterranean waters (Cebrian et al., 1996), which is characterized by the development of oligotrophic waters above the thermocline during summer, whilst in winter the water column is mixed and nutrients are abundant. Anyway, being strictly heterotrophic, red coral growth must be dependent on water trophic conditions. As other calcifying organisms, Red coral is also sensitive to acidification which impairs skeleton deposition (Bramanti et al., 2013; Cerrano et al., 2013).

The interactions among different stressors, already observed in other Mediterranean corals, is likely to be ecologically relevant for red coral also. Rodolfo-Metalpa et al. (2010) found that the seasonal change in temperature, over pCO_2, was the predominant factor controlling physiology and growth of the scleractinian *C. caespitosa*; Coma et al. (2009) reported that high nutritional levels can delay the appearance of necrosis in the gorgonian *P. clavata* exposed to elevated temperatures. Yet the understanding of the cause and effect mechanisms that underlie coral response to the environment is still fragmentary (e.g. Jokiel 2011 and references therein). Pörtner (2008), in a paper about the physiological bases of marine organisms sensitivity to acidification and warming, points out that the development of a cause and effect understanding is required beyond empirical observations, for a more accurate projection of ecosystem effects and for quantitative scenarios. The same study highlights that marine calcifiers sensitivity to ocean hypercapnia is a matter of several physiological processes being concomitantly affected. We argue this is equally true for the full set of relevant environmental parameters.

Here we develop and apply a mechanistic model for describing red coral colonies growth. The model describes the growth of the average coral polyp and colony accretion by polyps division and skeleton deposition, as a function of water temperature and food availability. The model is tested against available data and observed growth patterns and the calibrated model used to define fundamental properties of red coral potential niche, to quantify carbon fluxes, and it can be helpful in predicting productive and unproductive stocks.

In fact the only other models addressing red coral (also the only models addressing a Mediterranean coral species) are the matrix population models developed in Santangelo et al. 2007 and 2012 and Bramanti et al. 2009, which explore red coral demography and mass mortalities impacts on

populations. These models, although informative, assume constant colony growth rates and make no attempts to quantify polyps and colonies growth as a function of environmental conditions. Also considering other corals species, the few existing models mainly focus on specific processes (and related scales), such as calcification or morphogenesis. For instance, Hohn & Merico (2012; 2015) and Nakamura et al. 2013 all developed models for calcification in symbiotic corals, which describe the path of carbonate compounds from the seawater to coral skeleton on time scales from seconds to hours. Anthony et al. (2002) used energetic reasoning to assess the differential allocation of energy to soft tissue and skeleton across coral growth forms. From a quite different perspective, Merks et al. (2003) and Chindapol et al. (2013) looked into the morphogenesis of stony corals as the result of the collective behavior of many coral polyps subject to different local hydrodynamic conditions but didn't consider the differentiation of metabolic activities apart from generic growth. Hoogenboom & Connolly (2009) used a process-based model to characterize the fundamental niche of reef corals in flow-light space and for different colony sizes but didn't consider several aspects of organism energetics. Finally rough habitat suitability models have been proposed based on empirical or semi-empirical reasoning (McCulloch et al., 2012; Guan et al., 2015). The first and only, as far as we know, attempt to model a whole colony considering organism energetics and food limitation was carried out by Kim & Lasker (1998) to explore factors (trophic shading) that may constrain growth in colonial organisms.

From a modelling perspective, our approach relies on the coupling of a bioenergetic individual growth model, a type of model already successfully applied to a variety of organisms, including filter feeders, with a population dynamic model and a colony resource acquisition model that accounts for competition between polyps of the same colony. A similar approach has already been applied for other benthic filter feeders (Solidoro et al. 2000; 2003) to model animals response to different scenarios of environmental conditions.

The final goal is to simulate changes in coral calcareous mass, biomass and polyps number over time under different environmental conditions and, by using growth as a proxy for organism well-being, to identify favorable and unfavorable settings. Moreover our model allows for the interpretation of growth patterns such as skeleton accretion rings formation and the properties of modular growth, in the light of organism energetics.

2.2 Materials and methods

Red coral model

The soft tissue of red coral body, which covers the axial skeleton, is composed of polyps, the fundamental modular units that filter, ingest and digest food particles, and of the mesoglea, an acellular collagen matrix. Polyps are potentially autonomous units, but a network of gastrovascular channels runs through the mesoglea and along the skeleton distributing resources to the entire colony. Calcareous spicules are also found within the mesoglea. Both skeleton and spicules are composed of Mg-rich calcite and organic matter (OM). The role of the organic part is unclear and various hypotheses have been formulated, ranging from calcification control to passive incorporation (Allemand et al., 2011). The axial skeleton cross section shows annual growth rings composed of thin dark bands, alternated by thick pale bands, corresponding to slow and fast growth respectively. According to Marschal et al., (2004) thin bands, that are richer in OM, are deposited during winter/spring, whilst thick bands are deposited during summer/autumn; i.e. it appears the most of the calcium carbonate is deposited during the period that is regarded as trophically unfavorable.

The model is organized in two levels/scales (Fig. 1); one accounts for the growth of a single coral polyp, including organic tissues and skeletal growth, the other accounts for the population dynamics of polyps within a colony. Model currencies are energy (in kJ) for polyp growth dynamics, converted to mass when appropriate, and number of polyps (NP) for colony accretion.

Individual polyp growth model

The core structure of the polyp growth sub-model (Fig. 2.1) relies on the approach proposed by von Bertalanffy (1938) for describing the relation between growth and metabolism in a living organism. Accordingly, the energy gained by food intake (E_{in}) is used to support metabolic costs (basal metabolism R_b and energetic costs related to skeletal deposition, R_s), and to

build coral polyp biomass (b_P, comprising both polyp body and mesoglea) , gametes (b_G) and skeletal organic matter (b_{OM}).

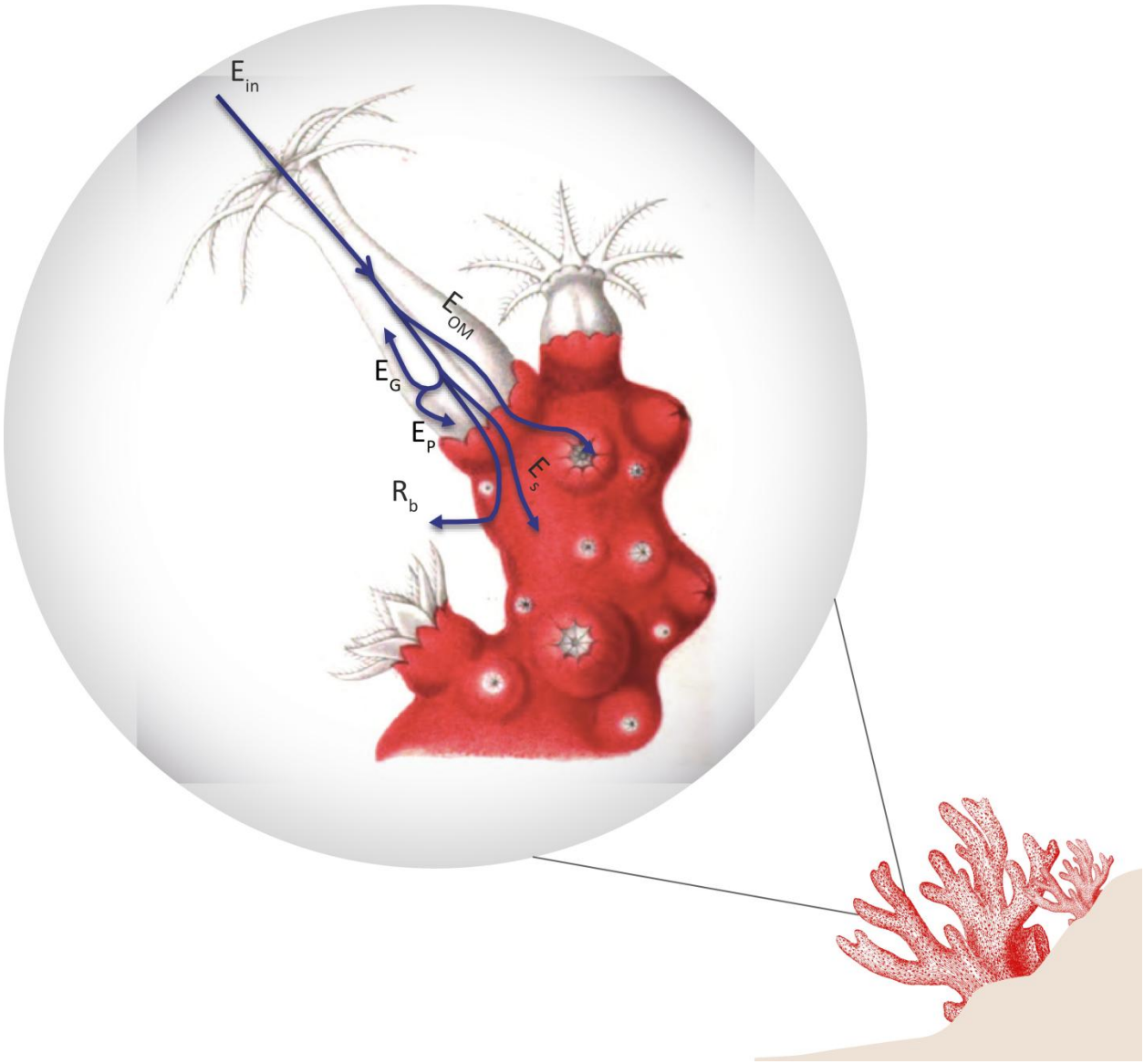

Fig. 2.1 Polyp growth sub-model scheme. Picture from the richly illustrated Histoire Naturel by Henri de Lacaze-Duthiers; graphic elaboration by Valentina Mosetti.

The anabolic flux, i.e. energy inflow, is therefore defined as

$$E_{in} = C_{max} \cdot f_c(F) \cdot f_{act}(T) \cdot b_P^n \tag{2.1}$$

where C_{max} is the maximum energy assimilation rate, n is an allometric parameter which accounts for the fact that energy inflow is proportional to polyps surface rather than weight, $f_{act}(T)$ describes the influence of temperature on polyps filtering activity, and $f_C(F)$ describe the influence of food concentration F in filtered water.

As for metabolic processes, we defined as basal metabolism the ensemble of processes supporting vital functions in the corals, such as basal respiration. By definition this processes cannot be stopped and related energy investments cannot be diverted to support other functions. Following common modeling practice and current ecophyisology theory we assume that R_b is a function of living biomass b_P, and Temperature, T. It can be measured by oxygen consumption in "resting" conditions. We assume skeletal and gametes biomass (once built) do not have maintenance costs, and therefore do not contribute to R_b.

$$R_b = R_{b,max} \cdot f_r(T) \cdot b_P^m \tag{2.2}$$

Where $m = 1$. A formal theory of energy allocation to skeleton versus tissue growth in calcifying organisms is currently lacking. However, Anthony et al. (2002) found that basal metabolic rates are the main descriptors of energy investment into skeleton in two species of reef corals. Furthermore, specific literature indicate that red coral skeleton is laid down continuously though all the coral lifespan (Santangelo et al. 2007, Pirori et al. 2013, Bramanti et al, 2013). Therefore we considered skeletal deposition to be a permanent cost, similarly to basal metabolism. However, since skeletal deposition might be considered proportional to the surface of a coral, rather than to its biomass, we assumed E_s (the energy per polyp allocated to skeletogenesis) to be a function of T and b_P to the power of n.

$$E_s = E_{s,max} \cdot f_r(T) \cdot b_P^n \tag{2.3}$$

Where $E_{s,max}$ is the maximal energy flux per unit surface area. This energy can then be converted in skeletal mass (s_{carb}, calcite) by using the calcification cost, e, proposed in Anthony et al (2002):

$$\frac{ds_{carb}}{dt} = e \cdot E_s \tag{2.4}$$

Skeleton dissolution is not possible within the model as E_s is always positive.

As already remarked, the skeleton also includes an organic fraction, but skeletal organic fraction has to be formed with a different kinetic (with respect to the inorganic one) in order to generate the yearly accretion rings patterns seen in *C. rubrum* (Marschal et al. 2004, Priori et al. 2013). Marschal et al. (2004) found that OM rich bands develop during the cold season and with high food abundance (Rossi and Gili 2005). After such evidence we inferred that red coral relies on some compounds supplied by food in order to acquire the building blocks for new OM synthesis; E_{OM} is then considered to be a feeding related cost:

$$E_{OM} = \alpha \cdot E_{in} \quad \text{and} \quad \frac{ds_{OM}}{dt} = \varepsilon \cdot \alpha \cdot E_{in} \tag{2.5}$$

where α is an energy partitioning coefficient (fraction of E_{in} allocated to OM formation) and ε the energy to mass conversion coefficient.

Incidentally, it is possible to notice that our approach is not too different from the one proposed in a dynamic energy budget model (Fablet et al. 2011, Pacuerie et al. 2012) for describing the energetic costs related to deposition of calcareous otoliths in fish, there defined as a weighted sum of anabolic and catabolic fluxes.

The difference between energy intake, E_{in}, and the permanent energetic costs (R_b, E_s, E_{OM}) defines the energy surplus, sometime also called scope for growth, *sfg*, which is partitioned between energetic costs related to the synthesis of polyps and gametes, with a partitioning coefficient β. In particular we assume that energy is invested in reproduction only when a surplus is available ($sfg \geqslant 0$); In this case $E_G=(1-\beta)sfg$. In fact Tsounis et al. (2006b) surveyed the yearly cycle of gametes development in red coral and found little development took place from approximately September to December, coinciding with the lowest seawater carbon concentrations (Rossi and Gili 2005).

Conversely, if permanent catabolic costs exceed the anabolic ones and *sfg* is lesser than zero, then gametogenesis is stopped ($E_G=0$) and permanent energetic costs are balanced by a reduction in polyp biomass. Accordingly, energy partitioning is described by,

$$sfg = E_{in} - R_b - E_s - E_{OM} \tag{2.6}$$

$$E_P = min(sfg, \quad \beta \cdot sfg) \tag{2.7}$$

$$E_G = max(0, \quad (1-\beta)\, sfg) \tag{2.8}$$

while the biomass counterpart reads,

$$\frac{db_P}{dt} = \varepsilon \cdot min(sfg, \quad \beta \cdot sfg) \tag{2.9}$$

$$\frac{db_G}{dt} = \varepsilon \cdot max(0, \quad (1-\beta) \cdot sfg) \tag{2.10}$$

Similarly gametes and organic matter cannot lose weight due to the absence of maintenance costs. However, once a year, in August, gametes are released and b_G resets to $b_G=0$ (Vighi 1972, Santangelo, 2003, Tsounis et al. 2006b).

Influence of temperature

Water temperature affects all biological processes. We modelled the influence of temperature on polyps filtering activity, $f_{act}(T)$, after experimental observations on polyps activity, measured as percentage of open polyps in a colony (the underlying hypothesis is that open polyps feed whilst closed ones do not). The curve parameters are derived by fitting data from Previati et al. (2007), which measured polyp activity rates in red corals over the range 14 - 25°C. The function is a sigmoid shaped function ranging from 0 to 1. for parameters description and values see table 2.1.

$$f_{act}(T) = 1 + exp\left(\frac{T_{ah}}{T_a} - \frac{T_a}{T}\right) \tag{2.11}$$

Respiration and metabolic costs depend upon T in agreement with an unimodal, asymmetric curve. Among possible choice we decided to use the formulation proposed in Heitzer et al. (1991). The function has been fitted against the data on O_2 consumption rates measured for red coral over the range 14 - 25°C (Previati et al. 2007). O_2 fluxes have been converted to energetic equivalents according to Gneiger (1983). for parameters description and values see table 2.1.

$$f_r(T) = \frac{\frac{T}{T_1} \cdot exp\left(\frac{T_r}{T_1} - \frac{T_r}{T}\right)}{1 + exp\left(\frac{T_{rl}}{T_l} - \frac{T_{rl}}{T}\right) + exp\left(\frac{T_{rh}}{T_h} - \frac{T_{rh}}{T}\right)} \tag{2.12}$$

Influence of trophic condition

The actual energy intake can be reduced also by a lack of particulate matter in the filtered water. Following a very common modelling practice, here we assume that actual energy inflow is the product of the maximum amount of energy a polyp can process, C_{max}, and a Monod-Michaelis-Menten function on the food concentration, F, experienced by the polyps:

$$f_c(F) = \frac{F}{k_F + F} \tag{2.13}$$

where k_F is the semi-saturation constant. Please note that F might be different from bulk food concentration (see trophic shading paragraph below).

Polyps population dynamics

Polyps population dynamic, i.e. the evolution of polyps number, N_P, over time, is modelled as:

$$\frac{dN_P}{dt} = r_{max} \cdot f_{gem}(\bar{b}_P) \cdot {N_P}^x \tag{2.14}$$

Where $\bar{b}_P$ is the average polyp biomass (see below), r_{max} is the maximum net population growth rate and x is an empirical coefficient, both derived from fitting the data (polyps at age) in Santangelo et al. 2007.

f_{gem} [0:1] is a sigmoid shaped function of polyp mass, $\bar{b}_P$, that describes the dependency of polyp gemmation rate from polyp size (see table 2.1); the underlying assumption is that polyps can undergo asexual reproduction only when a minimal size is attained (Sebens 1980), it is defined as:

$$f_{gem}\left(\bar{b}_P\right) = \frac{1}{1 + exp\left(\frac{b_{ss}}{b_{ah}} - \frac{\bar{b}_P}{b_{ah}}\right)} \tag{2.15}$$

No mortality term has been considered in the formulation of polyps population dynamics because although partial mortality events due to external causes (predation, disease, starvation, breaking) seem to be quite common among red coral (Garrabou and Harmelin 2002), there's no conclusive evidence for polyps dying of old age before the colony (but see. Vielzeuf et al. 2008).

Control function	Parameters	Value	Units	Source
Food assimilation	k_F	0.0184	$\mu g_C\ cm^{-3}$	Estimated by the fitting procedure
Activity rate	T_{ah}	92014	K	Fitting from Previati et al. 2010
	T_a	294.4	K	Fitting from Previati et al. 2010
Respiration rate	T_r	3170	K	Fitting from Previati et al. 2010
	T_1	293.15	K	Fitting from Previati et al. 2010
	T_{rl}	-57547	K	Fitting from Previati et al. 2010
	T_l	287.55	K	Fitting from Previati et al. 2010
	T_{rh}	96549	K	Fitting from Previati et al. 2010
	T_h	296.75	K	Fitting from Previati et al. 2010
Gemmation rate	b_{ss}	1.68e-4	kJ	Estimated by the fitting procedure
	b_{ah}	1.07e-5	kJ	Estimated by the fitting procedure

Table 2.1 Control functions parameter values and sources

Sub-models coupling

The integration of the population dynamic model and the individual polyp model permits to upscale the red coral model from the individual to the colony level. This integration would call for a development of age class model. However here we considered all the colony's polyps equal to an average individual and variables pertaining to the single polyp are averaged over the colony. This choice should be considered as a first approximation only, but it is useful to describe the interaction between a colony and its environment, also considering that polyps are relatively small and reach the adult size pretty quickly, possibly also using colony's shared resources.

The coupling of the polyp growth and polyps population dynamics implies that the average gamete and polyp biomass, $\bar{b}_P$ and $\bar{b}_G$, change as,

$$\frac{d\bar{b}_P}{dt} = \frac{\partial b_P}{\partial t} - \frac{B_P}{N_P}\frac{\partial N_P}{\partial t} = \varepsilon \cdot min(sfg, \quad \beta\, sfg) - \frac{\bar{b}_P}{N_P} r_{max} \cdot f_{gem}(b_P) \cdot {N_P}^x \tag{2.16}$$

$$\frac{d\bar{b}_G}{dt} = \frac{\partial b_G}{\partial t} - \frac{B_G}{N_P}\frac{\partial N_P}{\partial t} = \varepsilon \cdot min(sfg, \quad \beta\, sfg) - \frac{\bar{b}_P}{N_P} r_{max} \cdot f_{gem}(b_P) \cdot {N_P}^x \tag{2.17}$$

Conversely, the skeleton related fluxes, E_s and E_{OM}, join a single pool common to all polyps so that total calcite weight, S_{carb}, and total OM weight, S_{OM}, behave linearly with N_P and became:

$$\frac{dS_{carb}}{dt} = e \cdot N_P \cdot E_s \tag{2.18}$$

$$\frac{dS_{OM}}{dt} = \varepsilon \cdot N_P \cdot \alpha \cdot E_{in} \tag{2.19}$$

The set of differential equations is solved at monthly time steps with Runge Kutta 4th order method. Whole colony weight (W_{Col}) at time t results from the sum of the various components once proper conversion coefficients (see Table 2.2) have been applied:

$$W_{Col}(t) = S_{carb}(t) + S_{OM}(t) + N_P(t) \cdot \left(\bar{b}_P(t) + \bar{b}_G(t)\right) \tag{2.20}$$

Intra-colonial competition and trophic shading

The actual food concentration experienced by a polyp might differ from the bulk concentration away from the colony, because of competition among polyps from the same colony. In fact, in colonial organisms inner polyps might filter water that has been already partially filtered by outer polyps (Kim and Lasker 1998). This effect have been parameterized as following. Let Q be the water flow through a colony and F_b the bulk food concentration. Then the variation of the mass of food, M, in a control volume V around a colony of surface area S is:

$$\frac{dM}{dt} = Q \cdot (F_b - F) - C_{max} \cdot f_{act}(T) \cdot f_c(F) \cdot S \tag{2.21}$$

where F is the food concentration in the control volume and the surface S is dimensionally related to $N_P \cdot \bar{b}_P^{2/3}$. Assuming that stationary conditions are reached rather quickly, we can equate the right hand side of the equation to zero and solve for F, which gives,

$$F^2 + F \cdot \left(k_F - F_b + \frac{C_{max} \cdot f_{act}(T) \cdot S}{Q}\right) - k_F \cdot F_b = 0 \tag{2.22}$$

that admits just one positive solution:

$$F = \frac{-(k_F - F_b + \boldsymbol{G}) + \sqrt{(k_F - F_b + \boldsymbol{G})^2 + 4k_F F_b}}{2} \tag{2.23}$$

where

$$\boldsymbol{G} = \frac{C_{max} \cdot f_{act}(T) \cdot S}{Q} \tag{2.24}$$

is the ratio between maximal colony assimilation rate at a given temperature and water flow per unit area.

This way, if the polyps processing capability is much lower than water supply, G is small and F roughly equal to F_b, whereas in the opposite case, F is greatly reduced. Now let the control volume V be cubic so that the area of a face is $A_S = V^{2/3}$, and let the flow be oriented normally to two faces so that,

$$Q = v \cdot A_S = v \cdot V^{2/3} \tag{2.25}$$

where v is flow speed. If we assume that a branching coral grows according to a space filling pattern (Kruszyński et al. 2007) so that the colony surface area S per unit of control volume V is roughly constant,

$$\frac{S}{V} = k_1 \tag{2.26}$$

we can express G also as a function of water velocity and coral surface area:

$$\boldsymbol{G} = \frac{C_{max} \cdot f_{act}(T) \cdot S}{Q} = \frac{C_{max} f_{act}(T) S^{1/3}}{v\, k_1^{-2/3}} \tag{2.27}$$

Boundary conditions and initialization

The baseline simulation is forced with monthly average water temperature, recorded at l'Estartit, Catalan coast, over the period 1973 - 1997, (Cebrián et al. 1996, Fiorillo et al. 2013) and monthly average total Carbon, C_{tot} ,

measured at 20m depth above the benthic community, considered as a proxy for available food (Medes islands, Catalan coast, 1997 - 1998, Rossi and Gili 2005). Temperature recorded at 35m depth is used in most of the simulations. The initial value for $\bar{b}_P$ and N_P are set to 10^{-5} kJ and one polyp respectively whilst S_{carb}, S_{OM} and $\bar{b}_G$ initial values are set to zero. The simulation begins in August, when spawning usually takes place (Tsounis et al. 2006b).

Model calibration

Model calibration is performed on data sets where the three variables polyps number, colony weight and age were measured in red coral populations. The sets are from Santangelo et al. 2007 (13 data points averaged from a larger sample of 1802 colonies, polyps and age data, fig 4a, blue dots) and Priori et al. 2013 ($n = 69$ colonies, polyps, dry weight and age data, Fig. 2.2a, b and Fig. 2.3a, b, red dots). The two sets of accretion data reflect a number of red coral growth features. Santangelo et al. 2007 data, that were obtained from a single red coral population and for a rather large sample are very regular and point at exponential growth of the colony (via polyps gemmation) during at least the first decade of a colony's life. On the other hand Priori et al. 2013 data depict growth features that are highly dependent on life history traits, possibly microclimatic conditions and/or partial mortality events, to the point that no clear correlation emerges between age and polyps nor age and weight. If the two sets are compared, it can be inferred that the initial phase of exponential growth must cease as colony grows bigger, possibly due to competition for food and/or space between polyps of the same colony (Kim and Lasker 1998) and/or with neighbouring organisms, including red coral itself.

Given the variability of the calibration sets no single growth curve can satisfactorily approximate all the experimental data. Thus we assumed they represent the time trajectories of different colonies grew in different trophic conditions. The scope of parameterization was thus to fit the data against a set of model runs (that generate a growth surface in N_P, W_{Col}, time space), obtained by changing the flow speed v in eq. (2.27), This is equivalent to setting lower F_b values or decreasing polyps activity, or any other combination of factors that change the number G. The hypothesis we

tested with this approach is that local trophic conditions alone are capable of producing most of the observed variability in growth.

Model fitting is performed on eight selected uncertain parameters (α, β, k_F, $R_{b,max}$, $E_{s,max}$, $\bar{b}_{ss}$, $\bar{b}_{ah}$, k_1, see Tables 2.1, 2.2) with a monte carlo simulation. The algorithm minimizes of the sum of squared distances between each experimental point in N_P, W_{Col}, time space and the generated growth surface. The distances are computed on standardized data coordinates as units on N_P, W_{Col} and time axes are different. Both simulated and experimental data are standardized with mean and standard deviation of the experimental set to maintain the ratio between the two sets. Also The sum of the R_b and E_s terms is converted to oxygen consumption and confronted with the respiration rates measured in Previati et al. 2007. The sum of squared distance between measured and simulated respiration is also minimized by the fitting procedure.

Red coral grazing intensity

To estimate the grazing intensity of a typical red coral population we used data on age classes areal distribution from Santangelo et al., 2007 and the carbon intake rates per colony calculated by the model for the same age classes.

Suitability estimation

The calibrated model is also used to estimate the fundamental niche of red coral with respect to available food and temperature. We use the variation of coenenchyme biomass ($\bar{b}_P \cdot N_P$) over a time period t - t_0, ΔB_{coen}, as a proxy for organism-level fitness (Maltby 1999, Hoogenboom and Connolly 2009).

$$\Delta B_{coen} = \frac{N_P(t) \cdot \bar{b}_P(t) - N_P(t_0) \cdot \bar{b}_P(t_0)}{N_P(t_0) \cdot \bar{b}_P(t_0)} \tag{2.28}$$

ΔB_{coen} is computed over a range of (constant) temperatures and bulk food concentrations and for different colony sizes, defined by initializing the model with different $\bar{b_P}(t_0)$, $N_P(t_0)$ pairs from a baseline simulation. ΔB_{coen} is computed over 10 years as we are looking for long term effects on species distribution. The resulting zero ΔB_{coen} isoclines are indicative of fundamental niche borders in T, F_b space for the specified size class at a fixed flow speed. The model was coded in MatLab and the code is available from the authors upon request.

Parameter	Description	Value	Units	Source
n	scaling exponent	2/3	-	-
m	scaling exponent	1	-	-
α	b_{OM} allocation coefficient	0.1482	-	Estimated by the fitting procedure
β	$\bar{b}_P$ allocation coefficient	0.7606	-	Estimated by the fitting procedure
v	flow speeds	[0.8 : 4]	cm h^{-1}	-
k_1	shape coefficient	0.5191	cm^2 cm^{-3}	Estimated by the fitting procedure
$R_{b,max}$	max. respiration rate	0.1107	kJ g_{AFDM}^{-1} $month^{-1}$	Estimated by the fitting procedure
$E_{s,max}$	max. $CaCO_3$ energy allocation rate	0.0982	kJ cm^{-2} month	Estimated by the fitting procedure
C_{max}	max. assimilation rate	0.1408	kJ $month^{-1}$ cm^{-2}	Tsounis et al. 2006, Picciano & Ferrier-Pagès 2007
r_{max}	max. gemmation rate	2.664	y^{-1}	Fitted from Santangelo et al. 2007
x	allometric scaling exponent	0.563	-	Fitted from Santangelo et al. 2007
-	conversion coefficient	45.7	kJ g_C^{-1}	Brey 2001 and refs therein
-	molecular weight of O_2	3.2e4	mg mol^{-1}	-
-	oxyenthalpic equivalent	473	kJ mol_{O2}^{-1}	Gnaiger, 1983
ε	biomass energy content	27.203	kJ g_{AFDM}^{-1}	Brey 2001 and refs therein
e	$CaCO_3$ metabolic cost	0.152	kJ g_{CaCO3}^{-1}	Anthony et al. 2002

Table 2.2 Model parameters values and conversion coefficients and relative sources.

2.3 Results

Fitting to experimental data, polyps and colony weight

The model generates growth trajectories (a growth surface in N_P, W_{Col}, time space, Fig. 2.2a, b and Fig. 2.3a, b) that approximate most of the calibration data points just by varying flow speed (or equivalently G). This result is in line with the conjecture, suggested by calibration sets and expert's opinions, that colonies accretion depends strongly on the local environment and point at hydrodynamic and trophic conditions as major factors affecting colonies growth.

Polyps population dynamics(Fig 2.3a) follow an initial phase of exponential growth that closely matches Santangelo et al. 2007 data for high flow speeds. This exponential growth is dampened as N_P increases, as it can be also inferred from the experimental data. This behaviour is due to decreasing $\bar{b}_P$ with age, negatively affecting the f_{gem} function that controls gemmation rate.

Whole colony mass is mostly composed of $CaCO_3$. New skeleton is produced trough all the lifetime, the simulated growth curves (Fig. 2.3b) are initially exponential but approach linearity as $\bar{b}_P$ decreases with age.

Features of live tissue growth

The simulated live tissue ($\bar{b}_P$) shows a marked seasonal cycle (Fig. 2.3c, d): positive growth lasts approximately from January to June, when energy gain exceeds losses, and is followed by a negative growth phase from approximately July to December. This effect depends strongly on temperature regimes affecting both the gain and loss terms and on seasonality of food supply. In fact the biomass seasonal cycle is more marked when the model is forced with temperature records from relatively shallow (up to 35m) waters, that are characterized by wide temperature variations; Biomass oscillations are instead dampened if the less variable deep waters records (50 to 80m) are used to force temperature (not shown).

The same seasonality is present also in skeletal organic matter, S_{OM} (Fig 2.2d), and gametes, $\bar{E}_G$, dynamics.

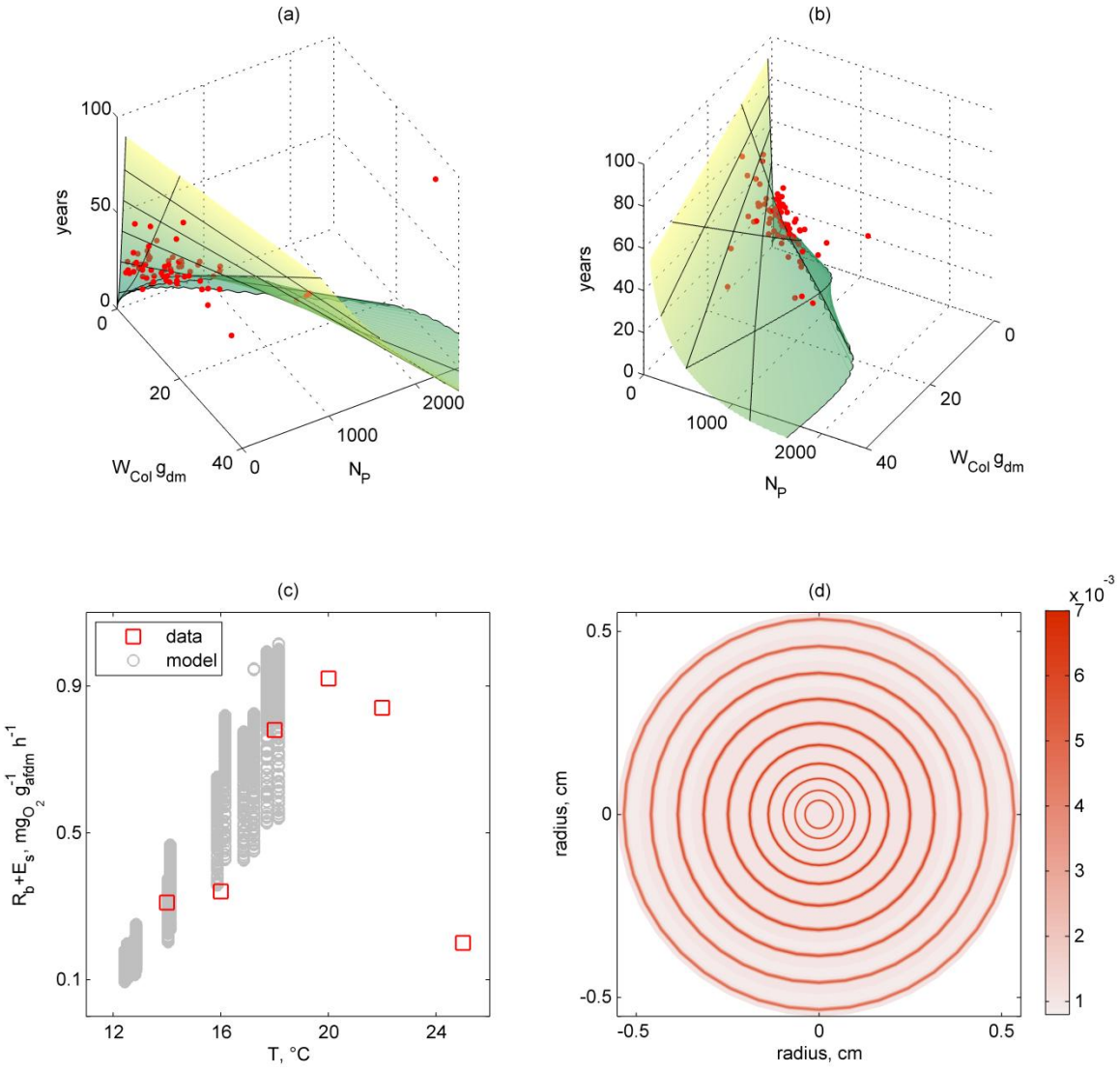

Fig. 2.2 Model results and fitting. (a),(b): two views of the colony growth surface, model results (green surface) and experimental data (red dots, Priori et al. 2013). (c): Total respiration, gray circles: model results, red squares: data from Previati et al. 2010. (d): Representation of skeletal banding as a stylized branch cross section, colorbar units are OM weight over total skeleton weight ($S_{OM} + S_{carb}$).

The single polyp (Fig. 2.3c) and gametes (not shown) simulated growth trajectories are characterized by a maximum within the first decade of life, followed by an exponential decay with an horizontal asymptote reached after about 20-30 years. The position of the maximum varies depending on external conditions (feeding, temperature). Two major processes contribute to this pattern. One concerns the trophic shading effects that limit food intake per polyp for high polyps number, resulting in decreasing E_P and E_G after the maximum; the other concerns f_{gem} limiting polyps gemmation at low E_p, thus slowing down biomass decrease.

Coenosarc and gametes biomass per colony ($= N_P \cdot \bar{b}_P$ and $N_P \cdot \bar{b}_G$ respectively, Fig 2.3d, gametes dynamics not shown) are characterized by determinate growth. Decreasing growth rates with colony size are mostly due to polyps population dynamics via f_{gem} that limits new polyps production at low $\bar{b}_p$ and is thus closely tied to the $\bar{b}_P$ evolution.

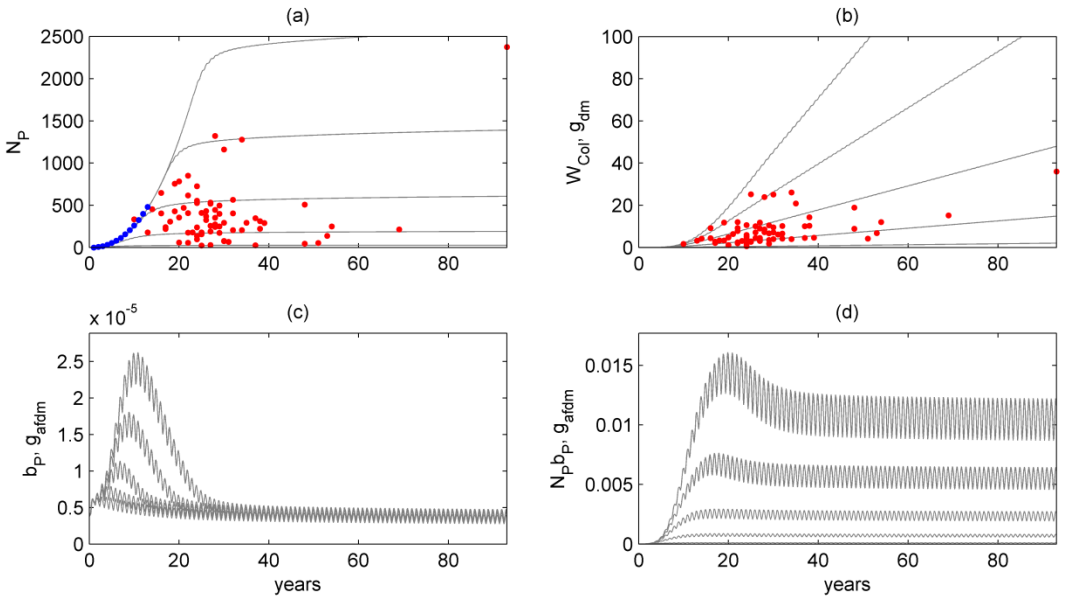

Fig. 2.3 Simulation results (multiple runs with varied v). red dots: experimental data from Priori et al. 2013, blue dots: data from Santangelo et al. 2003. (a): Polyps number. (b): Colony weight (skeleton and organic tissues). (c): Average polyp weight. (d): Coenosarc biomass ($=N_P\bar{b}_P$).

Features of skeleton growth

$CaCO_3$ deposition (Fig. 2.2d) also follows a seasonal pattern but with reverse order with respect to organic tissues, including E_{OM}. Most of the skeleton is deposited during the warmer period, when the E_s term is maximum due to high temperatures. And whilst live tissue growth slows down as a result of the balance between energetic intake and losses, the skeleton grows at a mostly constant pace.

The model simulates the differential incorporation of $CaCO_3$ and organic matter in the coral skeleton described in Marschal et al. 2004. During cold months environmental conditions are favourable for tissue growth, hence much organic matter is deposited whilst $CaCO_3$ flux is low due to low respiration rates; since organic matter flux is larger than $CaCO_3$ flux, this results in the deposition of little material (thin band), relatively rich in organic matter. On the contrary during warm months trophic conditions are poor and little organic matter is produced whilst $CaCO_3$ flux is high due to high respiration rates, resulting in the deposition of a thick band poor in organic matter. The average proportion of S_{OM} to S_{carb} in the skeleton is underestimated with respect to the values reported in Allemand and Tambutté 1996 (0.012 - 0.017).

Suitability Plots/ Niche estimation

As far as fundamental niche estimation is concerned (Fig. 2.4) our model predicts that smaller colonies have potential for positive growth over a wider region in F_b -T space than large colonies do, especially at low food concentrations. This means a large colony is more demanding in terms of food requirements to sustain its size when temperatures are also high, whilst small colonies can thrive over a broader range of conditions. In Fig. 2.4 the zero isocline ($\Delta B_{coen} = 0$) is indicative of the niche borders for different size classes and, unlike the rest of the isoclines, its position is not affected by the time window over which ΔB_{coen} is computed.

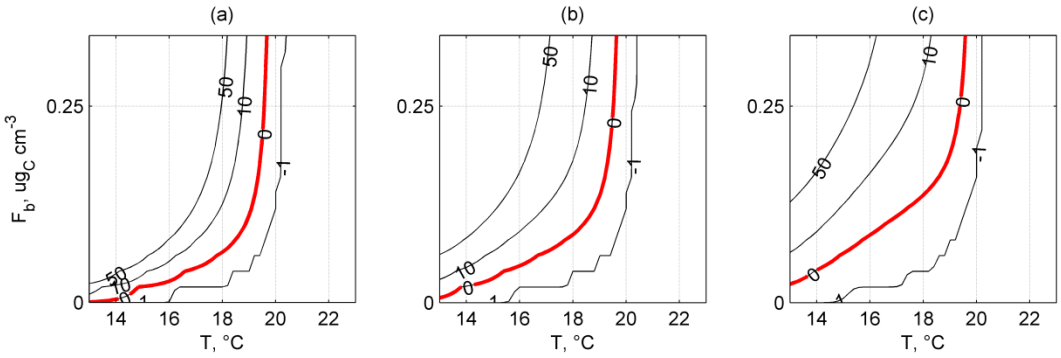

Fig. 2.4 Suitability diagrams computed as coenenchyme biomass change (ΔB_{coen}) over 10 y simulation. ΔB_{coen} values are plotted against different temperatures and bulk food concentrations, at fixed flow speed ($v = 3.03$ cm h^{-1}) and for different colony sizes. (a): small colony: 11 polyps, 0.1e-4 g_{afdm}/polyp, (b): medium colony: 70 polyps, 0.2e-4 g_{afdm}/polyp, (c): large colony: 847 polyps, 0.05e-4 g_{afdm}/polyp). The zero isoclines (in red) represent the distribution limits for the specified colony size. Other isoclines are merely indicative of trends as their position depends on simulation time.

Grazing Intensity

The estimated grazing intensity of a typical red coral shallow population composed mainly of relatively young colonies, such as the one sampled in Santangelo et al., 2007 is of 0.17 mg_C m^{-2} d^{-1} which is within the range estimated in Tsounis et al., 2006b (0.15 - 1.5 mg_C m^{-2} d^{-1}).

2.4 Discussion

In the present work we developed a colony growth model to better understand the influence of environmental variables, temperature, food concentration, hydrodynamic regime, on the accretion of C. rubrum colonies. We produced simulations that match measured growth patterns as well as multiple observed features of red coral development and of its

interactions with the environment. Furthermore the model allows for the interpretation of those features in the light of red coral metabolic organization. The originality of the approach lies in the choice of modelling C. rubrum as a colony of individuals, where single polyp and colony dynamics influence each other and the outcomes emerge from the interplay of the two.

Niche Estimation

By using growth potential as a proxy for organism well-being, we derived an estimation of red coral requirements, in terms of average water temperature and food concentration, to sustain positive growth, i.e. its fundamental niche in temperature-food space.

We found the limits of C. rubrum distribution (as identified by the zero-growth isoclines in Fig. 2.4) to be dependent on colony size: large colonies are more demanding than small ones with regard to temperature and food availability. These findings may help explain the observations made by Garrabou et al. (2001) that medium and large-sized colonies of *C. rubrum* from shallow waters suffered higher mortality incidence than small ones during a mass mortality event that occurred jointly with a positive temperature anomaly and summery food shortage.

Results also have implications regarding the size distribution of red coral colonies: as noted by many, shallow populations are usually composed of crowded patches of small individuals while larger colonies are found at higher depths (Santangelo & Bramanti, 2010; Garrabou et al., 2001, 400-600 colonies/m^2 and Tsounis et al., 2006a, 150-250 colonies/m^2 in shallow waters, compared to Priori et al., 2013 and Rossi et al., 2008, 10-50 colonies/m^2 in deep waters); this appears to be primarily a consequence of overharvesting of the shallow, easily accessible populations that selectively removes the large specimens (Santangelo and Bramanti 2010). Our findings indicate that large colonies are also more likely to undergo negative growth in shallow waters, where they experience both high temperatures and food shortage at the same time during late summer, and are thus less likely to be found near the upper limits of C. rubrum distribution. A similar size gradient with small individuals dominating the upper distributional limit has been reported by Sebens (2002) concerning the distribution of sea

anemones in relation to environmental parameters. If this temperature effect on size distribution is superimposed to the harvesting effect, large colonies occurrence could be further limited to elevated depths as mean sea temperatures increase. Increasing trend of harmful heat waves events will also increase this risk.

Differently Hoogenboom and Connolly (2009) found that the niche size of reef corals in flow-light space, as calculated with a process-based model, was positively related to colony size. Hogenboom and Connolly model uses daily integrated energy acquisition (photosynthesis) as a proxy for fitness, but since organism energy budget is not computed, it is not possible to assess if such rate is enough to sustain positive growth across different colony sizes; also size dependence of photosynthesis rate is calculated solely according to mass exchange kinetics from fluid mechanics theory, thus neglecting possible trophic shading effects, which the authors aknowledge.

For the sake of simplicity we imposed a fixed fraction of growth to be devolved to gametes development over a colony's life. Numerous studies (Tsounis et al., 2006a; Cupido et al., 2012; Priori et al., 2013) found fertility (gametes size/number per polyp) to be positively related to colony size in different Mediterranean gorgonians, including red coral. This suggests a greater energetic investment in reproductive output for the bigger specimens. The hereby predicted summery budget deficit issues may thus be further exacerbated in large colonies due to increased spawning investments.

Seasonality, trophic shading and constraints to growth

The simulated live tissue biomass displays seasonal cycles of positive and negative growth which are strongly dependent on temperature regimes and are thus more marked when the model is forced with shallow waters thermal records. Similarly Rossi and Tsounis 2007 and Tsounis et al. 2006b uncovered a seasonality in energy storage molecules concentrations (proteins, carbohydrates, lipids) and gametes development in shallow (16-18 m) red coral colonies, whilst in deep populations (45m) seasonality was detectable only for proteins and gametes development. The same seasonal pattern is also typical of other Mediterranean colonial benthic invertebrates

(Coma et al., 1994 and 1998) and appears to be related to NW Mediterranean climatology.

The simulated evolution of the whole colony live tissue biomass (Fig. 2.3d) is indicative of determinate growth, i.e. there exists an upper limit to colony size. The point is not trivial, in fact it is generally assumed that colony resource acquisition is simply a linear function of the number of modules, colonies would thus be free from the constraints that limit the size of the single modules and could growth indefinitely, simply adding new modules (Sebens, 1987). It is presently unclear whether colonial organisms are determinate or indeterminate growers, but data red coral size and age classes distribution (Priori et al. 2013) show that red coral has the characteristics of constrained growth.

In our model colony size limits, instead of being imposed with allometric constraints (as done in Kim and Lasker 1998), emerge as a consequence of trophic sahding, i.e. the competition for a limited resource (food) between the polyps of a same colony. This is in line with the argument found in Kim and Lasker 1998 that density dependent effects on resource capture rates, analogous to self shading in trees, may effectively limit maximal size in modular species that would otherwise exhibit indeterminate (exponential) growth. We also found that this result is not generally extendable to any colonial organism as the assumption in eq. (2.26) does not apply to any growth shape (e.g. it does not apply for a sphere), and will result in uptake rates that scale linearly with modules number, hence in unconstrained growth, for massive growth forms. Our implementation provides thus a theoretical background for a conjecture (the existence and relevance of trophic shading phenomena and their implications for growth determinacy or indeterminacy in colonial and modular organisms) that to date rests on anecdotal evidence and speculative arguments.

The model predicts the average polyp biomass to decrease with age once a maximal value is reached early in life as a result of competition between polyps. In support of our findings an inverse relationship between the two quantities have been described by Porter (1976) for Caribbean corals; Kim and Lasker (1998) proposed that such negative correlation can result from the additive effects of module size and colony size on self-shading and thus the ability of a colony to capture resources.

Features of Skeletal growth

Despite current research is increasingly shedding light on the processes involved in biomineralization, the present understanding of the mechanisms of integration between coral major metabolic processes and skeleton formation remains very weak (Allemand et al. 2013). In the present work we addressed this issue by relating skeleton formation to coral energy budget with the fraction of metabolism devoted to calcite deposition and the (proposed) energetic cost required per unit of $CaCO_3$ deposited. This modelling choice has been proven effective in reproducing observed patterns. At the same time it remains thrifty with respect to assumptions and parameters requirements, relatively to the finer-scale modelling approaches to biocalcification found in Hohn and Merico 2012 and Nakamura et al. 2013. Our approach aims at modelling calcified structures growth at whole organism level and can be considered as a simplification of such models.

Skeletal growth modelling choices are similar to those in Fablet et al. (2011) and Pecquerie et al. (2012). In such works, and in this one as well, the temperature dependences affecting skeletal deposition are those affecting the relevant physiological rates and temperature effects on $CaCO_3$ precipitation kinetics are neglected. The question whether inorganic deposition kinetics that are observed in seawater stay valid in the gel-like extracellular calcifying medium is currently debated (Allemand et al. 2013). However, the observation that the most of the $CaCO_3$ (the thick bands in the skeleton) is laid down during the warmest months, is easily linked to inorganic $CaCO_3$ precipitation being favoured at high temperatures (Zeebe and Wolf-Gladrow 2001). Our study suggests an alternative, perhaps complementary, mechanism for the observed seasonality in $CaCO_3$ deposition. Also the underestimation of the proportion of OM to $CaCO_3$ in the skeleton may suggest that the mechanism of OM incorporation is not entirely passive, as implemented here, in fact many studies (see Tambutté et al. 2007 for a review) suggest that OM plays a structural role in skeleton formation, so that the two fractions should obey some kind of stoichiometric law.

Whilst live tissue growth slows down with age, our results point at indeterminate skeletal growth, seemingly leading to the unrealistic condition of the coenosarc getting thinner and thinner over a colony's life. This could have been changed by lowering energy allocation to skeleton as

colony grows, this fix however seemed too much of an artefact. Indeed constant basal diameter growth rates have been observed in red coral by Santangelo et al. (2007), Priori et al. (2013), Bramanti et al. (2014) over wide sets of ages, and Bramanti et al. (2014) found the surface area increment in C. rubrum skeleton cross sections to be well fitted by a linear equation, indicating constant increment along colony life span. Other explanations are possible: 1. the coenosarc thinning actually happens but is so slow it isn't such a big deal over a colony's lifespan. 2. additional cortex mineralization compensates for coenosarc thinning; in fact Weinbauer et al. (2000) reported levels of cortex mineralization as high as 76±6% on weight basis for red coral.

Our model agrees with observations by Marschall et al. (2004) in placing maximal $CaCO_3$ deposition during the warm months, when biomass, on the contrary, displays negative growth. The same seasonal pattern has been described by Rodolfo-Metalpa et al. (2009) in the Mediterranean coral *Cladocora Caespitosa*. Although seemingly paradoxical, weak coupling between tissue and calcified structures growth is known to occur in bivalves (Hilbish 1989), fish otoliths (Neat et al. 2008) and has been reported for scleractinian corals by Anthony et al. (2002) that measured positive skeletal growth rates even in experimental treatments where tissue growth was negative.

Even though $CaCO_3$ deposition is regarded as energetically cheap (Palmer 1992, Anthony et al. 2002, McCulloch et al. 2012), it clearly entails some metabolic cost for the coral. We suggest that Skeletogenesis is sustained during energy shortage times at the expenses of the reserves accumulated during the previous favourable period.

2.5 References

Allemand D., Bénazet-Tambutté S. 1996. Dynamics of Calcification in the Mediterranean Red Coral, Corallium rubrum (Linnaeus) (Cnidaria, Octocorallia). The Journal of Experimental Zoology, 276, 270-278.

Allemand D., Tambutté É., Zoccola D., Tambutté S. 2013. Coral calcification, cells to reefs. In Coral reefs: An ecosystem in transition, Springer Netherlands. pp 119-150.

Anlauf H., D'Croz L. O'Dea A. 2011. A corrosive concoction: The combined effects of ocean warming and acidification on the early growth of a stony coral are multiplicative. Journal of Experimental Marine Biology and Ecology 397, 13-20.

Anthony K. R. N., Connolly S. R. Hoeg-Guldberg O. 2007. Bleaching, energetics, and coral mortality risk: Effects of temperature, light, and sediment regime.Limnol. Oceanogr., 52(2), 716-726.

Ballesteros E. 2006. Mediterranean coralligenous assemblages: a synthesis of present knowledge. Oceanogr. Marine Biology Annual Reviews 44 , 23-195.

Bramanti L., Magagnini G., DeMaio L., Santangelo G. 2005. Recruitment, early survival and growth of the Mediterranean Red Coral Corallium rubrum (L 1758), a four-year study. J. Exp. Mar. Biol. Ecol. 314, 67–78.

Bramanti L., Iannelli M., Santangelo G. 2009. Mathematical modelling for conservation and management of gorgoniancorals: young and olds, could they coexist? Ecological Modelling220, 2851-2856.

Bramanti, L., Movilla, J., Guron, M., Calvo, E., Gori, A., Dominguez-Carrió, C., Grinyó, J., Lopez-Sanz, A., Martinez-Quintana, A., Pelejero, C., Ziveri, P., Rossi, S. 2013. Detrimental effects of Ocean Acidification on the economically important Mediterranean red coral (Corallium rubrum). Blackwell Publishing Ltd (2013), Article in press.

Brey T. 2001. Population dynamics in benthic invertebrates. A virtual handbook. Version 01.2. http://www.thomasbrey.de/science/virtualhandbook

Cebrián J., Duarte C.M., Pascual J. 1996 Marine climate on the Costa Brava (northwest Mediterranean) littoral. Publ. Espec. Inst. Oceanogr. 22, 9-21.

Cerrano C., Cardini U.,Bianchelli S., Corinaldesi C., Pusceddu A., Danovaro R. 2013. Red coral extinction risk enhanced by ocean acidification. Scientific reports, 3, 1457,doi:10.1038/srep01457

Cerrano C, Bavestrello G, Bianchi CN, Cattaneo-Vietti R, Bava S, Morganti C, Morri C, Picco P, Sara G, Siccardi A, Sponga F. 2000. A

catastrophic mass-mortality episode of gorgonians and other organisms in the Ligurian Sea (Northwestern Mediterranean), summer 1999. Ecology Letters, 3, 284-293.

Chindapol N., Kaandorp J.A., Cronemberger C., Mass T., Genin A. 2013 Modelling Growth and Form of the Scleractinian Coral Pocillopora verrucosa and the Influence of Hydrodynamics. PLoS Comput Biol 9(1): e1002849. doi:10.1371/journal.pcbi.1002849

Coma R., Gili J.M., Zabala M., Riera T. 1994. Feeding and, prey capture cycles in the aposymbiotic gorgonlan Paramuricea clavata. Mar. Ecol. Prog. Ser., 1152, 57-270.

Coma R., Ribes M., Gili J.M., Zabala M. 1998. An energetic approach to the study of life-history traits of two modular colonial benthic invertebrates. Mar. Ecol. Prog. Ser., 162, 89-103.

Coma R., Ribes M., Serrano E., Jimenéz E., Salat J., Pascual J. 2009. Global warming-enhanced stratification and mass mortality events in the Mediterranean. PNAS 106/15, 6176-6181.

Cupido R., Cocito S., Bordone A., Santangelo G. 2008. Response of a gorgonian (Paramuricea clavata) population to mortality events: recovery or loss? Aquatic Conserv.: Mar. Freshw. Ecosyst. 18, 984-992.

Cupido R., Cocito S., Manno V., Ferrando S., Peirano A., Iannelli M., Bramanti L., Santangelo G. 2012. Sexual structure of a highly reproductive, recovering gorgonianpopulation: quantifying reproductive output. Marine Ecology Progress Series. 469, 25-36.

Fablet R., Pecquerie L., de Pontual H., Høie H., Millner R., Mosegaard H., Kooijman S. A. L. M. 2011. Shedding Light on Fish Otolith Biomineralization Using a Bioenergetic Approach. PLoS ONE 6(11): e27055. doi:10.1371/journal.pone.0027055.

Fabry, V. J., Seibel, B. A., Feely, R. A., and Orr, J. C. 2008. Impacts of ocean acidification on marine fauna and ecosystem processes. – ICES Journal of Marine Science, 65, 414-432.

Fabricius K. E., Langdon C., Uthicke S., Humphrey C., Noonan S., De'ath G., Okazaki R., Muehllehner N., Glas M. S., Lough J. M. 2011. Losers and winners in coral reefs acclimatized to elevated carbon dioxide concentrations. Nature climate change, 1, 165-169.

Fiorillo I., Rossi S., Gili J.M., Alvà V., López-González P.J. 2013. Seasonal cycle of sexual reproduction of the Mediterraneansoft coral Alcyonium acaule (Anthozoa, Octocorallia). Marine Biology, 160, 719-728.

Garrabou J., Harmelin G. 2002. A 20-year study on life-history traits of a harvested long-lived temperate coral in the NW Mediterranean: insights into conservation and management needs. Journal of Animal Ecology, 71, 966-978.

Garrabou, J., Perez, T., Santoretto, S., Harmelin, J.G., 2001. Mass mortality event in red coral Corallium rubrum populations in the Provence region (France, NW Mediterranean). Mar. Ecol. Prog. Ser. 217, 263-272.

Gneiger E. 1983. Calculaton of energetic and biochemical equivalents of respiratory oxygen consumption. In Gnaiger, E., Forstner, H. (eds): Polarographic oxygen sensors. Springer, Berlin.

Heitzer A., Kohler H. E., Reichert P., Hamer G. 1991. Utility of Phenomenological Models for Describing Temperature Dependence of Bacterial Growth. Applied and environmental Microbiology, 57(9), 2656-2665.

Hilbish T. 1986. Growth trajectories of shell and soft tissue in bivalves: Seasonal variation in Mytilus edulis L. J. Exp. Mar. Biol. Ecol. 96, 103-113.

Hoeg-Guldberg O. 1999. Climate change, coral bleaching and the future of the world's coral reefs. Marine and Freshwater Research 50(8), 839-866 .

Hohn S., Merico A. 2012. Modelling coral polyp calcification in relation to ocean acidification. Biogeosciences, 9, 4441–4454.

Holcomb M. C., McCorkle D. C., Cohen A. L. 2010. Long-term effects of nutrient and CO2 enrichment on the temperate coral Astrangia poculata (Ellis and Solander, 1786). J Exp Mar Biol Ecol. 386, 27-33.

Houlbrèque F., Tambutté E., Allemand D., and Ferrier-Pagès C. 2004. Interactions between zooplankton feeding, photosynthesis and skeletal growth in the scleractinian coral Stylophora pistillata. The Journal of Experimental Biology 207, 1461-1469.

Hoogenboom M. O., Connolly S. R. 2009. Defining fundamental niche dimensions of corals: synergistic effects of colony size, light, and flow. Ecology, 90-3, 2009, 767-780.

Jokiel, P. L. 2011. Ocean acidification and control of reef coral calcification by boundary layer limitation of proton flux. Bullettin of marine science. 87-3, 639-657.

Kim, K. and H. R. Lasker. 1998. Allometry of resource capture in colonial cnidarians and constraints on modular growth. Funct. Ecol. 12, 646-654.

Kooijman S. A. L. M. 2010. Dynamic Energy Budget theory for Metabolic Organisation. Cambridge University Press.

Maltby L. 1999. Studying stress: The importance of organism level responses. Ecol. Appl., 9, 431-440.

Marschal C., Garrabou J., Harmelin J.G., Pichon M., 2004. A new method for measuring growth and age of the precious red coral Corallium rubrum (L). Coral Reefs 23, 423–432.

McCulloch M., Falter J., Trotter J., Montagna P. 2012. Coral resilience to ocean acidification and global warming through pH up-regulation. Nature Climate Change 2, 623-627.

MerksR.M.H., HoekstraA.G., Kaandorp J.A., Sloot P.M.A. 2004. Polyp Oriented Modelling of Coral Growth. Journal of Theoretical Biology, 228, 559-576.

Nakamura T., Nadaoka K., Watanabe A. 2013. A coral polyp model of photosynthesis, respiration and calcification incorporating a transcellular ion transport mechanism. Coral Reefs 32, 779-749.

Neat F.C., Wright P., Fryer R.J. 2008. Temperature effects on otolith pattern formation in Atlantic cod Gadus morhua. J Fish Biol 73, 2527-2541.

Pecquerie L., Fablet R., de Pontual H., Bonhommeau S., Alunno-Bruscia M., Petitgas P., Kooijman S. A. L. M. 2012. Reconstructing individual food and growth histories from biogenic carbonates. Marine ecology progress series, 447, 151-164.

Perez, T., Garrabou, J., Sartoretto, S., Harmelin, J.G., Francour, P. & Vacelet, J. 2000. Mortalité massive d'invertébrés marins: un événement sans précédent en Méditerranée nord-occidentale. Comptes Rendus de l'Académie des Sciences Série III, Life Sciences 323, 853-865.

Picciano M. Ferrier-Pagès C. 2007. Ingestion of pico- and nanoplankton by the Mediterranean red coral Corallium rubrum. Marine Biology, 150, 773-782.

Porter J.W. 1976. Autotrophy, heterotrophy, and resource partitioning in Caribbean reef-building corals. American Naturalist 110, 731-742.

Pörtner, H. O. 2008. Ecosystem effects of ocean acidification in times of ocean warming: a physiologist's view. Marine ecology progress series. 373, 203-217.

Previati M, Scinto A, Cerrano C, Osinga R. 2010. Oxygen consumption in Mediterranean octocorals under different temperatures. Journal of Experimental Marine Biology and Ecology 390, 39-48.

Priori C., Mastascusa V., Erra F., Angiolillo M., Canese S., Santangelo G. 2013. Demography of deep-dwelling red coral populations: Age and reproductive assessment of a high valuable marine species. Estuar. Coast. Shelf Sci. 118, 43-49.

Rodolfo-Metalpa R. 2009. Response of the temperate coral Cladocora caespitosa to mid- and long-term exposure to pCO2 and temperature levels projected in 2100. Biogeosciences Discuss., 6, 7103–7131.

Rossi S. Gili J. M. 2005. Composition and temporal variation of the near-bottom seston in a Mediterranean coastal area. Estuarine coastal and

shelf science. 65, 385-395.

Rossi S.,Gili J.M., Coma R., Linares C., Gori A., Vert N. 2006 Seasonal cycles of protein, carbohydrate and lipid concentrations in Paramuricea clavata: (anthozoa, octocorallia): evidences for summer-autumn feeding constraints. Marine Biology 149, 643-651.

Rossi S., Tsounis G. 2007. Temporal and spatial variation in protein, carbohydrate, and lipid levels in Corallium rubrum (Anthozoa, Octocorallia). Marine Biology 152, 429-439.

Santangelo, G., Abbiati, M., 2001. Red coral: conservation and management of an overexploited Mediterranean species. Aquat. Conserv. Mar. Freshwater Ecosyst. 11, 253-259.

Santangelo G., Carletti E., Maggi E., Bramanti L.2003. Reproduction and population sexual structure of the overexploitedMediterranean red coral Corallium rubrum. Mar Ecol Prog Ser 248, 99-108.

Santangelo G, Bramanti L, Iannelli M (2007) Population dynamics and conservation biology of the over-exploited Mediterranean Red coral. J Theor Biol. 244, 416-423.

Santangelo G., Bramanti L. 2010. Quantifying the decline in Corallium rubrum populations. Marine Ecology Progress Series, 418, 295-297.

Santangelo G., Cupido R., Cocito S., Bramanti L., Tsounis G., Iannelli M. 2013. Demography of long-lived octocorals: survival and local extinction. Proceedings of the 12th International Coral Reef Symposium, Cairns, Australia, 9-13 July 2012.

Sebens K. P. 1980. The regulation of asexual reproduction and indeterminate body size in the anemone Anthopleura elegantissima (Brandt). Biol. Bull. 158, 370-382.

Sebens K. P. 2002. Energetic Constraints, Size Gradients, and Size Limits in Benthic Marine Invertebrates. Integ. and Comp. Biol., 42, 853-861.

Solidoro C., Pastres R., Melaku Canu D., Pellizzato M., Rossi R. 2001. Modelling the growth of Tapes philippinarum in Northern Adriatic lagoons. Mar. Ecol. Prog. Ser. 199, 137-148.

Solidoro C., Melaku Canu D., Rossi R. 2003. Ecological and economic considerations on fishing and rearing of Tapes phillipinarum in the lagoon of Venice. Ecological modelling 170, 303-318.

Tambutté S, Tambutté É, Zoccola D, Allemand D. 2007. Organic matrix and Biomineralization of scleractinian corals. In: Baeuerlein E (ed) Handbook of Biomineralization: Biology aspects and Structure Formation. Wiley-VCH, pp 243-259

Tsounis G., Rossi S., Laudien J., Bramanti L., Fernández N., Gili J-M., Arntz W. 2005. Diet and seasonal prey capture rates in the Mediterranean red coral (Corallium rubrum L.). Marine Biology 149-2,

313-325.

Tsounis G., Rossi S., Gili J.M., Arntz W. 2006a. Population structure of an exploited benthic cnidarian: the red coral case study. Marine Biology 149, 1059-1070.

Tsounis G., Rossi S., Aranguren M., Gili J.M., Arntz W.E. 2006b. Effects of spatial variability and colony size on the reproductive output and gonadal development cycle of the Mediterranean red coral (*Corallium rubrum* L.). Marine Biology 148, 513-527.

Tsounis G., Rossi S., Grigg R.W., Santangelo G., Bramanti L., Gili J.M. 2010. The Exploitation and Conservation of Precious Corals. Oceanography and Marine Biology Annual Review 48, 161-212.

Tsounis G., Rossi S., Bramanti L., Santangelo G. 2013. Management hurdles in the sustainable Management of *Corallium rubrum*. Marine Policy 39: 361-364.

Torrents O., Tambutté E., Caminiti N., Garrabou J. 2008. Upper thermal thresholds of shallow vs. deep populations of the precious Mediterranean red coral *Corallium rubrum* (L.): Assessing the potential effects of warming in the NW Mediterranean. Journal of Experimental Marine Biology and Ecology 357, 7-19

Vielzeuf, D., Garrabou, J., Baronnet, A., Grauby, and Marschal, C. (2008) Nano to macroscale biomineral architecture of red coral (Corallium rubrum). American Mineralogist, 93, 1799–1815.

Vighi M., 1972. Étude sur la reproduction du Corallium rubrum (L.). Vie Milieu vol XXIII fase 1, sér A, 21-32

von Bertalanffy, L. 1938. A quantitative theory of organic growth. Hum. Biol. 10, 181-213.

Weinbauer M. G., Brandstätter F., Velimirov B. 2000. On the potential use of magnesium and strontium concentrations as ecological indicators in the calcite skeleton of the red coral (*Corallium rubrum*). Marine Biology 137, 801-809.

Zeebe, R.E., Wolf-Gladrow, D.A. 2001. CO_2 in Seawater: Equilibrium, Kinetics, Isotopes, Vol. 65 of Elsevier Oceanography Book Series, Elsevier, Amsterdam, 1st Edn.

3. Biologically mediated and abiotic mechanisms for light enhanced calcification (LEC) and the cost of carbonates deposition in corals.

Abstract

Zooxanthellate corals are known to increase calcification rates under the light, a phenomenon called light enhanced calcification, that is believed to be mediated by symbionts photosynthetic activity. There is a lot of controversy on the mechanism behind this phenomenon with hypotheses coarsely divided between abiotic and biologically mediated mechanisms. At the same time evidence is building up that calcification in corals relies on active ion transport to deliver the skeleton building blocks into the calcifying medium, hence it is a costly activity.

Here we build on generally accepted conceptual models of the coral calcification machinery and of the energetics of coral-zooxanthellae symbiosis to develop a model that can be used to separate the biologically mediated and abiotic effects of metabolic rates (respiration and photosynthesis), temperature and seawater chemistry.

We tested this model on a dataset relative to the Mediterranean scleractinian *Cladocora caespitosa* (an acidification resistent species) and we conclude that most of the variation in calcification rates due to photosynthesis and temperature can be attributed to biologically mediated mechanisms, in particular to the metabolic energy supplied to the active ion transports. Abiotic effects are also present but of smaller magnitude, though they could be more relevant for acidification sensitive species.

Based on these findings and on a literature review we suggest that the energetic aspect of coral calcification has been so far overlooked, and that a key parameter that should be measured in order to test this is the metabolic cost of calcification.

3.1 Introduction

As argued by Pörtner (2008), marine organisms sensitivity to acidification is a matter of several physiological processes being concomitantly affected. Despite the huge research effort seen in recent years, the effects of seawater chemistry on marine calcifiers remains an elusive topic, as stated by Allemand et al. (2011) in an extensive review on coral calcification; that review opens with two quotes, written almost one century apart by scientists engaged with coral calcification:

A question which has common interest both for zoologist and palaeontologist is the relation of the soft parts of the polyp to the hard calcareous or horny skeleton produced in most corals. (Ogilvie 1896)

The poor understanding of calcification mechanisms in corals results from a lack of information on tissue / skeleton interactions and temporal / spatial patterns in skeleton morphogenesis. (Le Tissier 1987)

Both these authors recognize that the key to understand biocalcification lies in the interactions between the living parts of the coral and the skeleton, an aspect that is currently often overlooked in many research studies.

Few doubts exist coral calcification is an energy demanding process. Corals, trough their metabolism, allocate some part of the energy budget they obtain from food and photosynthesis to calcification (Dubinsky & Jokiel 1994), and convert it to calcium carbonate. The conversion rate (in the economic sense) of energy invested to calcium carbonate deposited is the [unitary] metabolic cost of calcification.

Jokiel (2011) proposed that the observed effects of acidified seawater on coral calcification are mediated by diffusion limitation of net H^+ transport away from the coral. This is equivalent to the argument from Cohen & Holcomb (2010) that under acidified conditions corals must spend more energy to remove protons from the calcifying medium in order to maintain calcification rates. These arguments point at an increase in the cost of calcification under acidified conditions.

Many studies make use as input parameter proposed metabolic costs of calcification (Anthony et al. 2002; McCulloch et al. 2012). The exact value of such cost is in fact unknown (Allemand et al. 2011). The only experimental estimate to date was carried out by Palmer (1992) on a mollusk and yielded an estimated cost of 100 to 200 kJ/mol. More recently the cost of calcification has been identified with the difference in chemical potential between coelenteron and ECM (about 3-6 kJ/mol, McCulloch et al. 2012), the Gibbs free energy of ATP hydrolysis coupled with membrane transport proteins stoichiometry (about 30 kJ/mol, Anthony et al. 2002) or the Gibbs free energy of ATP hydrolysis coupled with membrane transport proteins stoichiometry and other transport mechanisms (about 20 kJ per mol, Hohn & Merico 2015). Though these estimates fall short in that they do not account for the inefficiencies that any real life transport process entails and so can result in unphysical behaviors. Furthermore it could be argued that if the cost of building one mole of skeleton was that low, calcifiers would face little trouble in compensating for acidification effects.

To understand how much energy is needed per amount of skeleton it is crucial to understand how the coral allocates energy to calcifiction. The problem is not trivial as it involves both the coral host physiological activity and that of its algal symbionts which are also involved in the phenomenon of light enhanced calcification (LEC). Higher calcification rates (3x on average, Gattuso et al. 1999) are consistently observed during daytime and this effect is believed to be mediated by symbionts photosynthetic activity (Gattuso et al. 1999; Allemand et al. 2011). LEC is an highly debated topic and various non mutually exclusive hypotheses exist (reviewed in Gattuso et al. 1999). All the hypotheses can be coarsely grouped into the two categories of biologically mediated and abiotic mechanisms.

Three major environmental parameters are believed to play crucial roles in calcification: seawater chemistry, temperature and light. All three of these parameters are believed to act in a two-fold fashion on the process of calcification with biologically mediated and abiotic effects: light bears a clear relation with photosynthetic activity, hence with coral energy budget and investment in calcification, but also photosynthesis alters the carbon budget in the coelenteron, producing changes in chemical gradients that ultimately affect carbonates deposition. Temperature is clearly a major determinant of metabolic rates, but it also has effects on carbonates chemistry, including calcification rates which are favoured at high

temperatures. Carbonates chemistry is universally considered a major determinant of chemical gradients within the coral but also is believed to affect photosynthesis (which may be carbon-limited) and respiration (that is depressed in case of hypercapnia, Pörtner 2008).

Whilst most studies focus on what we here defined abiotic effects, some authors (Goreau & Goreau 1959; Chalker & Taylor 1975) mention the energetic coupling between symbionts and host as a possible cause of LEC. Syntrophic symbioses, like the one that happens in many coral species, can be conveniently understood in the light of host and symbiont energetics, combined with evolutionary reasoning: symbiosis must be beneficial, in terms of fitness, for both the host and the symbiont whilst the two actors must retain selfish behaviour (sensu Dawkins 1976). These concepts have been incorporated in the syntrophic symbiosis models developed by Dubinsky & Jokiel (1994) and Muller et al. (2009). In these models zooxanthellae produce an excess of photosyntate that is translocated to the coral host and it thus represents additional energy available for whatever metabolic purpose must be fulfilled, whilst (in the Muller & Nisbet model) the coral supplies its symbionts with waste material (nutrients) that serve as substrate for algal photosynthesis. The interesting outcome of this setup is that, although the regulation mechanism is entirely passive, it suffices to obtain a stable relationship; furthermore this relationship shifts from mutualism to parasitism as environmental conditions change, thus providing also a candidate trigger for bleaching events.

We believe the key to understand the biological mechanisms involved in LEC lies in the energetic coupling between coral and zooxanthellae metabolism and calcification. It is however also likely that purely abiotic mechanisms play major roles in determining calcification response to seawater chemistry. Arguably both abiotic and biological phenomena may be relevant and it would be interesting to be able to discern the effects.

The experimental results from Al-Horani et al. (2003) and Venn et al. (2011) and the conceptual models of the calcification physiological machinery from McConnaughey & Whelan (1997) opened the gates to a deeper understanding of the cause and effect mechanisms that regulate coral sensitivity to acidification. Still lot though remains to be understood; the small spatial and temporal scales of the processes involved make many possibly useful experiments impractical: many studies couldn't resolve some aspect due to lack of knowledge about some state variable (e.g. Schneider &

Erez 2006 and refs therein). Carbonates chemistry is considered to be a key factor involved in coral calcification. The system of carbonates in seawater is completely determined with any two of its variables, though measuring such variables into the sub micrometric ECM is demanding, so that it's chemical characteristics are to date mostly unknown.

Models represent a viable way to test existing hypotheses and suggesting new experiments.

Hohn & Merico (2012; 2015) compared different conceptual models of coral calcification to determine which one produced the better agreement with the experiments from Al-Horani et al. (2003). The authors found the model that performed better was the one that incorporated all three of the proposed metabolic pathways (active transport, paracellular diffusion, transcellular diffusion) involved in calcification. Coincidently it was also possible to test hypotheses on the contributions of the different metabolic pathways to calcification: in their model Calcium reaches the skeleton mainly rough the active pathway and Carbon trough transcellular CO_2 diffusion, whilst trough the paracellular pathway solutes diffuse back from ECM to coelenteron.

Nakamura et al. (2013) used a similar model to test the plausibility of the oxygen hypothesis (Allemand et al. 2011) for light enhanced calcification (LEC), concluding that oxygen-boosted respiration may be responsible for the increase in calcification during daytime.

Here we propose a model of coral calcification built on the conceptual scheme developed in McConnaughey & Whelan 1997, Hohn & Merico 2012 and 2015, Nakamura et al. 2013, and implement realistic kinetics of active trans-membrane transport (Smith & Crampin 2004). The model is applied on experimental data for the Mediterranean coral *Cladocora caespitosa* (Rodolfo-metalpa et al. 2010) and used to (1) assess the cost of calcification and it's response to external parameters and physiological rates, (2) compare the biologically mediated and abiotic contributions to LEC from temperature, metabolic rates (Photosynthesis and respiration) and seawater chemistry.

3.2 Materials and methods

Case study

The model is applied on the dataset provided in Rodolfo-Metalpa et al. 2010. This very valuable study assessed the differential influence of Temperature and pCO_2 on the metabolic rates (gross photosynthesis, dark respiration, calcification) in the Mediterranean coral *Cladocora caespitosa*. The data set constitutes of four treatments: 1. Baseline temperature (according to replicate) and baseline pCO_2 (400 ppm), 2. Baseline temperature and increased pCO_2 (700 ppm), 3. Increased temperature (+3°C with respect to the corresponding baseline temperature replicate) and baseline pCO_2, 4. increased temperature and increased pCO_2. Each treatment comprises six replicates assessed in different seasons. For this study only the summer and winter replicates were used because both gross photosynthesis and dark respiration were measured. A table of the experimental conditions used in the model is provided in Table 3.1.

Model Topology, State Variables and Scales

This model's rationale is to follow the paths of the chemical species and metabolic fluxes physiologically relevant to biocalcification (either in a direct or indirect way) from seawater to coral skeleton trough compartments within the coral living body. We make the simplifying assumption (after Nakamura et al. 2013) that seawater is separated from the skeleton by two consecutive compartments: the coelenteron and the calcifying medium (ECM). A scheme of the model is provided in Fig. 3.1., all model parameters and sources are listed in Table 3.2.

Treatment	Temperature	TA	DIC	pH	Gross photosynthesis	Dark respiration	Calcification
	°C	umol kg-1	umol kg-1	-	nmol cm-2 h-1	nmol cm-2 h-1	nmol cm-2 h-1
a	21.7	2538	2201	8.06	0	-606.618	102.7
b	21.7	2538	2201	8.06	1455.883	-606.618	247.8
c	13.4	2540	2262	8.1	0	-121.324	36.4
d	13.4	2540	2262	8.1	165.4416	-121.324	80.2
e	24.5	2541	2203	8.01	0	-816.176	143.3
f	24.5	2541	2203	8.01	1555.147	-816.176	266.8
g	16.4	2540	2254	8.06	0	-595.588	45.2
h	16.4	2540	2254	8.06	1113.97	-595.588	101.2
i	21.7	2543	2317	7.87	0	-452.206	99.7
j	21.7	2543	2317	7.87	1466.916	-452.206	232.0
k	13.4	2538	2378	7.87	0	-121.324	35.0
l	13.4	2538	2378	7.87	341.912	-121.324	71.8
m	24.5	2546	2315	7.84	0	-716.912	106.3
n	24.5	2546	2315	7.84	1731.622	-716.912	241.0
o	16.4	2545	2374	7.85	0	-419.118	42.4
p	16.4	2545	2374	7.85	694.853	-419.118	108.4

Table 3.1 experimental data from Rodolfo-Metalpa et al. 2010 used in this study, calcification rates are measured with the alkalinity anomaly technique.

The chemical species considered are the Ca^{2+} ion and those pertaining to the carbonates system, whose chemistry in seawater is rather well known. The reported presence of the enzyme carbonic-anhydrase, which speeds up the equilibration of the carbonates system, in corals ECM (see Bertucci et al. 2013 for a review) may hinder the validity of kinetics derived for seawater (Zeebe & Wolf-Gladrow 2001), whilst, at the same time, suggests that the carbonate system should be reasonably close to equilibrium within the model compartments. Given this reasoning and due to the fact that the whole carbonates system has two degrees of freedom (i.e. is completely determined by any two of the variables involved), we chose as state variables to describe the carbonates system the two conservative quantities dissolved inorganic carbon (DIC) and total alkalinity (TA), as done in Nakamura et al. (2013), and use equilibrium relations (as explained later in this section) to calculate the other (dependent) state variables: H^+, OH^-, CO_2, HCO_3^- and CO_3^{2-}. Whenever some model process involves the dependent state variables, the resulting flux is converted in DIC and/or TA fluxes as explained through this section.

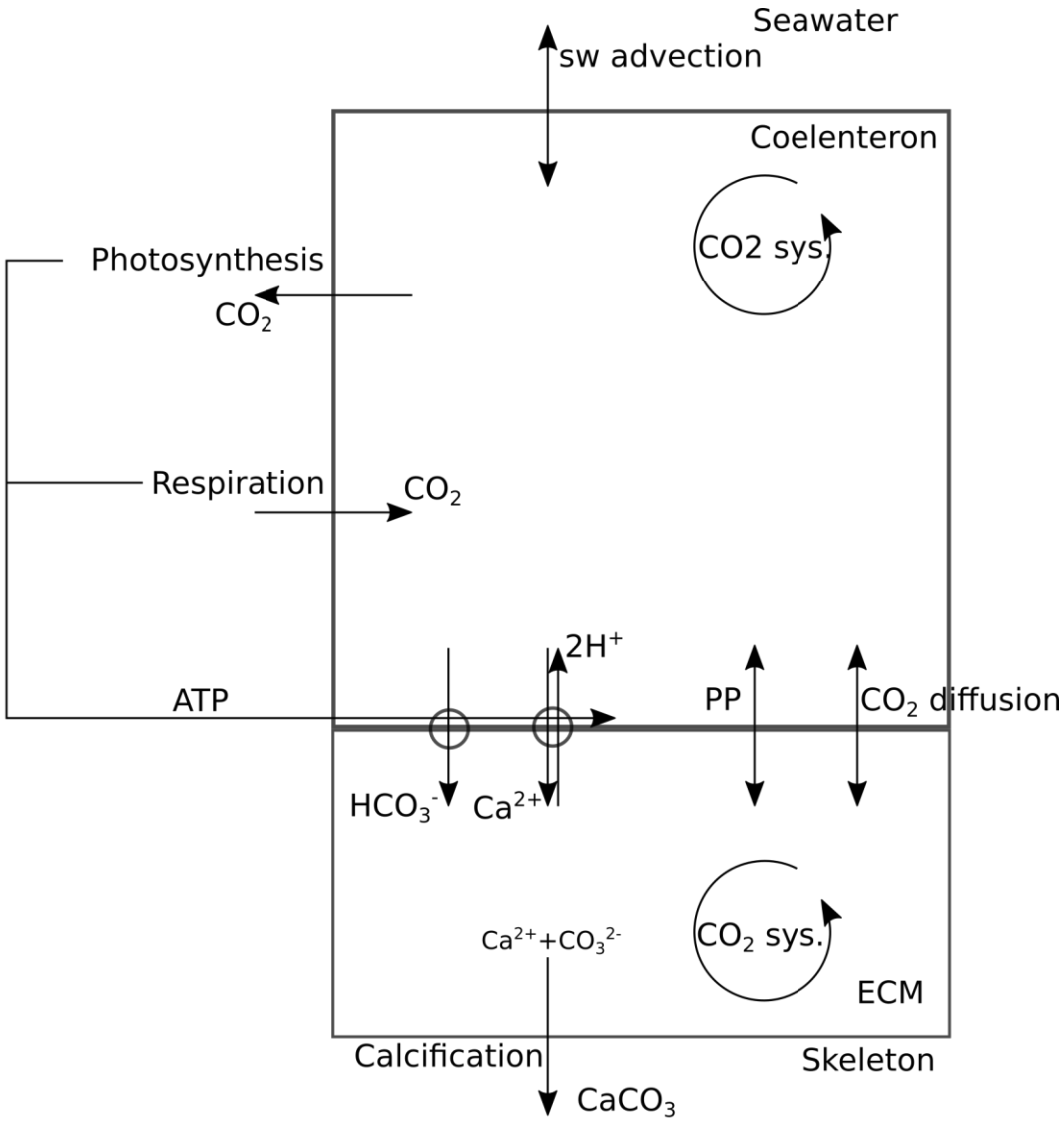

Fig. 3.1 Model conceptual scheme, PP: paracellular diffusion pathway.

parameter	description	value	units	source
h_{coe}	coelenteron height	3000	um	assumed
h_{ecm}	ECM height	5	um	assumed
k_p	aragonite precipitation rate constant	1.1 e-3	umol cm^{-2} s^{-1}	Burton & Water 1990
n_p	aragonite precipitation rate constant	1.63	-	Burton & Water 1990
k_d	aragonite dissolution rate constant	2.7 e-2	umol cm^{-2} s^{-1}	Walter & Morse 1985
n_d	aragonite dissolution rate constant	2.5	-	Walter & Morse 1985
-	Oxyenthalpic equivalent	473	kJ mol^{-1}	Gnaiger & Forstner 1983
ΔG_{ATP}	Gibbs free energy of ATP hydrolysis	30.5	kJ mol^{-1}	-
-	Respiratory quotient	1	mol_C $molO_2^{-1}$	assumed
Sal	Salinity	38.1	psu	Rodolfo-metalpa et al. 2010
k_{CO2}	CO2 permeability constant	2.04 e-4	cm s^{-1}	estimated
k_{pp}	paracellular pathway permeability	2.96 e-4	cm s^{-1}	estimated
s	diffusion coefficient	1.02 e-02	cm s^{-1}	estimated
alpha	fraction of Pg allocated to calcification	0.29068	-	estimated
beta	fraction of R allocated to calcification	0.2383	-	estimated
v_H	proportionality constant	5.41 e-3	cm s^{-1}	estimated
$E0_c$	Ca-ATPase concentration	3.57 e+3	umol cm^{-2}	estimated
$k1f_c$	Ca-ATPase rate constant	5.56E+00	cm^2 $umol^{-1}$	estimated
$k2f_c$	Ca-ATPase rate constant	4.03E+02	s^{-1}	estimated
$k3f_c$	Ca-ATPase rate constant	5.97E+01	s^{-1}	estimated
$k1b_c$	Ca-ATPase rate constant	5.27E-01	cm^2 $umol^{-1}$	estimated
$k2b_c$	Ca-ATPase rate constant	3.85E+01	s^{-1}	estimated
$k3b_c$	Ca-ATPase rate constant	3.12E-01	cm^2 $umol^{-1}$	estimated
$E0_b$	BAT concentration	4.71E+00	umol cm^{-2}	estimated
$k1f_b$	BAT rate constant	4.70E+00	cm^2 $umol^{-1}$	estimated
$k2f_b$	BAT rate constant	4.82E+01	s^{-1}	estimated
$k3f_b$	BAT rate constant	3.58E+00	s^{-1}	estimated
$k1b_b$	BAT rate constant	6.71E-05	cm^2 $umol^{-1}$	estimated
$k2b_b$	BAT rate constant	7.49E+00	s^{-1}	estimated
$k3b_b$	BAT rate constant	1.55E-02	cm^2 $umol^{-1}$	estimated

Table 3.2 All model parameters and sources.

All transport processes are computed per unit surface area and the growth of the colony is not resolved. As shown in chapter 1 the massive growth shape of *Cladocora caespitosa* would ensure that vital rates do not depend colony size.

Photosynthesis and respiration

Gross photosynthesis, *Pg*, and respiration, *R*, are forced in the model with the values measured by Rodolfo-Metalpa et al. (2010) as mol O_2 per unit area per unit time. Photosynthesis removes one mol DIC from the coelenteron per mol O_2 produced whilst respiration increases coelenteron DIC by one mol per mol O_2 consumed.

Carbonate system equilibria and physico-chemical constants

The components of the carbonate system, H^+, CO_2, HCO_3^- and CO_3^{2-}, are calculated in each compartment from DIC, TA, temperature and salinity, assuming that chemical equilibrium is reached at each time step, according to the equilibrium relation in (Zeebe & Wolf-Gladrow 2001). For the sake of simplicity we consider just the carbonates contribution to alkalinity and neglect, e.g. borates.

The carbonic acid dissociation constants and solubility product of water are calculated from temperature and salinity according to Millero 2007. Aragonite solubility constant is calculated from temperature and salinity according to Zeebe & Wolf-Gladrow 2001. Water density, ρ, is also calculated from temperature and salinity according to (Millero & Poisson 1981) and used trough the model to convert volumes to masses when needed.

Passive transport processes

The exchanges from seawater to coelenteron are modelled as an advection process governed by concentration gradients:

$$\vec{J}_{sw-coel} = s(\overrightarrow{SV}_{sw} - \overrightarrow{SV}_{coel}) \tag{3.1}$$

Where $\vec{J}_{sw-coel}$ is the vector of the fluxes of the state variables from seawater to coelenteron (mass/ surface · time), $\overrightarrow{SV_{sw}}$ and $\overrightarrow{SV_{coel}}$ are the vectors of the state variables, $SV_i = \left[DIC_i, TA_i, Ca_i^{2+}\right]$, in seawater and coelenteron respectively (concentrations), s is the advection coefficient (with units of speed).

Also the exchanges of state variables between coelenteron and ECM trough the paracellular pathway and the permeation of CO_2 trough cell layers are described as advective/diffusive phenomena:

$$\vec{J}_{coel-ecm} = k_{pp}(\overrightarrow{SV_{coel}} - \overrightarrow{SV_{ecm}}) \tag{3.2}$$

$$J_{CO2} = k_{CO2}(CO_{2,coel} - CO_{2,ecm}) \tag{3.3}$$

Where $\vec{J}_{coel-ecm}$ is the vector of the fluxes between coelenteron and ECM trough the paracellular pathway, J_{CO2} is the CO_2 flux from coelenteron to ECM trough the living tissue, $CO_{2,coel}$ and $CO_{2,ecm}$ are CO_2 concentrations in coelenteron and ECM respectively, and k_{pp}, k_{CO2} are permeability coefficients (with units of speed). The J_{CO2} flux exchanges 1 mol DIC per mol CO_2 transported.

Aragonite precipitation and dissolution

Aragonite precipitation and dissolution kinetics are modelled after Burton & Water 1990 and Walter & Morse 1985 as:

$$J_{CaCO3} = k_p(\Omega - 1)^{n_p}(\Omega \geqslant 1) + k_d(1 - \Omega)^{n_d}(\Omega < 1) \tag{3.4}$$

where J_{CaCO3} is the Aragonite precipitation or dissolution flux (mass per unit time per unit area), k_p, n_p are empirical coefficients for precipitation kinetics, k_d, n_d are empirical coefficients for dissolution kinetics and Ω is the saturation state of aragonite defined as,

$$\Omega = \frac{Ca^{2+}_{ecm}\ CO^{2-}_{3,ecm}}{K_{ar}} \tag{3.5}$$

where K_{ar} is the solubility constant of aragonite calculated from temperature and salinity according to Zeebee & Wolf-Gladrow (2001). J_{CaCO3} flux consumes 1 mol DIC and 2 mol TA from the ECM per mol $CaCO_3$ precipitated and vice-versa in case of dissolution.

Active transport processes

Two active transport processes are present: A Ca-ATPase (McConnaughey & Whelan 1997; Allemand et al. 2004) pump that exchanges 1 mol Ca^{2+} for 2 mol H^+ at the cost of 1 mol ATP (Gattuso et al. 1999) between coelenteron and ECM, and a bicarbonate active transport (BAT, Furla et al. 2000; Zoccola et al. 2015) that exchanges 1 mol HCO_3^- between coelenteron and ECM at the cost of 1 mol ATP. According to Zoccola et al. (2015) other ions such as Cl^- and/or Na^+ are likely involved in the BAT functioning, though those have been neglected as they are not relevant for skeletogenesis and unlikely to be rate-limiting due to high concentrations in seawater.

Pumps functioning is modelled after Smith & Crampin (2004) whom proposed a biophyisically-based model of a sodium-potassium antiporter as a four steps cyclic enzymatic reaction comprising both the forward and backward cycles. Such model is based on a reduction scheme from a 15-stage kinetic model that lumps together the fast reactions. To limit the number of unknown parameters we further simplified Smith and Crampin model by assuming that 1. the binding of two H^+ ions in the Ca-ATPase is lumped together in a single reaction, 2. the binding reactions of Ca-ATPase with Ca^{2+} and of BAT with ions other than HCO_3^- are much faster than the

other steps due to high Ca^{2+}, Cl^-, Na^+, etc. concentrations and can therefore be neglected. This leaves us with two 3-stage reactions that can be written as:

$$E1_c + 2H^+_{ecm} \rightleftharpoons E2_c \tag{3.6}$$

$$E2_c + ATP \rightleftharpoons E3_c \tag{3.7}$$

$$E3_c \rightleftharpoons E1_c + 2H^+_{coel} \tag{3.8}$$

and,

$$E1_b + HCO^-_{3,coel} \rightleftharpoons E2_b \tag{3.9}$$

$$E2_b + ATP \rightleftharpoons E3_b \tag{3.10}$$

$$E3_b \rightleftharpoons E1_b + HCO^-_{3,ecm} \tag{3.11}$$

for CaATPase and BAT respectively. Where E1, E2, E3 are the three possible states of Ca-ATPase (subscript c) and BAT (subscript b), whose total concentration is conservative and equals E0 = E1+E2+E3.

In the model we do not compute ATP concentration within the cell but rather we define the metabolic flux that is devoted to running the active transports (see next section). Given this constraint we chose to model reaction kinetics based on fluxes rather than concentrations, as proposed by Kooijman (2009); the fluxes of chemical species (indicated with dots over variable names) reaching the pumps are considered to be linearly proportional to concentrations: e.g. $\dot{H}^+_i = v_H H^+_i$ with v_H a proportionality constant with units of speed. Forward and backward reactions are considered as 1st order kinetics with reaction constants k1f, k2f, k3f and

k1b, k2b, k3b for the forward and backward cycles respectively and the whole system for the Ca-ATPase can be written as:

$$\frac{dE1}{dt} = -k_{1f}\ E1\ 2\dot{H}^{+}_{ecm} + k_{1b}\ E2 + k_{3f}\ E3 - k_{3b}\ E1\ 2\dot{H}^{+}_{coel} \tag{3.12}$$

$$\frac{dE2}{dt} = k_{1f}\ E1\ 2\dot{H}^{+}_{ecm} - k_{1b}\ E2 - k_{2f}\ E2\ A\dot{T}P + k_{2b}\ E3 \tag{3.13}$$

$$\frac{dE3}{dt} = k_{2f}\ E2\ A\dot{T}P - k_{2b}\ E3 - k_{3f}\ E3 + k_{3b}\ E1\ 2\dot{H}^{+}_{coel} \tag{3.14}$$

By solving at stady state, the expression for the flux trough Ca-ATPase is derived:

$$J_{CaATPase} = \frac{E0\left(k_{1f}\ k_{2f}\ k_{3f}\ A\dot{T}P\ 2\dot{H}^{+}_{ecm} - k_{1b}\ k_{2b}\ k_{3b}\ 2\dot{H}^{+}_{coel}\right)}{den} \tag{3.15}$$

$$\begin{aligned} den = {} & k_{2f}\ k_{3f} A\dot{T}P + k_{2f}\ k_{3b}\ 2\dot{H}^{+}_{coel}\ A\dot{T}P + k_{1f}\ k_{2f}\ 2\dot{H}^{+}_{ecm}\ A\dot{T}P \\ & + k_{1f}\ k_{3f}\ 2\dot{H}^{+}_{ecm} + k_{2b}\ k_{3b}\ 2\dot{H}^{+}_{coel} + k_{1b}\ k_{3b}\ 2\dot{H}^{+}_{coel} \\ & + k_{1f} k_{2b}\ 2\dot{H}^{+}_{ecm} + k_{1b}\ k_{2b} + k_{1b}\ k_{3f} \end{aligned} \tag{3.16}$$

So that each cycle transports two mol protons from ECM to coelenteron and one mol Ca^{2+} from coelenteron to ECM while consuming 1 mol ATP; flow is in opposite direction if the pump functions in reverse. The $J_{CaATPase}$ flux moves 2 mol TA from coelenteron to ECM per mol $2H^{+}$, and vice-versa if the pump functions in reverse.

BAT flux (J_{BAT}) expression is analogous to that of CaATPase and can be derived by substituting $2\dot{H}^{+}_{coel}$ with $H\dot{C}O^{-}_{3,ecm}$ and $2\dot{H}^{+}_{ecm}$ with $H\dot{C}O^{-}_{3,coel}$ in

eq. 15 and 16. The kinetic constants for the two transports are of course different so that the BAT and Ca-ATPase have separate parameterizations. the J_{BAT} flux moves 1 mol DIC and 1 TA from coelenteron to ECM under normal functioning and vice-versa if the pump functions in reverse.

ATP flux to Ca-ATPase and BAT

The energetic flux that is used to run the active transports is considered to be a weighted sum of respiration and photosynthesis metabolic fluxes. Even though zooxanthellae clearly do not directly supply energy to Ca-ATPase and BAT, we assume, after Dubinsky & Jokiel 1994 and Muller et al. 2009, they produce some excess photosintate that is translocated to the host and can be used for whatever purpose, including running the ion transport machinery. This mechanism is clearly a simplification, the translocation of photosynthetic energy to the coral host would imply an increase in light respiration and the energy consumed by the active transports will indeed appear solely in the respiratory flux, though it should suffice as a first approximation assuming that the machinery operates at steady state. The ATP flux is:

$$\dot{ATP} = \Delta G_{ATP}\left(\alpha\, \Delta H_{Pg}\, Pg + \beta\, \Delta H_R\, R\right) \tag{3.17}$$

Where Pg and R fluxes are converted from O_2 to energy with the oxyenthalpic equivalents according to (Gnaiger & Forstner 1983) and then to mol ATP by assuming a Gibbs free energy of 30.5 kJ per mol ATP; α and β are the fractions of Pg and R that are devoted to the active transports. ATP flux is then partitioned between Ca-ATPase and BAT according to their concentrations:

$$\dot{ATP}_{BAT} = \frac{E0_b}{E0_b + E0_c}\dot{ATP} \tag{3.18}$$

$$A\dot{T}P_{CaATPase} = \frac{E0_c}{E0_b + E0_c} A\dot{T}P \tag{3.19}$$

Model master equations

Surface based fluxes are converted to concentrations by dividing for the height of the relevant compartment, h_{coel} and h_{ecm} so that the whole system of differential equations can be written as:

$$\frac{dDIC_{coel}}{dt} = \left(-J_{BAT} + \vec{J}_{sw-coel,1} - \vec{J}_{coel-ecm,1} - J_{CO2} - Pg + R\right)/h_{coel} \tag{3.20}$$

$$\frac{dTA_{coel}}{dt} = \left(-J_{BAT} - 2J_{CaATPase} + \vec{J}_{sw-coel,2} - \vec{J}_{coel-ecm,2}\right)/h_{coel} \tag{3.21}$$

$$\frac{dCa_{coel}}{dt} = \left(-J_{CaATPase} + \vec{J}_{sw-coel,3} - \vec{J}_{coel-ecm,3}\right)/h_{coel} \tag{3.22}$$

$$\frac{dDIC_{ecm}}{dt} = \left(J_{BAT} + \vec{J}_{coel-ecm,1} + J_{CO2} - J_{CaCO3}\right)/h_{ecm} \tag{3.23}$$

$$\frac{dTA_{ecm}}{dt} = \left(J_{BAT} + 2J_{CaATPase} + \vec{J}_{coel-ecm,2} - 2J_{CaCO3}\right)/h_{ecm} \tag{3.24}$$

$$\frac{dCa_{ecm}}{dt} = \left(J_{CaATPase} + \vec{J}_{coel-ecm,3} - J_{CaCO3}\right)/h_{ecm} \tag{3.25}$$

This system is solved with a Runge-Kutta-Fehlberg variable step-size method with error control tolerance 10^{-6} and initialized with a 0.01s timestep.

Model calibration

The model was run for a simulation time of 500s, largely sufficient to reach a steady state, with external conditions corresponding to the experimental setups (T, Sal, DIC, TA) and vital rates measurements (Pg, R) in Rodolfo-Metalpa et al. 2010 and was calibrated by minimizing the sum of squared errors between the measured and simulated calcification rates (those measured with the alkalinity anomaly technique, see Rodolfo-Metalpa et al. 2010). The data set was also used to run simulation experiments (see below).

Cost of calcification

The instantaneous metabolic cost of calcification can be calculated as the ratio between the sum of the energy fluxes reaching Ca-ATPase and BAT and the calcification rate.

Simulation experiments

After determining the set of parameter values that approximates at best the measured calcification rates, the model was used to run simulation experiments.

To evaluate how the compartments and transport rates behave under light and dark conditions (i.e. in the presence or absence of photosynthesis), the model was run for a total simulation time of 2000 s with alternating light and dark conditions lasting for 500 s each and other conditions as from the *b* setup (see Table 3.1).

Abiotic and biologically mediated effects on calcification

The model was also used to discern between the biologically mediated and abiotic effects of photosynthesys (light), respiration, seawater chemistry and temperature on calcification rates and calcification costs.

We assume that the only effect of light is that of stimulating photosynthesis (but see Cohen et al. 2016); this in turn alters the DIC balance in the coelenteron (abiotic effect) and the ATP flux to the active transports (biologically mediated effect). Thus increasing photosynthesis in the model should simulate the LEC phenomenon. To separate the biologically mediated effect of photosynthesis the model was run at all light setups with ATP fluxes derived with Pg values ranging from 0.5 to 1.5 the baseline setup value. To separate the abiotic effect of light instead the model was run at all setups with Photosynthetic DIC and TA fluxes derived with Pg values ranging from 0.5 to 1.5 the baseline setup value. We adopted the same procedure also to separate the biologically mediated and abiotic effects of respiration, but here all setups were used.

The model doesn't incorporate any law of temperature dependence for Pg and R, thus to separate the biologically mediated effects of temperature the model was run at all setups with Pg and R values from increased temperature setups substituted with Pg and R values from the corresponding baseline temperature setup and vice versa. This method is constrained by the experimental dataset and permits the assessment of two temperature differences only: -3 and +3 °C. Please note that here, contrary to what done for Pg, R, the effects of modified rates on coelenteron carbonates budget are included in the biologically mediated group. In fact we consider that the abiotic effects of temperature are those for which seawater phyisco-chemical constants account for. To separate the abiotic effect of temperature instead the model was run at all setups with all physico-chemical constants calculated from Temperatures ranging from -5 °C to +5 °C the baseline setup value.

To separate the abiotic effects of different components of carbonates chemistry (DIC, TA) the model was ran at all setups with either DIC or TA values ranging from 0.9 to 1.1 their original setup value. Same as for Temperature, the model doesn't incorporate any law that ties Pg nor R to seawater chemistry, also Rodolfo Metalpa et al. (2010) state there's no

significant correlation between pCO_2 and Pg nor pCO_2 and R. Nonetheless it is possible to assess potential biologically mediated effects of pCO_2 (suggested to exist in Pörtner 2008) by running the model at each setup with Pg and R values of baseline setups equal to those of the corresponding acidified setup and vice versa. This method is constrained by the experimental setup and permits the assessment of two pCO_2 differences only: -300 and +300 ppm, corresponding to a change in DIC of roughly ±5%.

3.3 Results

Calibration

The model correctly simulates the observed calcification rates under all of the experimental conditions (Fig 3.2a).

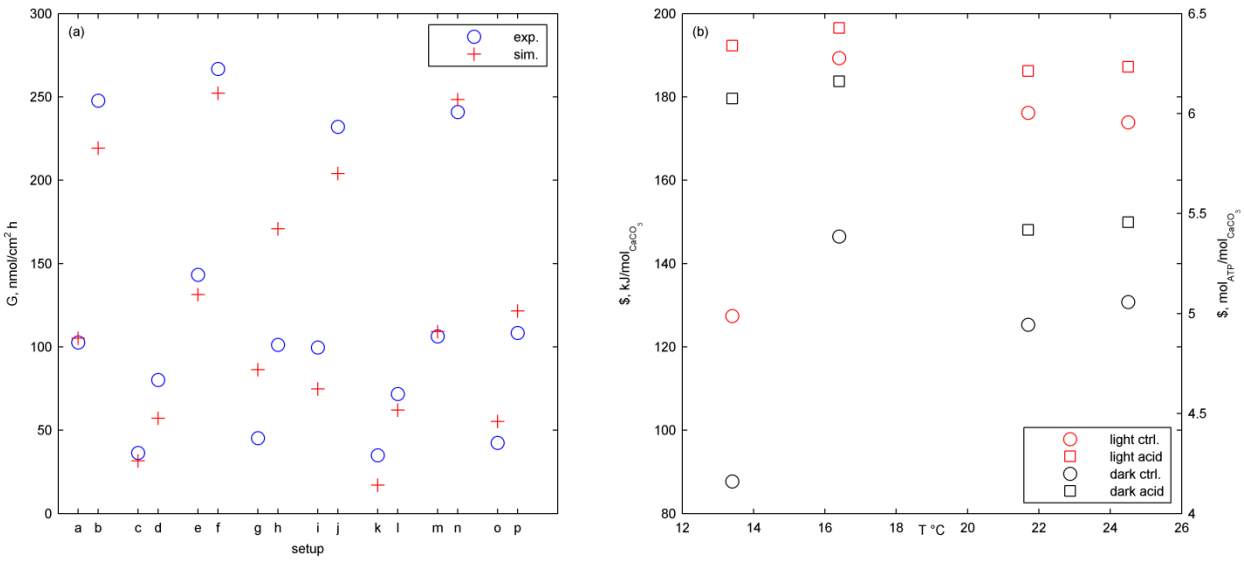

Fig. 3.2 (a) Calcification rates at all experimental setups, observed vs. simulated values. (b) Calcification costs at all model setups.

Compartments behaviour

The model compartments behaviour under light and dark conditions (Fig. 3.3) agrees with the experimental observations from Al-Horani et al. 2003 and with the modelling results from Hohn & Merico 2012 and 2015 and Nakamura et al. 2013: the ECM pH is always higher than external pH and higher in the light than in the dark. ECM Ca^{2+} concentration is also higher than the external value and higher in the dark than in the light. Active ion pumping has the effect of increasing both DIC and TA in the ECM with respect to the coelenteron. Ω in the ECM is also higher than in seawater, ranging from about 13 in the light to about 8 in the dark, this reflects on the related calcification rates. Under dark conditions DIC coming mainly from respiration accumulates in the coelenteron due to the absence of the photosynthesis sink, so that it diffuses back to seawater; on the contrary under light conditions coelenteron DIC drops as it is used for photosyntetic activity, so that the diffusive flux is directed from seawater into the coelenteron. Transcellular CO_2 flux is always directed from coelenteron to ECM but is consistently smaller than the rest of the fluxes and has little overall effect.

Cost of light and dark calcification under different temperatures and pCO_2

The estimated costs of calcification under the experimental conditions used in Rodolfo-Metalpa et al. 2010, Fig 3.2b, ranges between about 88 kJ/mol_{CaCO3} or 2.9 mol_{ATP}/mol_{CaCO3} to about 196.5 kJ/mol_{CaCO3} or 6.4 mol_{ATP}/mol_{CaCO3}. At each temperature and pCO_2 dark calcification is more cost effective than light calcification, even though the calcification rates are smaller in the dark; also the costs under acidified conditions are always higher with respect to control. The biggest differences between costs in control vs acidified treatments are seen under dark conditions, on the contrary light calcification is only slightly more costly under acidified conditions except for the 13.4 °C treatment where the difference is substantial.

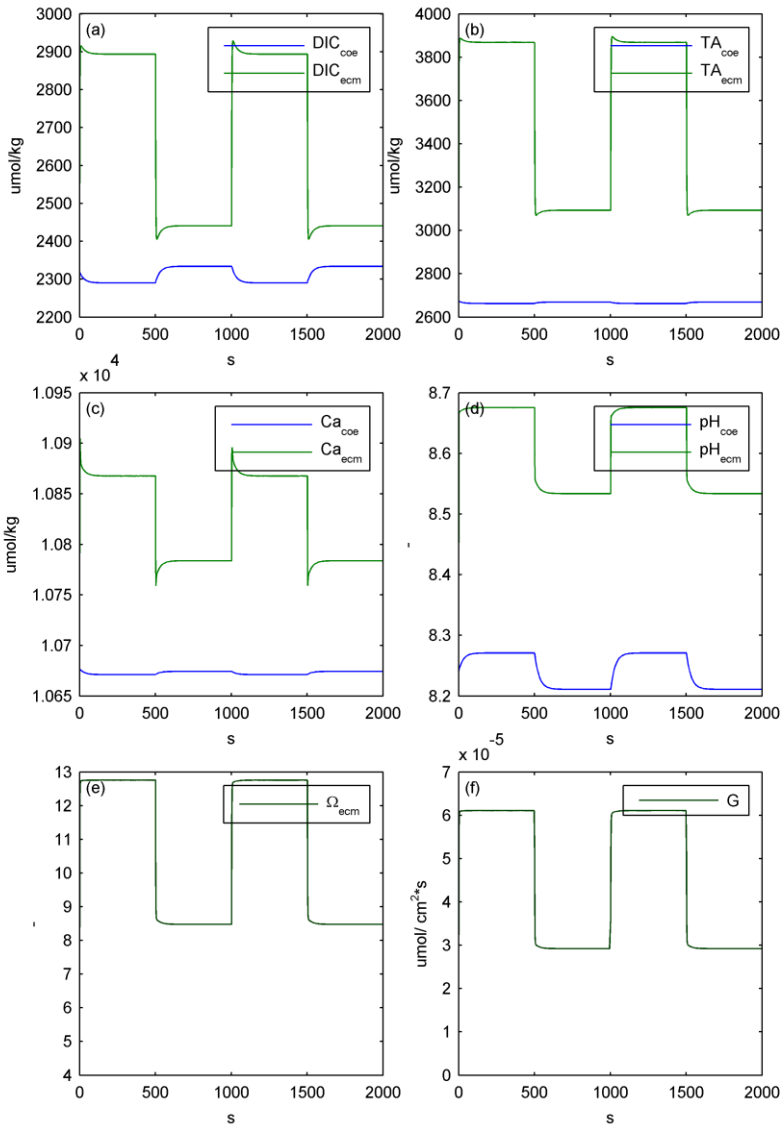

Fig. 3.3 State variables behaviour under alternating light (0:500 and 1000:1500 s) and dark (500:1000 and 1500:2000 s) conditions. (a) DIC, (b) TA, (c) Ca^{2+}, (d) pH, (e) aragonite saturation, (f) Calcification rate.

For instance at 21.7 °C the cost of dark calcification under control pCO_2 is about 125.3 kJ/mol_{CaCO3} or 4.1 mol_{ATP}/mol_{CaCO3}, whereas under acidified conditions is about 148.1 kJ/mol_{CaCO3} or 4.8 mol_{ATP}/mol_{CaCO3}. At the same temperature light calcification costs about 175.4 kJ/mol_{CaCO3} or 5.8 mol_{ATP}/mol_{CaCO3} under control conditions and about 187 kJ/mol_{CaCO3} or 6.1 mol_{ATP}/mol_{CaCO3} under acidified conditions.

The analysis of the material fluxes between the models compartments permits to interpret these patterns bearing in mind that the final costs are the ratio between the ATP flux that reaches the active transports (or the sum of Ca-ATPase and BAT transport rates) and the calcification rates. High transport rates and low calcification rates both have the effect of increasing costs and vice versa.

Influence of photosynthesis (light) and respiration

The overall effect of increased photosynthesis is that of increasing both calcification rates and costs. The observed difference in light and dark calcification rates (LEC) is largely due to photosynthesis boosting the energetic flux that reaches the active transports (biologically mediated effect, Fig 3.4a,b). An increase in photosynthesis causes a substantial increase in both calcification rates and costs. The abiotic component (Fig 3.4c,d) is also present and is related to the different carbon budget of the coelenteron with or without photosynthesis, it has the effect of increasing calcification rates and decreasing costs for increasing photosynthesis rates, thus it acts in synergy with the biologically mediated effect, but its effects are roughly one order of magnitude lower. The biologically mediated effects of respiration (Fig. 3.5) are similar to those of *Pg*, whilst the abiotic effects are entail decreasing calcification rates and increasing costs for increasing *R*.

The difference between light and dark costs is due to the high active transport rates under light conditions, stimulated by photosynthetic energy, that overload the ECM with Ca^{2+}, DIC and TA with respect to the coelenteron, so that these ECM solutes move back to the coelenteron trough the paracellular pathway following the concentration gradient; this also happens under dark conditions but to a lesser extent due to the lower active transport rates. As a consequence calcification in the light is less cost-effective than in the dark, because a substantial fraction of the skeleton building blocks that are transported to the ECM at the expense of energy do not end up in the skeleton but diffuse back to the coelenteron instead; Nonetheless light calcification still can be sustained at higher rates due to a substantial excess of metabolic energy from photosynthesis.

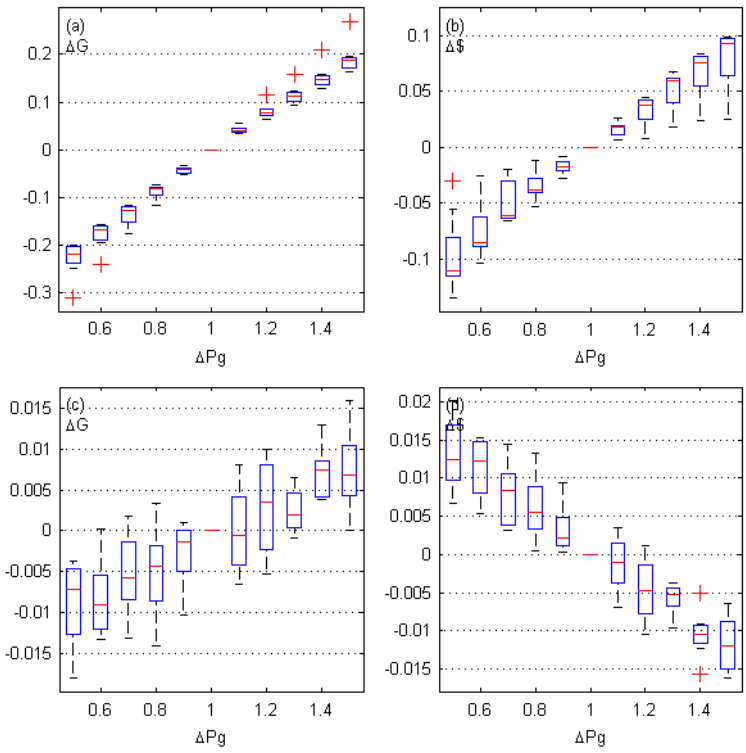

Fig. 3.4 biologically mediated (a, b) and abiotic (c, d) effects of photosynthesis on calcification.

Effect of temperature on calcification rates and costs

The overall effect of temperature is that of a substantial increase in calcification rates and related costs. The largest part of the variation is biologically mediated (Fig 3.6a,b): increasing temperatures stimulate Pg and R and provide additional energy for the active transcellular pathway. This of course within the temperature variation range of the experimental setups. Arguably as the limits of *C. Caespitosa* thermortolerance range are approached metabolic rates will drop. As for the abiotic effect of temperature (Fig 3.7c,d), calcification rates increase and calcification costs decrease with increasing temperature, according to $CaCO_3$ deposition kinetics, though the abiotic effects, even if present, are one order of magnitude lower than the biologically mediated ones.

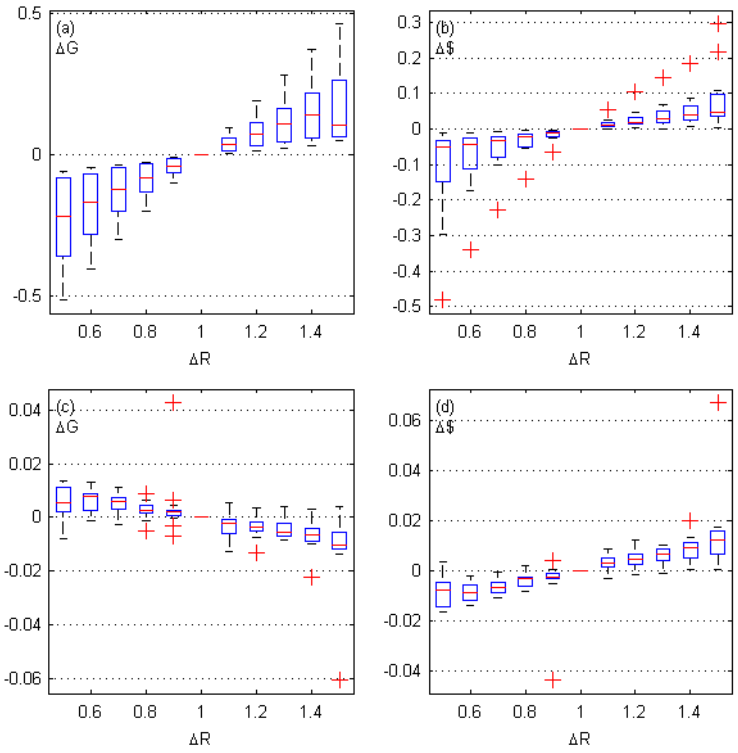

Fig. 3.5 biologically mediated (a, b) and abiotic (c, d) effects of respiration on calcification.

Influence of seawater chemistry

The overall effects of pCO_2, as already remarked in Rodolfo Metalpa et al. 2010, are low with respect to those of temperature and light. The biologically mediated component (Fig 3.7a,b) is the less important of the two contributions and results in a decrease in calcification for increasing pCO_2, coupled with a decrease in costs. This contribution is due to respiration and photosynthesis rates being respectively slightly decreased (always, Tab 3.1) and slightly increased under acidified conditions. As for the abiotic effects of carbonates chemistry (Fig 3.7c,d,e,f), an increase in seawater DIC causes a decrease in calcification rates and an increase in costs, whilst an increase in seawater TA causes an increase in calcification rates and a decrease in costs.

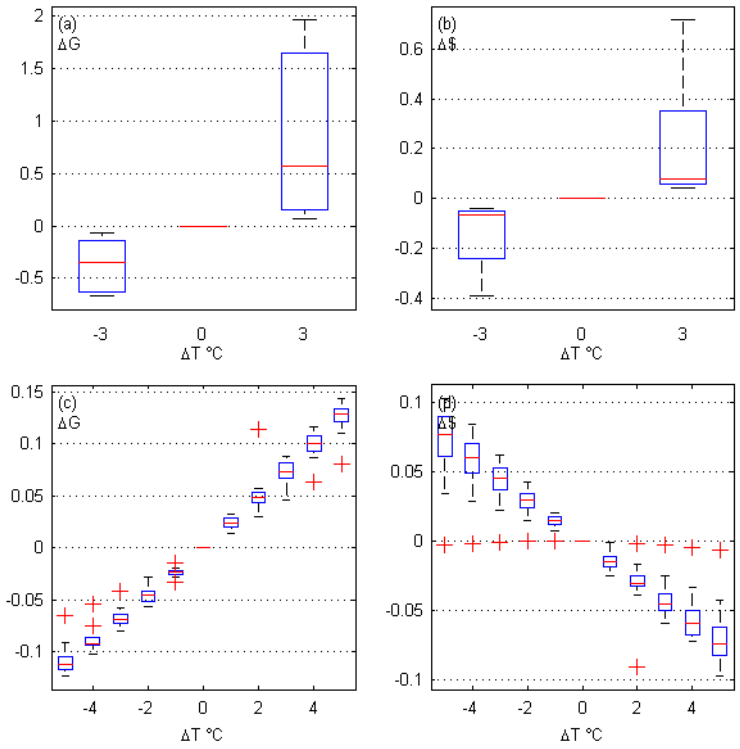

Fig. 3.6 biologically mediated (a, b) and abiotic (c, d) effects of temperature on calcification.

3.4 Discussion

Our model successfully simulates the experimental calcification rates determined by Rodolfo-Metalpa et al. (2010), as well as the qualitative compartments response to external conditions described in Al-Horani et al. 2003. The resulting material fluxes are also qualitatively in agreement with the modelling results from Hohn & Merico 2015.

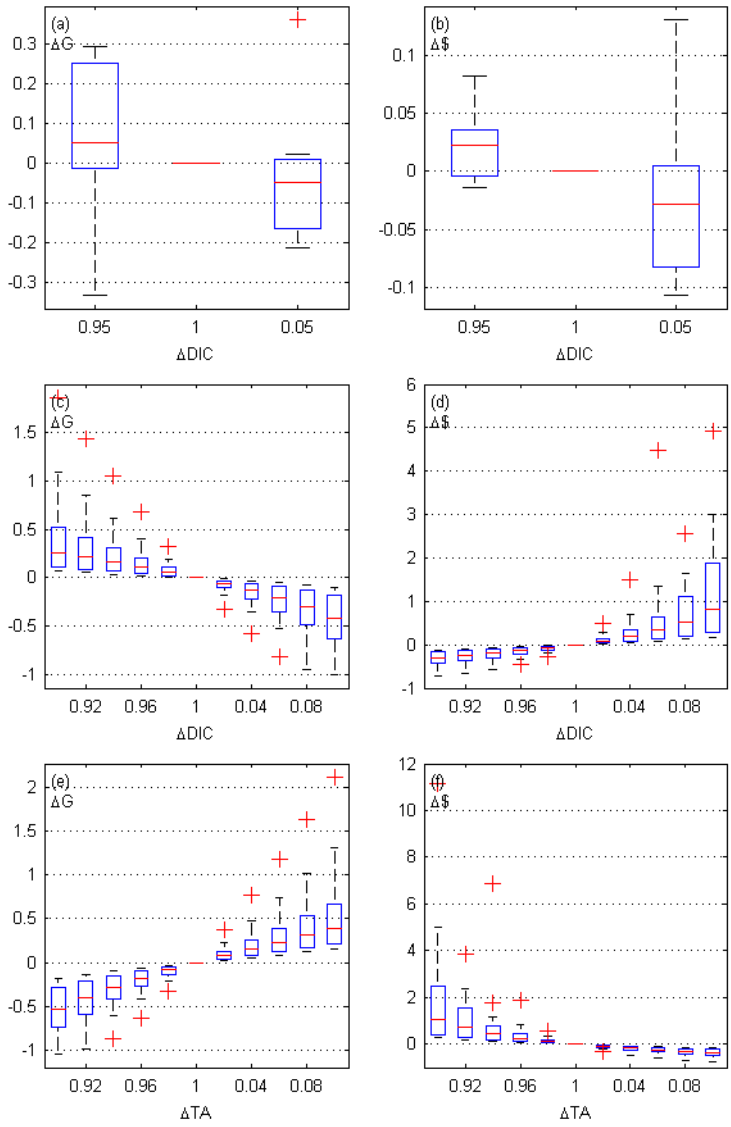

Fig. 3.7 (a, b) Biologically mediated effects of DIC, (c, d) abiotic effects of DIC (e, f) abiotic effects of TA.

Calcification Cost

Our estimates of the metabolic cost of calcification (ranging around 100-200 kJ/mol) are much larger than the values previously proposed based on theoretical reasoning and more in line with Palmer (1992) experimental estimate. We obtained such estimates by implementing realistic biophisically-based active transport kinetics (Smith & Crampin 2004) where

the transport rates are influenced by both concentration gradients and available energy. In our opinion the commonly assumed values for the cost of calcification have a number of limitations as they do not account for transport inefficiencies and may produce unphysical behaviour: for instance, if the cost for transporting 1 mol of solute was invariantly 1 mol ATP, it would suffice to set the chemical gradient greater than ΔG_{ATP} to obtain a perpetual motion engine. Also the previously reported costs are (in our opinion) suspiciously low if compared to common biomass synthesis costs (Gnaiger & Forstner 1983). With such low costs many corals would face little trouble in allocating some extra energy to calcification when acidification kicks in. Our result instead is indicative of a conspicuous investment into skeleton and may be important to understand the relations between biocalcification and climatic variability. Since to date only one experimental estimate of the cost of calcification is available, and none for corals, we suggest further experiments to test this. However we also stress that most studies target tropical species whilst we use data from a Mediterranean one which is also little sensitive to acidification.

Regardless the exact value of the calcification cost we also found it to have an overall positive relation with calcification rates: the more the coral calcifies the less efficient is the conversion of energy to calcium carbonate. This may seem paradoxical though it can be understood bearing in mind that the cost in the absence of a metabolic investment would be zero and rates would still be positive due to seawater oversaturation.

Contribution of the different pathways to calcification

We found that both calcium and carbon enter the ECM mainly through the active transcellular pathway; this is in line with the findings from Furla et al. (2000) that found calcification rates in the reef coral *Stylophora pistillata* to be impaired by both Ca-ATPase and BAT selective inhibitors. As found by Hohn & Merico (2015), the passive paracellular pathway is a sink rather than a source of carbon and calcium in the ECM. Finally the transcellular diffusion pathway is scarcely influential.

LEC and contributions to calcification.

In our model the main factor contributing to LEC is the excess metabolic energy provided by photosynthesis that stimulates active transcellular transport activity. The other major contribution to calcification rate is temperature which acts in a similar fashion as light does, by stimulating photosyntesis and respiration. Abiotic contributions are also present but are largely minoritary with respect to biologically mediated effects. The effects of seawater chemistry, both abiotic and biologically medited, on the other hand, are less pronounced than those of temperature and light. This was however expected because the original experiments from Rodolfo-Metalpa et al. 2010 concluded that *C. Caspitosa* is an acidification resistant species.

Our model builds on an accredited conceptual model of the physiology of coral calcification (McConnaughey & Whelan 1997), already tested for different purposes trough modelling applications (Hohn and Merico 2012; 2015, Nakamura 2013), and incorporates realistic kinetics for the active transcellular pathway (Smith & Crampin 2006) that depend both on concentration gradients and available energy. Our coupling between metabolic rates (Pg, R) and the calcification machinery is based on the models of syntrophic simbioses developed in Dubinsky & Jokiel 1994 and Muller et al. 2009; in such models, and in ours as well, the zooxanthellae translocate some excess photosynthate to the coral host that can use it for whatever purpose, and some of this energy is indeed used to run the active transports.

The hypothesis that calcification in corals is energy limited and that LEC is due to photosyntate translocation from symbionts to host has already been formulated (Goreau & Goreau 1959; Chalker & Taylor 1975) but is rather overlooked (e.g. Allemand et al. 2011 and Gattuso et al. 1999 and references therein). A positive correlation between photosynthesis and calcification is beyond doubt, but LEC is more often attributed to the photosynthetic uptake of CO_2 which would increase carbonate ion concentration and facilitate precipitation of $CaCO_3$ (Cohen et al. 2016).

However also increased respiration rates (a source of CO_2) are widely reported to be correlated with enhanced calcification: Holcomb et al. (2014) found that addition of glucose or glycerol, coupled with increased oxygen stimulated both respiration and dark calcification in bleached S. pystillata microcolonies (but not in un-bleached ones), and concluded that dark

calcification may be oxygen limited in zooxanthellate corals. (Anthony et al. 2002) found respiration rates to be the main factor affecting calcification in two species of reef corals. Also in the data used for this study (Rodolfo-Metalpa et al. 2010) both photosynthesis and respiration rates correlate positively with photosynthesis.

Since photosynthesis consumes carbon and respiration produces it, the two processes should, most of the times, display opposite effects if the prevailing mechanism was abiotic.

Evidence is building up that calcificaton in corals relies on active transport, hence it is an energy demanding process. This suggests calcification should be energy limited at least under some conditions.

Biological processes are indeed renown for being energy demanding (life, at least usually, doesn't happen spontaneously); The practice of studying biocalcification solely from a carbonates chemistry perspective is indeed very popular, perhaps because carbonates chemistry in seawater is rather well known and all the tools are at hand. This approach undoubtedly lead to a much deeper understanding of coral calcification and its relations with environmental parameters, especially in recent years; however ambiguous results are still abundant and many mechanisms have yet to be elucidated. We suggest that the energy limitation of active transport rates in corals may be much more important than previously thought and that further experiments should test this hypothesis.

3.5 References

Al-Horani, F. a, Al-Moghrabi, S.M. & De Beer, D., 2003. The mechanism of calcification and its relation to photosynthesis and respiration in the scleractinian coral Galaxea fascicularis. *Marine Biology*, 142(3), pp.419–426.

Allemand, D. et al., 2004. Biomineralisation in reef-building corals : from molecular mechanisms to environmental control. *General Palaeontology (Palaeobiochemistry)*, 3, pp.453–467.

Allemand, D. et al., 2011. Coral calcification, cells to reefs. In Z. Dubinsky & N. Stambler, eds. *Coral Reefs: An Ecosystem in Transition*. Dordrecht: Springer Netherlands, pp. 119–150.

Anthony, K.R.N., Connolly, S.R. & Willis, B.L., 2002. Comparative analysis of energy allocation to tissue and skeletal growth in corals. *Limnology and Oceanography*, 47(5), pp.1417–1429.

Bertucci, A. et al., 2013. Bioorganic & Medicinal Chemistry Carbonic anhydrases in anthozoan corals — A review. *Bioorganic & Medicinal Chemistry*, 21, pp.1437–1450.

Burton, E.A. & Water, L.M., 1990. The role of pH in phosphate inhibition of calcite and aragonite precipitation rates in seawater. *Geochimica et Cosmochimica Acta*, 54, pp.797–808.

Chalker, B.E. & Taylor, D.L., 1975. Light-enhanced calcification, and the role of oxidative phosphorylation in calcification of the coral Acropora cervicornis. *Proceedings of the Royal Society London*, 190, pp.323–331.

Cohen, A.L. & Holcomb, M., 2010. Why Corals Care About Ocean Acidification Uncovering the Mechanism. *Oceanography*, 22(4), pp.118–127.

Cohen, I., Dubinsky, Z. & Erez, J., 2016. Light Enhanced Calcification in Hermatypic Corals : New Insights from Light Spectral Responses. *Frontiers in Marine Science*, 2, pp.1–12.

Dawkins, R., 1976. the Selfish Gene. *30th Anniversary Edition--with a new Introduction by the Author*, pp.1–13.

Dubinsky, Z. & Jokiel, P.L., 1994. Ratio of energy and nutrient fluxes regulates symbiosis between zooxanthellae and corals. *Pacific Science*, 48(3), pp.313–324.

Furla, P. et al., 2000. Sources and mechanisms of inorganic carbon transport for coral calcification and photosynthesis. *The Journal of experimental biology*, 203, pp.3445–3457.

Gattuso, J.P., Allemand, D. & Frankignoulle, M., 1999. Photosynthesis and calcification at cellular, organismal and community levels in coral reefs: A review on interactions and control by carbonate chemistry. *Am. Zool.*, 39(1), pp.160–183.

Gnaiger, E. & Forstner, H., 1983. *Polarographic oxygen sensors: aquatic and physiological applications*, Springer-Verlag.

Goreau, T.F. & Goreau, N.I., 1959. The physiology of skeleton formation in corals. II. Calcium deposition by hermatypic corals under different conditions. *Biological Bulletin*, 117, pp.239–250.

Hohn, S. & Merico, A., 2012. Modelling coral polyp calcification in relation to ocean acidification. *Biogeosciences*, 9(11), pp.4441–4454.

Hohn, S. & Merico, A., 2015. Quantifying the relative importance of transcellular and paracellular ion transports to coral polyp calcification . *Frontiers in Earth Science*, 2(January), p.37.

Holcomb, M. et al., 2014. Coral calcifying fluid pH dictates response to ocean acidification. *Nature Scientific Reports*, pp.1–4.

Jokiel, P.L., 2011. Ocean acidification and control of reef coral calcification by boundary layer limitation of proton flux. *Bulletin of Marine science*, 87(3), pp.639–657.

Kooijman, S.A.L.M., 2009. *Dynamic energy budget theory for metabolic organisation, third edition* 3rd ed., Cambridge University Press.

McConnaughey, T.A. & Whelan, J.F., 1997. Calcification generates protons for nutrient and bicarbonate uptake. *Earth-Science Reviews*, 42(1-2), pp.95–117.

McCulloch, M. et al., 2012. Coral resilience to ocean acidification and global warming through pH up-regulation. *Nature Climate Change*, 2(8), pp.623–627.

Millero, F.J., 2007. The Marine Inorganic Carbon Cycle. *Chemical Reviews*, 107, pp.308–341.

Millero, F.J. & Poisson, A., 1981. International one-atmosphere equation of state of seawater. *Deep-Sea Research*, 28, pp.625–629.

Muller, E.B. et al., 2009. Dynamic energy budgets in syntrophic symbiotic relationships between heterotrophic hosts and photoautotrophic symbionts. *Journal of Theoretical Biology*, 259, pp.44–57.

Nakamura, T., Nadaoka, K. & Watanabe, A., 2013. A coral polyp model of photosynthesis, respiration and calcification incorporating a transcellular ion transport mechanism. *Coral Reefs*, 32(3), pp.779–794.

Ogilvie, M.M., 1896. Microscopic and Systematic Study of Madreporarian Types of Corals. *Philosophical Transactions of the Royal Society of*

London B: Biological Sciences, 187, pp.83–345.

Palmer, A.R., 1992. Calcification in marine molluscs: how costly is it? *Proceedings of the National Academy of Sciences of the United States of America*, 89(4), pp.1379–1382.

Pörtner, H.-O., 2008. Ecosystem effects of ocean acidification in times of ocean warming: a physiologist's view. *Marine Ecology Progress Series*, 373, pp.203–217.

Rodolfo-metalpa, R. et al., 2010. Response of the temperate coral Cladocora caespitosa to mid- and long-term exposure to p CO 2 and temperature levels projected for the year 2100 AD. *Biogeosciences*, 7, pp.289–300.

Schneider, K. & Erez, J., 2006. The effect of carbonate chemistry on calcification and photosynthesis in the hermatypic coral Acropora eurystoma. *Limnology and Oceanography*, 51(3), pp.1284–1293.

Smith, N.P. & Crampin, E.J., 2004. Development of models of active ion transport for whole-cell modelling: Cardiac sodium-potassium pump as a case study. *Progress in Biophysics and Molecular Biology*, 85(2-3), pp.387–405.

Le Tissier, M.D., 1987. *The nature and construction of skeletal spines in Pocillopora damicornis (Linnaeus)*. Newcastle upon Tyne.

Venn, A. et al., 2011. Live tissue imaging shows reef corals elevate pH under their calcifying tissue relative to seawater. *PLoS ONE*, 6(5).

Walter, L.M. & Morse, J.W., 1985. The dissolution kinetics of shallow marine carbonates in seawater: A laboratory study. *Geochimica et Cosmochimica Acta*, 49, pp.1503–1513.

Zeebe, R.E. & Wolf-Gladrow, D.A., 2001. *CO2 in Seawater: Equilibrium, Kinetics, Isotopes*, Amsterdam: Elsevier Ltd.

Zoccola, D. et al., 2015. Bicarbonate transporters in corals point towards a key step in the evolution of cnidarian calcification. *Nature Scientific Reports*, pp.1–11.

4. Increasing frequency of heat waves will cause the extinction of red coral shallow banks

Abstract

Frequency and severity of heat waves is expected to increase as a consequence of climate change with important consequences on human and ecosystems health (Seneviratne et al. 2013). However, while many studies explored heat wave impacts on terrestrial systems (Fischer et al. 2007, Schär et al. 2004), few studies dealt with marine systems, so that both the expected changes in marine heat waves occurrence and effects on marine organisms and ecosystems remain less understood and surprisingly poorly quantified.

Here we quantify how much more frequent, severe, and depth-penetrating marine heat waves will be in the next decades, and show that this will impact on many organisms that live in shallow water or have reduced motility (e motility, and related economic activities. In particular, shallow (up to 40 meters) banks of red coral - a commercially exploited benthic species endemic of the Mediterranean Sea and already subjected to heat-related mass mortality events - are doomed to extinction. Results also provide essential information to assess heat wave impacts on other species with no or reduced motility (e.g. bivalves), ecologically important habitats (e.g. coralligenous) and aquaculture activity.

4.1 Study

Climate change is expected to alter not only the average values of environmental properties, but also the extreme ones, as well as the frequency of occurrence of conditions nowadays considered as extreme (Fig. 4.1). This has the potential to significantly impact the state and dynamics of biological organisms by exposing them to conditions that are different from those they are adapted to and possibly outside their tolerance limits (Thompson et al. 2013). Furthermore, while many organisms have the capabilities to cope with and adapt to new conditions, this is not fast, nor free. Biological adaptation takes time, and coping with adverse conditions requires an energetic cost and leaves an organism stressed and more vulnerable to other pressures. Therefore acclimation mechanisms are likely to be effective for slow gradual changes, such as those occurring to averages values, but less effective in buffering the impact of extreme or episodic events.

Marine heat waves are events during which sea temperature exceeds a given threshold for a number of consecutive days. They might be severe because of the level of temperature, the duration of the event, or both. Obviously different organisms present different vulnerabilities to a given event, depending on species-specific thermal tolerance limits.

The effects of heat waves on land have been extensively analyzed (Wernberg et al. 2013, Garrabou et al. 2003, Marba & Duarte 2010), also because of consequences on human health and agriculture. The effects of heat waves on ocean properties and marine life have been less explored, possibly because of the buffering effect of ocean water, which confines the impacts to the upper part of the sea. However, marine heat waves effects can be quite relevant in shallow waters and for organisms which - being sessile or having reduced motility - cannot move to colder water. Similarly, heat waves will impact on organisms which - being exploited by aquaculture activities - are kept in surface water by floating cages (e.g. fishes) or devices (e.g. bivalves). Notable examples of significant impacts of heat waves on Mediterranean marine ecosystems are provided by the 1999 and 2003 summers, which caused mass mortality events in a variety of organisms (Garrabou et al. 2001, 2009) and caused relevant economic damages to aquaculture activities.

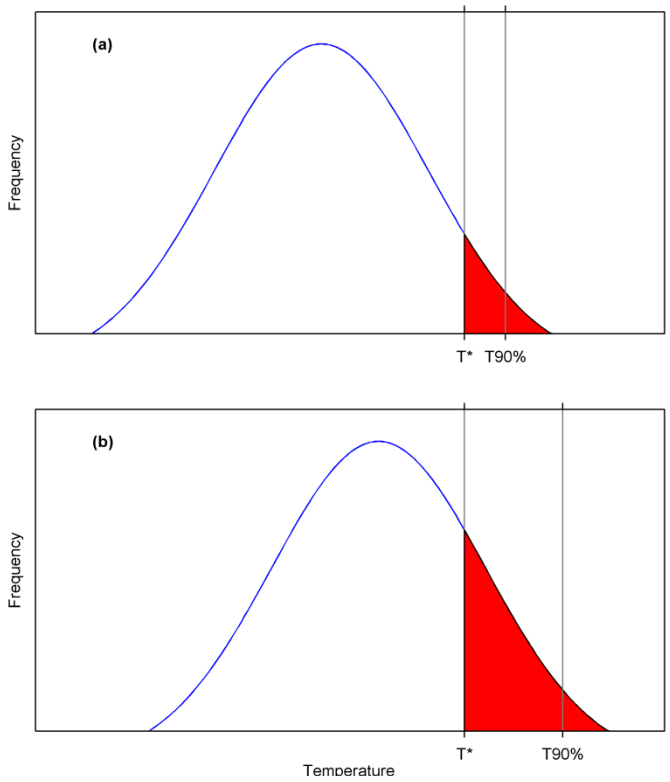

Fig. 4.1 Idealized present (a) and future (b) frequency distribution of temperature; under future conditions average and extreme temperatures will be higher, as well as the number of days exceeding a given threshold temperature (shaded area).

In this paper we: a) quantified the changes in spatial distribution, frequency and severity of marine heat waves in the Mediterranean Sea by analyzing projections from a state of the art, high resolution, physical oceanography model off-line forced by a standard IPCC climate change scenario; and b) produced risk assessment maps for red coral (*Corallium rubrum)*, by integrating the information on 3D spatial distribution of marine heat waves with a mortality model derived from experimental findings and knowledge on red coral physiology.

C. rubrum is a slow growing, long lived, gorgonian coral endemic of the Mediterranean. It is commonly found on hard substrates, on steep walls and overhangs, below 20 m depth and up to more than 100 m, and it is associated with the coralligenous communities (Tsounis et al. 2010). It is exploited by the jewelry industry since ancient times for its glossy red skeleton and currently considered over-harvested (Tsounis et al. 2010,

2013). Besides fishing, shallow red coral populations have been subject in summers 1999 and 2003 to mass mortalities that occurred jointly with positive summer temperature anomalies(Garrabou et al. 2001, 2009, Torrents et al. 2008).

Rossi and Tsounis (2007) and Coma et al. (2009) advocated that mass mortalities are triggered by a combination of increased metabolic demands, due to high temperature, and summery food shortage; however, prolonged exposure to high temperature is known to substantially increases mortality risk, as shown in Torrents et al. 2008.

We explored the potential effect of the forecasted increase in heat wave frequency and magnitude on natural banks of red coral. The response of such organisms, however, provides indications on the response of coralligenous communities too and, possibly, of other organisms. Furthermore, and importantly, our projections of heat wave occurrence can be readily used - in conjunction with specie specific thermal tolerance information - to assess the impact on marine heat waves on any marine organism for any point and any depth of the Mediterranean sea.

We quantified the spatial distribution of marine heat waves with reference to three temperatures: 25, 27 and 30°C. Model projections show that the number of consecutive days per year with temperature exceeding those thresholds expands under future conditions (Fig. 4.2). The change is not spatially homogeneous, with the eastern basin showing the highest increments. The surface layers undergo the largest change, whereas below 40m depths the differences between present and future conditions are negligible. Generally, the 25°C threshold is exceeded far more often than the 27°C threshold. Conversely, if heat waves are assessed against the 30°C threshold, the differences between present and future conditions are appreciable only in easternmost (and southernmost) coasts of the Levantine basin.

The spatial distribution of red coral mortality risk is illustrated in Fig. 4.3, which shows the classification of sites in *no mortality*, *partial mortality*, and *total mortality* risk classes, for different depths and under both contemporary and future conditions. The figure also indicates the sites in which red coral banks are observed (green dots). Mortality risk estimates were derived also for zones where red coral banks are currently not present, because we aim to map potential rather than realized distribution.

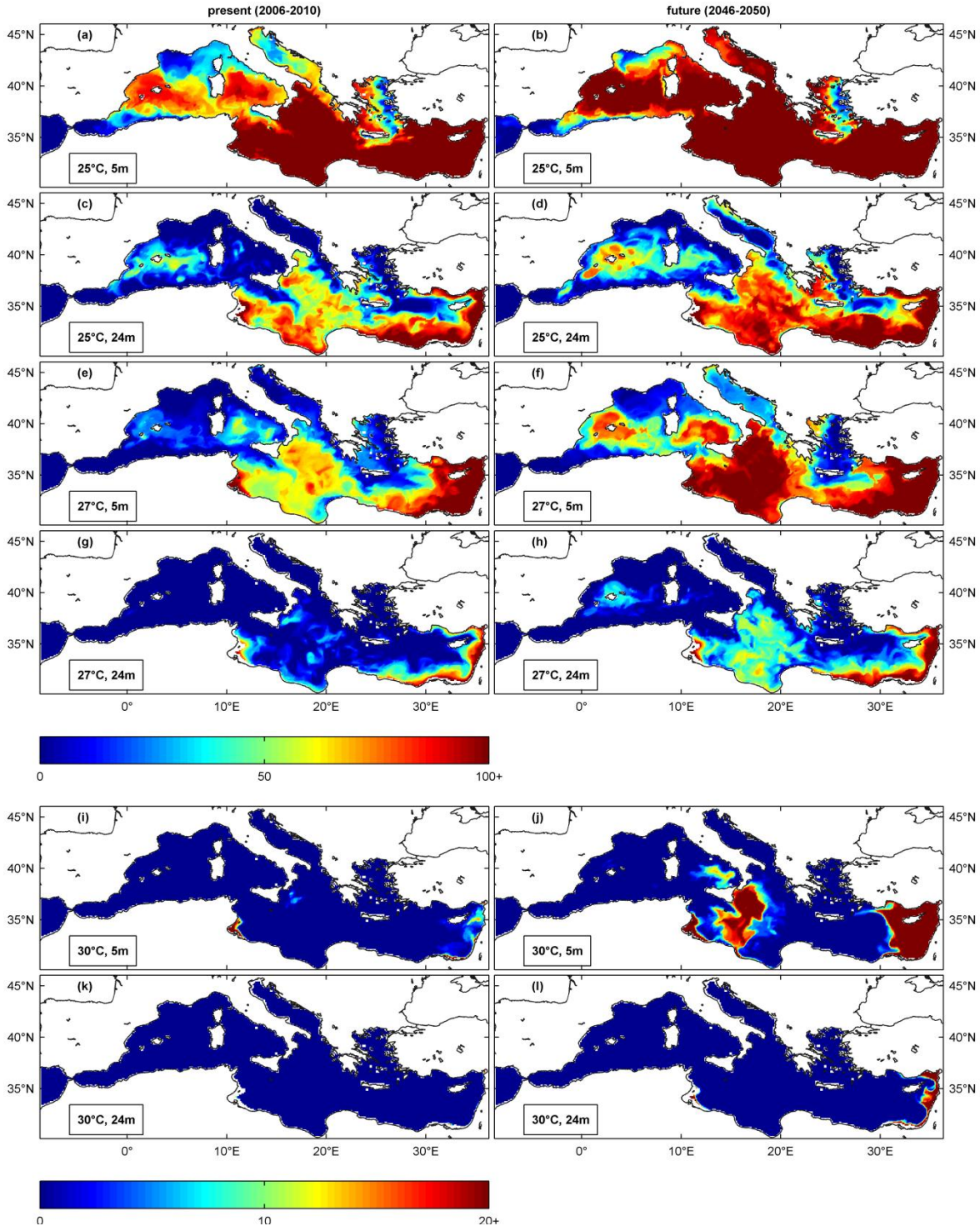

Fig. 4.2 Max yearly number of consecutive days with temperature above 25, 27 and 30°C, for present (2006-2010) and future (2046-2050) conditions at sample depths of 5, and 24 m.

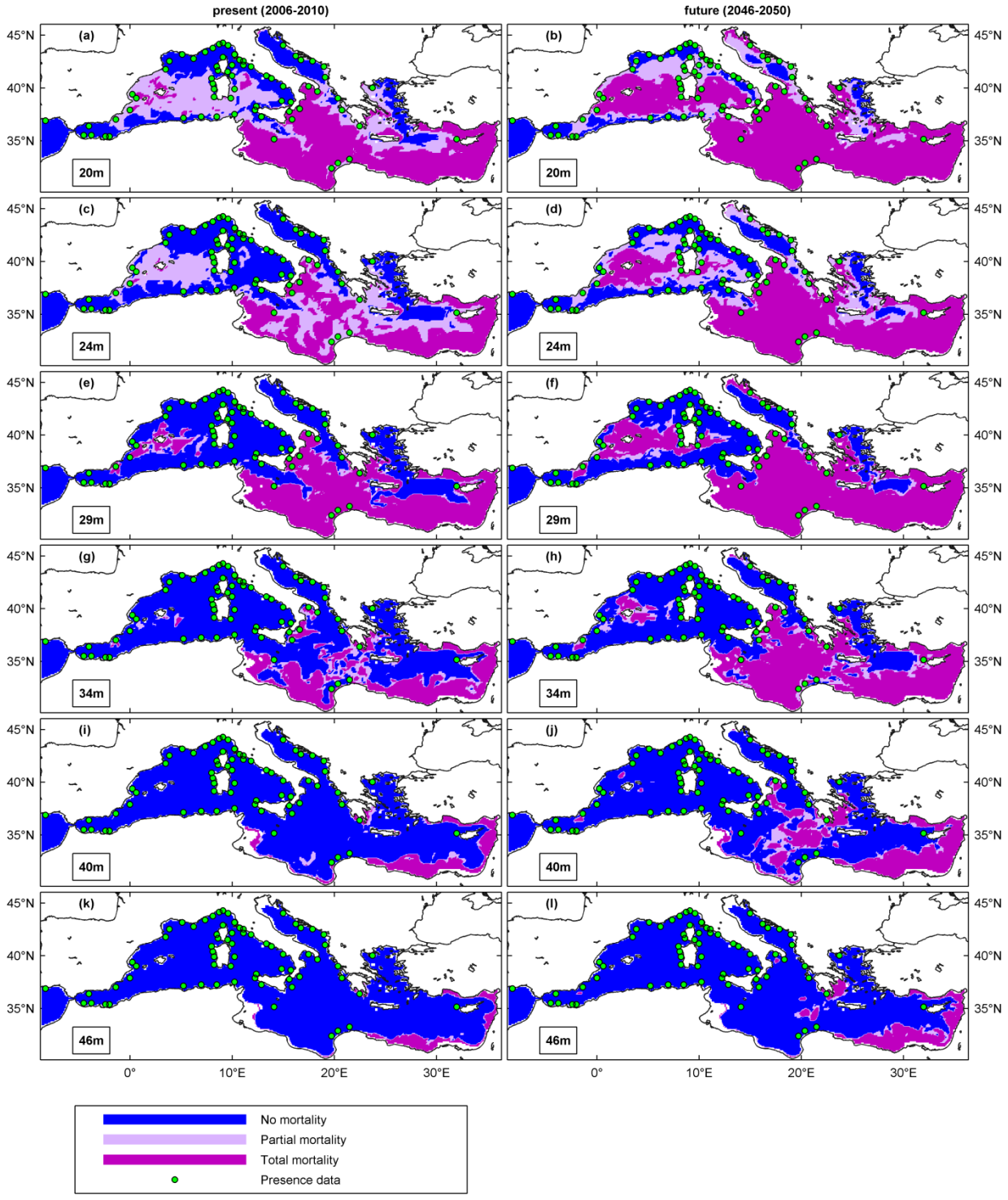

Fig. 4.3 Estimated red coral mortality risk under present and future conditions at different depths.

Results show how the presence records of red coral banks are spatially confined to the area currently classified as *no mortality*, or - in few cases - *partial mortality*.

Under present conditions extensive *partial mortality* zones are present in shallow waters in South Western Mediterranean and Western Tyrrhenian Sea. The extent of these zones becomes negligible below 34 m depth, which is consistent with the reported presences of deep banks. On the contrary no mortality risk is detected in the basins where red coral shallow banks have been most often signaled: Eastern Tyrrhenian Sea, Ligurian Sea and coastal zones of North Western Mediterranean. Extensive *total mortality* zones are a common feature of shallow waters in the eastern basin, including the Ionian and Aegean seas where red coral is present but extremely rare and found at depths greater than those interested by the heat waves related mortality here analyzed (Salomidi et al. 2009).

Under future conditions, the extensions of both the *partial* and *total mortality* areas increase. At 20m depth, in the North and Central Adriatic and North Tyrrhenian (currently classified as *no mortality* area) the higher occurrence of heat waves will significantly reduce the extension of *no mortality* areas, and the chance of survival of red coral shallow banks. Negative effects are projected also for banks along the Sardinia coast, the Sicily coast and the Greek seas.

As expected, the adverse impacts of heat waves markedly decrease with water depth, so that at around 40m the changes in mortality risk classes distribution are negligible, with the only exception of the coastal zones in the Levantine basin where red coral presence has - however - never been reported yet.

Future potential *total mortality* zones extend through all the Levantine and Ionian basins, up to the southern costs of Italy and Eastern Aegean Sea. South Tyrrhenian and South Western Mediterranean are also heavily impacted in the shallower portion of the bathymetric range (up to 35 - 40m). The Balearic Islands appear to be a particularly vulnerable zone within Western Mediterranean. Large mortality zones, mostly *partial mortality*, are present also in the Northern Tyrrhenian Sea and North Western Mediterranean, where shallow red coral banks are currently abundant, and in the Eastern Adriatic Sea at depths up to 35m. Few coastal zones do not present mortality risk at shallow depths; those include

the gulf of Marseille, the Alboran Sea and the coast affected by the Algerian current originated by cool Atlantic waters.

Our results support that summer heat waves of magnitude capable to cause massive mortality in red coral banks may become commonplace in the near future and could affect red coral as well as other typical coralligenous species. In fact, even though the exposure thresholds used in this study were determined for red coral, mortality events similarly affected several coralligenous species (Garrabou et al. 2001, Coma et al. 2009), pointing at comparable thermotolerance thresholds. Demographic studies (Santangelo et al. 2012) pointed out that, despite of recolonization phenomena, should these adverse events become more frequent, populations might not be able to recover.

The physiological mechanism underlying mortality has not yet been elucidated. Whilst some studies suggest a combined effect of increased metabolism and summery food shortage (Rossi & Tsounis 2007, Coma et al. 2009), recent studies point to a mismatch between oxygen supply and demand (verberk and Bilton 2011, Kleypas 2015). Although not mutually exclusive, we argue the second hypothesis may better explain the short time scales (few days) over which mortality events took place.

Impacts are predicted in geographical zones where shallow red coral banks are known to be present, including Eastern Tyrrhenian coasts, Sardinia and Corsica and the Spanish coast of Western Mediterranean. Few refuge zones will remain along the French and Algerian coasts and Alboran Sea. On the other hand populations dwelling below 40m depth are not predicted to be impacted significantly.

Several studies highlight that ectothermic species, such as corals or mussels, have the capability to tolerate exposure to temperatures close to the their upper limits, and even to adapt their thermal limits (Middlebrook et al. 2008, Buckley et al. 2001). However, it must be considered that acclimation might not be very effective for episodic exposures to extreme conditions, and thermal acclimation limits anyway exist. In fact, other studies reported a decrease in tolerance to high temperature after repeated exposures (Jones et al. 2008), and raised concerns about the capability of marine organisms to cope with a trend of increasing frequency of heat wave events. On the other hand, the recent extinction of vermetids along the Israeli coast (Galil 2013) already provides an example of the impact of temperature on

sensitive organisms. Furthermore, besides heat waves impacts, red coral is also subjected to other stressors, such as acidification and intense harvesting, so that heat waves impact will sum up, especially for the largest specimen that are the primary target of fisheries and also display the highest vulnerability to heat (Garrabou et al. 2001).

The impacts on red coral also exemplify analogous impacts that will occur to other species that have reduced motility or are confined to surface layers. Notably, aquaculture activities - which exploit the growth of organisms in floating devices - will surely be impacted by an increase in frequency of marine heat waves. As an example, temperature levels of 25°C have been identified as an upper limit for mussels normal physiological activities (Anestis et al. 2010), indicating that Mediterranean mussels already live close to their thermal acclimation limits. Furthermore total mortality of mussels has been observed when seawater temperature reached 28°C for more than 10 days (Ramon et al. 2007). Consequently, the projections in Fig. 4.2 (surface water) clearly suggest a significant reduction in the number of suitable farming sites, which are currently distributed all over the Mediterranean coasts. Similarly, coralligenous outcrops - a collective term referring to complex biogenic structure made by the outgrowth of encrusting calcareous algae on hard substrate in relatively shallow waters - would also suffer. Also in this case, mortality events might cause -besides ecological damages - a direct economic cost, because of the impacts on scuba diving tourism (Rodrigues et al. 2013).

4.2 Methods

Results of a 50 years (2000-2050) numerical simulation performed with a state of the art ocean model under RCP8.5 IPCC climate change scenario have been post-processed to assess physical properties of the Mediterranean Sea under contemporary (2006-2010) and future (2046-2050) conditions.

The physical model used for the projection is the NEMO model (Madec 2008, see also http://www.nemo-ocean.eu) already used in the Mediterranean Sea (Oddo et al. 2009, Lazzari et al. 2014), and also routinely used to produce short term forecast of the Mediterranean Sea

since 2007 (http://www.myocean.eu). For these specific simulations, the transport is computed with a horizontal resolution of 1/16 of degree (which corresponds to about 5 km) and with a vertical z-coordinate discretization in 43 levels with a grid spacing ranging from 3 meters in surface layers to 350 meters in the bottom layers (MED16 OGCM model, Béranger et al. 2005). A comparison of model output with projections made by an ensemble of five physical models of the Mediterranean Sea (Gualdi 2013) confirmed that our projections fall within the range projected by an ensemble of state of the art regional models of the Mediterranean Sea, and highlights how there is an high consensus in expecting a significant warming of the Mediterranean Sea in the next decades.

Post-processing of model output permitted us to reconstruct the spatial distribution (maps) of heat waves occurrence, by recording - for each point of the Mediterranean Sea and for each considered time period - the maximal number of consecutive days above a given temperature thresholds.

Upper thermal limits for red coral specimen have been estimated by Torrents et al. (2008), and are reported in Table 1. These authors exposed corals to different treatments (24, 25,27,30 °C) and concluded that exposure to different temperature thresholds result in partial or total mortality of the colonies, as summarized in Table 1. As an example, exposure for 3 consecutive days at 27°C would cause partial mortality, and exposure for 5 days to the same temperature will cause total mortality. Furthermore, different mortalities have been observed for specimen collected from shallow populations vs. deep populations. Deep corals result to be more sensitive to warming than the shallow ones, likely because the latter are acclimated to warmer temperature than the former.

Thresholds	Shallow population	Deep population
Days before partial mortality at 24°C	-	-
Days before partial mortality at 24°C	-	-
Days before partial mortality at 25°C	14	9
Days before total mortality at 25°C	-	19
Days before partial mortality at 27°C	3	2
Days before total mortality at 27°C	5	3
Days before total mortality at 30°C	1	1

Table 4.1 Upper thermal thresholds of Corallium rubrum adapted from Torrents et al. (2008).

Current and future mortality risk estimates have been derived by combining the spatial distribution of heat waves occurrence (Fig. 4.3) and the vulnerability information summarized in Table 4.1.

We assessed the mortality risk of colonies in the 0-30 meters depth range against thresholds derived from experiments on shallow specimen, and the mortality risk of deeper colonies against deep specimen thresholds. To minimize the effect of inter-annual variability two five-year periods have been considered (2006-2010 and 2046-2050). Mortality criteria were considered met if exposure threshold were exceeded at least once in each five-year period.

4.3 References

Anestis, A., et al. 2010. Response of Mytilus galloprovincialis (L.) to increasing seawater temperature and to marteliosis: metabolic and physiological parameters. *Comp. Biochem. Physiol., Part A: Mol. Integr. Physiol.* 156(1), 57–66.

Béranger, K., Mortier, L. & Crépon, M. 2005. Seasonal variability of water transport through the Straits of Gibraltar, Sicily and Corsica, derived from a high–resolution model of the Mediterranean circulation. *Prog. Oceanogr.* 66, 341–364.

Buckley, B. A., Owen, M. E. & Hofmann, G. E. 2001. Adjusting the thermostat: the threshold induction temperature for the heat shock response in intertidal mussel (genus Mytilus) changes as a function of thermal history. *J. Exp. Biol.* 204, 3571–3579.

Coma, R. et al. 2009. Global warming–enhanced stratification and mass mortality events in the Mediterranean. *Proc. Nat. Acad. Sci.* 106(15), 6176–6181.

Fischer, E.M., Seneviratne, S. I., Lüthi, D. & Schär, C. 2007. Contribution of land-atmosphere coupling to recent European summer heat waves. *Geophys. Res. Lett.* 34, L06707, doi:10.1029/2006GL029068.

Galil, B.S. 2013. Going going gone: the loss of a reef building gastropod (Mollusca: Caenogastropoda: Vermetidae) in the southeast Mediterranean Sea. *Zool. Middle. East.* 59, 179–182.

Garrabou, J., Perez, T., Santoretto, S. & Harmelin, J. G. 2001. Mass mortality event in red coral Corallium rubrum populations in the Provence region (France, NW Mediterranean). *Mar. Ecol. Prog. Ser.* 217, 263–272.

Garrabou, J. et al. 2009. Mass mortality in Northwestern Mediterranean rocky benthic communities: effects of the 2003 heat wave. *Glob. Change Biol.* 15, 1090-1103.

Gualdi, S. et al. 2013. The CIRCE Simulations: Regional Climate Change Projections with Realistic Representation of the Mediterranean Sea. *Bull. Amer. Meteor. Soc.* 94, 65–81.

Jones, S.J., Mieszkowska, N. & Wethey, D. S. 2008. Linking Thermal Tolerance to Biogeography: Mytilus edulis (L.) at its Southern Limit on the East Coast of the United States. *Biol. Bull.* 217, 73–85.

Kleypas, J. 2015. Invisible barriers to dispersal. *Science* 348:1086.

Lazzari, P. et al. 2014. The impacts of climate change and environmental management policies on the trophic regimes in the Mediterranean Sea:

Scenario analyses. *J. Mar. Syst.* 135, 137–149.

Madec, G. 2008. NEMO Ocean Engine. In: Note du Pole de Modelisation Institute Pierre-Simone Lapalce No 27 (IPSL), France, pp. 1288–1619.

Marba, N. & Duarte, C.M. Mediterranean warming triggers seagrass (Posidonia oceanica) shoot mortality. *Glob. Change Biol.* 16, 2366–2375.

Middlebrook, R., Hoegh-Guldberg, O. & Leggat, W. 2008. The effect of thermal history on the susceptibility of reef building corals to thermal stress. *J. Exp. Biol.* 211, 1050–1056.

Oddo, P. et al. 2009. A nested Atlantic–Mediterranean Sea general circulation model for operational forecasting. *Ocean Sci* 5(4), 461–473.

Ramon, M., Fernández, M. & Galimany, E. 2007. Development of mussel (Mytilus galloprovincialis) seed from two different origins in a semi-enclosed Mediterranean Bay (N.E. Spain), *Aquaculture* 264, 148–159.

Rossi, S. & Tsounis, G. 2007. Temporal and spatial variation in protein, carbohydrate, and lipid levels in Corallium rubrum (Anthozoa, Octocorallia). *Mar. Biol.* 152, 429–439.

Rodrigues, L.C., van den Bergh, J. C. J. M. & Ghermandi, A. 2013. Socio-economic impacts of ocean acidification in the Mediterranean Sea. *Mar. Policy* 38, 447 465.

Santangelo, G. et al. 2012. Demography of long–lived octocorals: survival and local extinction. In: Proceedings of the 12th International Coral Reef Symposium, Cairns, Australia, 9–13 July 2012.

Salomidi, M., Smith, C., Katsanevakis, S., Panayotidis, P. & Papathanassiou, V. 2009. Some observations on the structure and distribution of gorgonian assemblages in the eastern Mediterranean sea. In: Actes du 1er Symposium sur la Conservation du Coralligène et autres bio concrétions de Méditerranée. Tabarka, Tunisia, 16–17 Jan. 2009.

Schär, C., Jendritzky, G. 2004. Hot news from summer 2003. *Nature* 432, 559–560.

Seneviratne, S.I., Donat, M.G., Mueller, B., & Alexander, L. 2013. No pause in the increase of hot temperature extremes. *Nature Cim. Change* 4, 161–163.

Thompson, R.M., Beardall, J., Beringer, J., Grace, M. & Sardina, P. 2013. Means and extremes: building variability into community-level climate change experiments. *Ecol. Lett.* 16(6), 799–806.

Torrents, O., Tambutté, E., Caminiti, N. & Garrabou, J. Upper thermal thresholds of shallow vs. deep populations of the precious

Mediterranean red coral Corallium rubrum (L.): Assessing the potential effects of warming in the NW Mediterranean. *J. Exp. Mar. Biol. Ecol.* 357, 7–19.

Tsounis G., et al. 2010. The Exploitation and Conservation of Precious Corals. Oceanogr. *Mar. Biol.* 48, 161–212.

Tsounis, G., Rossi, S., Bramanti, L. & Santangelo, G. 2013. Management hurdles in the sustainable Management of Corallium rubrum. *Mar. Policy* 39, 361–364.

Verberk, W.C.E.P. & Bilton, D. T. 2011. Can oxygen set thermal limits and drive gigantism? *PLoS ONE* 6(7), doi:10.1371/journal.pone.0022610.

Wernberg, T. et al. 2013. An extreme climatic event alters marine ecosystem structure in a global biodiversity hotspot. *Nature Clim. Change*. 3, 78–82.

5. Calcareous Bio-Concretions in the Northern Adriatic Sea: Habitat Types, Environmental Factors that Influence Habitat Distributions, and Predictive Modelling

Annalisa Falace[1], Sara Kaleb[1], Daniele Curiel[2], Chiara Miotti[2], Giovanni Galli[1,3], Stefano Querin[3], Enric Ballesteros[4], Cosimo Solidoro[3], Vinko Bandelj[3]

1 Department of Life Sciences, University of Trieste, Trieste, Italia, 2 SELC Society Marghera, Venezia, Italia, 3 National Institute of Oceanography and Experimental Geophysics-OGS, Trieste, Italia, 4 Centre d'Estudis Avançats de Blanes-CSIC, Girona, España.

Published in *PLoS ONE*, 10(11), doi: 10.1371/journal.pone.0140931

Abstract

Habitat classifications provide guidelines for mapping and comparing marine resources across geographic regions. Calcareous bio-concretions and their associated biota have not been exhaustively categorized. Furthermore, for management and conservation purposes, species and habitat mapping is critical. Recently, several developments have occurred in the field of predictive habitat modeling, and multiple methods are available. In this study, we defined the habitats constituting northern Adriatic biogenic reefs and created a predictive habitat distribution model. We used an updated dataset of the epibenthic assemblages to define the habitats, which we verified using the fuzzy k-means (FKM) clustering method.

Redundancy analysis was employed to model the relationships between the environmental descriptors and the FKM membership grades. Predictive modelling was carried out to map habitats across the basin. Habitat A (opportunistic macroalgae, encrusting Porifera, bioeroders) characterizes reefs closest to the coastline, which are affected by coastal currents and river inputs. Habitat B is distinguished by massive Porifera, erect Tunicata, and noncalcareous encrusting algae (Peyssonnelia spp.). Habitat C (non-articulated coralline, Polycitor adriaticus) is predicted in deeper areas. The onshore-offshore gradient explains the variability of the assemblages because of the influence of coastal freshwater, which is the main driver of

nutrient dynamics. This model supports the interpretation of Habitat A and C as the extremes of a gradient that characterizes the epibenthic assemblages, while Habitat B demonstrates intermediate characteristics. Areas of transition are a natural feature of the marine environment and may include a mixture of habitats and species. The habitats proposed are easy to identify in the field, are related to different environmental features, and may be suitable for application in studies focused on other geographic areas. The habitat model outputs provide insight into the environmental drivers that control the distribution of the habitat and can be used to guide future research efforts and cost-effective management and conservation plans.

5.1 Introduction

Coralligenous outcrops are among the most diverse and representative Mediterranean benthic ecosystems, and they are produced by the interplay between calcareous organism building processes and physical and biological erosional processes (Ballesteros 2006). Several types of coralligenous morphologies have been identified in the literature (Ballesteros 2006, Bosence 1983, 1985, Di Geronimo et al. 2001a, 2001b, 2002, Bracchi et al. 2015). The main recognized morphologies are reef banks, which are flat structures (ranging from 0.5 to 4 m in height) built over more or less horizontal substrates, and coralligenous rims, which are structures that grow on vertical cliffs and are generally located in shallower waters (Ballesteros 2006, Bracchi et al. 2015, Pérès & Picard 1964, Laborel 1987).

Most scientists consider coralligenous outcrops to be seascapes or community mosaics rather than a single community. These biogenic structures are complex and contain areas dominated by algae, suspension feeders, borers, or even soft-bottom fauna living in the sediment deposited in cavities and holes (UNEP-MAP-RAC/SPA 2008). Certain dominant species that characterize the calcareous bio-concretions are long-lived engineering species, which makes this habitat extremely vulnerable to disturbances (Ballesteros 2006, UNEP-MAP-RAC/SPA 2008, Kipson et al. 2011, Salomidi et al. 2012).

Because of their extent, biodiversity, and implications for fisheries and carbon regulation, calcareous biogenic habitats are considered priority habitats at the European and regional levels (UNEP-MAP-RAC/SPA 2008, Canals & Ballesteros 1997, Martin et al. 2014).

Marine habitat classifications are performed to provide standard nomenclature and guidelines for describing, mapping, and comparing marine environments and associated assemblages across geographic regions (Costello 2001). Moreover, habitat classifications assist in the management of marine resources and the quantification of ecosystem processes and services at different temporal and spatial scales. Finally, habitats can be used as a surrogate for biodiversity, and they provide guidance for monitoring programs (Diaz et al. 2004). For example, the identification of thresholds between the ecological statuses of priority habitats in the

European Marine Strategy Framework Directive (MSFD, 2008/56/EC) of "Good" and "Not Good" is based on "Habitat Distribution," "Habitat Extent", and "Habitat Condition." The geomorphological features of coralligenous build-ups and their associated biota have not been exhaustively categorized. In particular, coralligenous build-ups that occur in areas where boulders are associated with sand and mud, such as in the northern Adriatic Sea to the Apulia region, should be considered a specific type (Costello & Emblow 2005). According to the European Habitats Directive (92/43/EEC), the marine rocky outcrop classification is included in the Annex I habitat types as "1170-Reefs" (36). In the context of the Barcelona Convention (UNEP/OCA/ MED WG149/5 Rev. 1, 2006), which is an elaboration of the CORINE biotopes nomenclature (Moss & Wyatt 1994), coralligenous biocoenosis (IV.3.1) is included within the circalittoral hard beds and rocks categories and contains 15 different facies (UNEP-MAP-RAC/SPA 2008). Finally, according to the MSFD, coralligenous biocoenoses fall into the categories "Facies and associations of coralligenous biocoenosis (III.6.1.35)" and "Shallow sublittoral rock and biogenic reef". However, these bulk categories are not appropriate for management purposes because they each encompass a large range of biogenic natural habitats that can differ significantly in their ecological and conservation features (Borg & Schembri 2002). Europe generally employs the European Nature Information System (EUNIS) habitat classification scheme (Davies & Moss 1999; http://eunis.eea.europa.eu); however, the development of the marine EUNIS classification is primarily based on Atlantic ecosystems, whereas Mediterranean ecosystems are roughly incorporated into the EUNIS list using habitats from the Barcelona Convention. Thus, coralligenous habitats are currently classified as "A4.26: Mediterranean coralligenous communities moderately exposed to hydrodynamic action" and "A4.32: Mediterranean coralligenous communities sheltered from hydrodynamic action" in the EUNIS system.

Despite their ecological, aesthetic, and economic value, complete and up-to-date baseline information on coralligenous outcrops is not available (Kipson et al. 2011), and most of the current information is derived from the western Mediterranean (Martin et al. 2014), where coralligenous outcrops are unlikely to occur in sedimentary zones, enclosed estuarine environments, and sandy areas with low salinities, such as river mouths (Martin et al. 2014). However, hundreds of calcareous bio-concretions are

scattered on the muddy-detritic bottom of the northern Adriatic Sea. These biogenic outcrops are considered to have a significant degree of similarity with coralligenous outcrops (Casellato & Stefanon 2008, Ponti et al. 2011, Curiel et al. 2012), although their composition and overall structure show striking differences (Curiel et al. 2012), and according to the EUNIS classification, they should be classified as a different habitat.

The increasing awareness of the importance and fragility of these habitats has led to global efforts to conserve these ecosystems according to several legally binding or voluntary international initiatives. For environmental research, resource management, and conservation planning, mapping is critical, although it is not an easy task in marine habitats that might be distributed over hundreds of square kilometers. In recent decades, many developments have occurred in the field of species and habitat distribution modeling, and multiple methods are now available (Elith et al. 2011, Guisan & Zimmermann 2000). The construction of a geographical distribution model requires observations of species/habitat occurrences and environmental variables that are considered to influence habitat suitability (Franklin & Miller 2009). The quantification of such species–environment relationships represents the foundation used to predict the likelihood of a species occurring at a given location (Guisan & Zimmermann 2000).

Currently, predictive habitat modeling is performed at regional or global scales and appears to be a cost-effective method of identifying the location of vulnerable marine habitats, such as coralligenous reefs, although this modeling does not provide habitat maps. Predictive habitat modeling provides insight into the environmental drivers that control the distribution of vulnerable marine habitats and can be used to guide research efforts (Martin et al. 2014, Davies & Guinotte 2011, Giakoumi et al. 2013).

In this study, we intend to provide (1) a definition of the different habitats constituting northern Adriatic biogenic reefs, (2) an assessment of the main physical and environmental variables accounting for their distribution and (3) a predictive habitat map to indicate the occurrence of biogenic reef habitats in the northern Adriatic Sea.

5.2 Material and Methods

Study area

The northern Adriatic Sea is the most dynamic sub-basin of the Mediterranean Sea (Artegiani et al. 1997, Russo & Artegiani 1996), and it is characterized by strong river runoff and wide seasonal and interannual variability in temperature and salinity. The Adriatic Sea is surrounded by mainland areas that exhibit sharp contrasts in tectonism, topography, climate, and fluvial inputs. Northwestern Adriatic shores are sedimentary and contain a continuous line of coastal lagoons. The water density gradient between the northern and the southern Adriatic Sea is the most important factor that triggers the movement of water in a primarily counterclockwise current that flows down to the Otranto Strait and into the Mediterranean Sea (Zore-Armanda 1969). River discharges show a remarkable seasonality, with the highest flow rates usually occurring in late spring and autumn. The concentration of inorganic nutrients is highly variable and is mainly related to river inputs (Burba et al. 1994).

From the Gulf of Trieste to the Po River delta, biogenic outcrops, locally known as "tegnùe" or "trezze", are scattered on the soft bottom, and they were first identified as beach rocks (Braga et al. 1969, Stefanon 1967, Stefanon 1970, Newton & Stefanon 1975). Recent studies have related their genesis to seeping methane, cementation, and lithification processes (Colantoni et al. 1998, Conti et al. 2002, Gordini et al. 2004, 2012, Stefanon & Zuppi 2000). These rocky outcrops are "calcareous bio-concretions" derived from the building action of calcareous organisms on hard substrata of diverse geological origins. The origins of the complex primary substrata consist of a carbonatic conglomeration of sandy sediments mixed with shells and other exoskeletons. The buildup process may be accelerated by the seepage of methane through the sediments and by subtidal freshwater streams (Gordini et al. 2012). The calcareous bio-concretions display a broad range of geomorphologies and extend from a few to several thousands of square meters. The offshore bio-concretions situated in front of the Venice Lagoon are sloped and stretch parallel to the coast. Several outcrops show large horizontal surfaces, whereas others are composed of scattered conglomerates of small rocks. The surrounding sea floor is mainly detritic

because it accumulates skeletons of species growing either in the sediment or in the neighboring outcrops.

Habitat typology

We used an updated spatial dataset based on information provided by peer-reviewed articles, regional, national, and international reports and by recently unpublished data obtained by the authors to produce an overview of the epibenthic assemblages associated with the northern Adriatic calcareous bio-concretions. Data on macroalgal assemblages were obtained from studies performed over an approximately 30-year period (Ponti et al. 2011, Curiel et al, 2012, Curiel et al. 2001, 2010a, 2010b. Curiel & Molin 2010, Ponti & Mescalchin 2008, Solazzi & Tolomio 1981) as well as from recent studies.

Data on benthic invertebrates were obtained from peer-reviewed articles (Casellato & Stefanon 2008, Ponti et al. 2011, 2014, Gabriele et al. 1999, Casellato et al. 2005, 2007, Mizzan 1992) and national unpublished reports (Faresi 2010, ARPAV 2010, Magistrato Alle Acque di Venezia–Corila-SELC 2006).

Habitat typology was established by expert judgment based on knowledge of the assemblages and the updated dataset. This typology was then verified on a large scale using 33 outcrops for which comparable data were available (Fig 5.1).

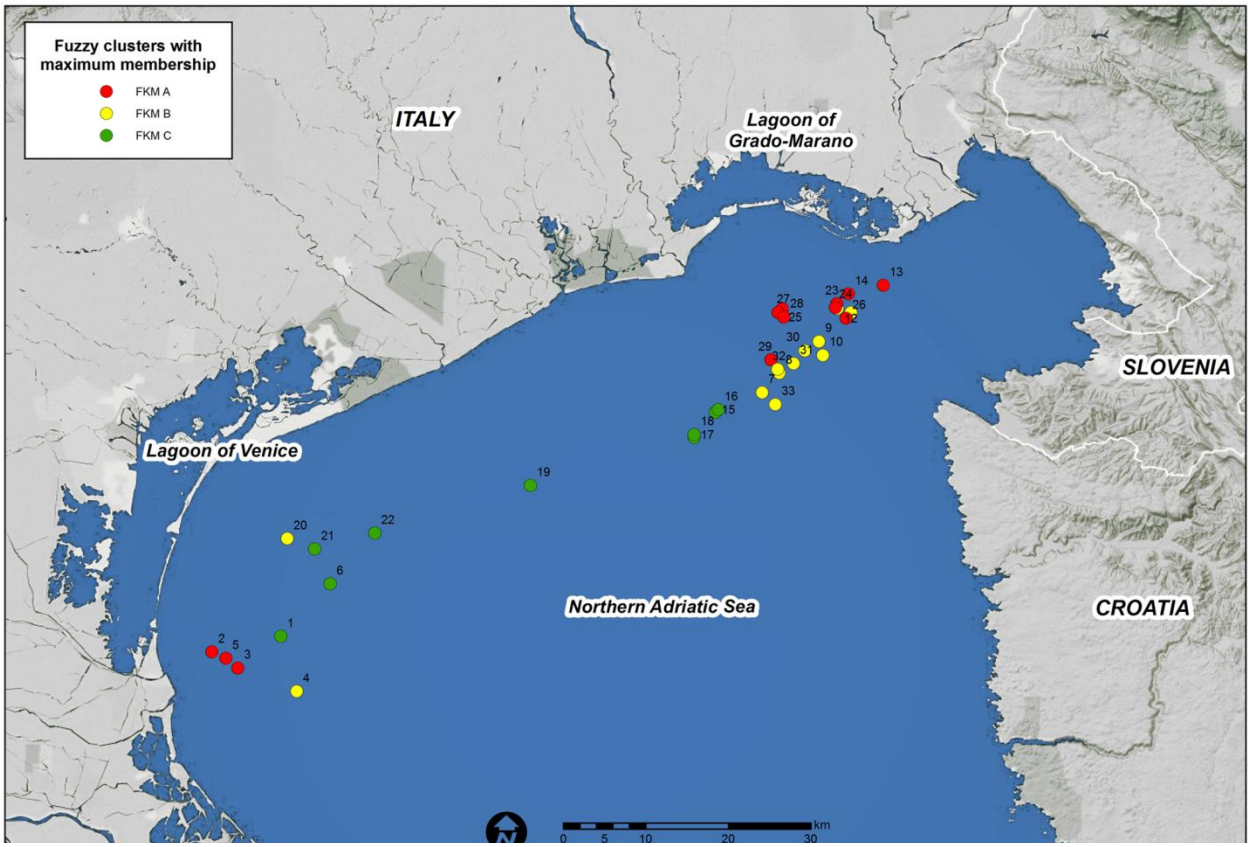

Fig. 5.1 Occurrences of the 3 habitat typology outcrops across the northern Adriatic Sea (original copyright 2015).

Fuzzy clustering methods

To evaluate the habitat typology produced through "a priori expert judgment," we used the fuzzy k-means (FKM) clustering method (Bezdek 1981) and performed the clustering with the parameter of fuzziness set to 2 and the number of random initializations set to 1000. All FKM calculations were performed using the fclust package for R (Ferraro & Giordani 2015).

Environmental database

Data on water temperature, salinity, dissolved oxygen and chlorophyll a, and ammonium, nitrate and phosphate concentrations were extracted from

the dataset of vertical seawater profiles collected by Solidoro et al. (2009) from 1986–2006; ii) the Regional Water Authority (ARPA Veneto, 1985–2004) in monthly or biweekly measurements performed along 20 transects orthogonal to the Veneto coast and extending offshore up to 5 nautical miles; and iii) the Regional Water Authority (ARPA-FVG, 2009–2012) in monthly measurements performed at 21 monitoring stations along the Friuli-Venezia Giulia coastline (Table 5.1). The surface (shallowest record) and bottom (deepest record) values of all variables were extracted for winter (January, February, and March), spring (April, May, and June), summer (July, August, and September) and autumn (October, November, and December).

ACRONYM	VARIABLE	UNITS OF MEASURE	Data source
TEMP	Water temperature (surface and bottom, median and range)	°C	Solidoro et al. (2009); ARPA Veneto; ARPA FVG
SAL	Salinity (surface and bottom, median and range)		Solidoro et al. (2009); ARPA Veneto; ARPA FVG;
DOX	Dissolved oxygen (surface and bottom, median and range)	mL L^{-1}	Solidoro et al. (2009); ARPA Veneto
AMON	Ammonium concentration (surface and bottom, median and range)	µmol L^{-1}	Solidoro et al. (2009); ARPA Veneto; ARPA FVG
NTRA	Nitrate concentration (surface and bottom, median and range)	µmol L^{-1}	Solidoro et al. (2009); ARPA Veneto; ARPA FVG
PHOS	Phosphate concentration (surface and bottom, median and range)	µmol L^{-1}	Solidoro et al. (2009); ARPA Veneto; ARPA FVG
CPHL	Chlorophyll a (surface and bottom, median and range)	µg L^{-1}	Solidoro et al. (2009); ARPA Veneto; ARPA FVG
Vmean	Mean velocity (surface and bottom)	m s-1	Ocean circulation model
Vmax	Max velocity (surface and bottom)	m s-1	Ocean circulation model
Depth	Bottom depth	m	GEBCO 30 arc-second grid http://www.gebco.net/

doi:10.1371/journal.pone.0140931.t001

Table 5.1 Environmental descriptors, measurement units, and data sources. All of the variables except depth were extracted at the surface and the bottom.

A minimum depth of 5 m was imposed for the bottom values. We calculated the median seasonal values of each parameter on a 2.5 x 2.5 km grid, and we calculated a yearly median only if data were present for all 4 seasons to prevent biases caused by different sampling efforts in different seasons. Because the data were spatially sparse and a number of grid cells were left empty, we extrapolated information to grid cells without data by means of the moving window method (Solidoro et al. 2009). For each cell, the median for at least 10 data points within the surrounding cells in a search radius of 20 km was calculated to determine the missing temperature, salinity, and chlorophyll a values. For the remaining variables, we used a search radius of 30 km and at least 6 data points. The same procedures were applied to derive ranges of variation between the 95th and

5th percentiles of distribution for each parameter at the surface and the bottom. We used the 95th and 5th percentiles instead of the absolute maximum and minimum values, respectively, to prevent occasional extreme data from biasing the range calculations. The gridded results of the median and value ranges for each surface and bottom variable were exported and geo-referenced as geographic information system (GIS) raster layers.

Hydrodynamic data were extracted from a high-resolution numerical model of the northern Adriatic Sea. The simulation was performed by customizing theMITgcm (Massachusetts Institute of Technology general circulation model), which is a three-dimensional, finite-volume general circulation model. The numerical experiment presents a higher resolution (4-fold higher, which is ˜750 m in the horizontal direction) version of the simulation described in Querin et al. 2013, and it is focused on the northern Adriatic Sea for the year 2008. The computational grid is composed of 30 vertical levels. The model neglects tides and short gravity waves (wind waves).

For the bottom velocities, we sampled the first grid elements above the deepest cells to produce a fully developed velocity field and avoid boundary layer effects at the bottom. The velocities were averaged over a 2.5 x 2.5 km grid and then geo-referenced as GIS raster layers.

For the bathymetry, we downloaded the GEBCO 30 arc-second grid from the General Bathymetric Chart of the Ocean (GEBCO 2014. Database: GEBCO_2014 Grid version 20150318; http://www.gebco.net/) and extracted data at the coordinates of the outcrops as well as data on the 2.5 x 2.5 km grid to ensure consistency among the explanatory variables.

All of the GIS computations were performed using QGIS (QGIS Development Team 2015).

Direct gradient analysis method

A redundancy analysis (RDA) (van den Wollenberg 1977, Rao 1964) was used to model the relationship between the environmental descriptors and the FKM membership grades (Bandelj et al. 2012). The biotic data table was transformed using the Hellinger transformation (Legendre & Gallagher

2001) prior to performing the RDA to avoid the species abundance paradox (Legendre & Legendre 2012).

The number of environmental predictors was the same as the number of samples; therefore, an RDA with all of the environmental variables would not be constrained. Furthermore, it has been shown that explained variance continues to increase when including variables, even if they are random or insignificant (McCune 1997, Peres-Neto et al. 2006). To reduce the number of explanatory variables while still preserving their explanatory power, we chose a two-step procedure and divided the explanatory variables into 3 subsets: a subset including the median and value ranges for 7 water quality parameters at the surface; a subset including the median and value ranges for 7 water quality parameters at the bottom subset; and a hydrodynamic subset including values for 4 variables. For each of these subsets, an RDA was performed, the axes were tested for significance, and the significant explanatory variables were selected by forward selection using a double stopping criterion (Blanchet et al. 2008). The significant explanatory variables of each subset were then used along with the depth values as the explanatory variables of the final RDA model. Variation partitioning (Brocard et al. 1992) was applied to the 3 groups of variables and the depth values in the final RDA model to study their mutual relationships.

To predict the fuzzy cluster membership grades over a grid covering the Italian sector of the northern Adriatic, we applied canonical coefficients from the final RDA model to the values of the selected environmental variables in each of the 2.5 x 2.5 km bins. The results were projected in GIS as geo-referenced raster maps.

All of the analyses were performed using the vegan (Oksanen et al. 2015), ade4 (Dray & Dufour 2007) and packfor (Dray 2013) packages for R.

5.3 Results and Discussion

Habitat classification: Biodiversity

Most of the studies conducted on the epibenthic assemblages of the northern Adriatic bio-concretions are qualitative. Only the most recent research (Ponti et al. 2011, 2014, Curiel et al. 2012; unpublished data) has reported quantitative data, although these studies are generally restricted to small or medium spatial scales or consider the flora and fauna separately. A total of 573 taxa have been reported, which includes a relatively high number of macroalgae (191 taxa) (Supplementary information, Checklist) considering the biogeographical context and the dispersal of outcrops on muddy sandy bottoms far from coastal sources of spores and propagules. More shallow bio-concretions are mainly characterized by taxa that are widespread in nearby lagoons (Falace et al. 2009a, 2009b, Sfriso & Curiel 2007, Sfriso et al. 2009, Curiel et al. 1999, 2009) and the Gulf of Trieste shoreline (Falace et al. 2010), and they include turf-forming or laminar taxa. All of the calcareous species of macroalgae, which are acknowledged as the most important coralligenous bioconstructors (Boudouresque 1973, Ballesteros 1992, Hong 1980), have been reported, even if most have low coverage. The highest coverage of bioconstructors, particularly Lithophyllum incrustans and Mesophyllum spp., is found on the outcrops located at a depth of 23–25 m and at a distance _10 km from the coast.

However, a number of common coralligenous taxa (UNEP-MAP-RAC/SPA 2008) are found in low amounts or at extremely rare frequencies (i.e., Palmophyllum crassum, Flabellia petiolata, Halimeda tuna).

The most numerous of the 382 animal taxa are Mollusca (107 taxa), Polychaeta (92 taxa), Porifera (59 taxa), and Crustacea (50 taxa) (Supplementary information, Checklist). Most of these epibenthic invertebrates are filter feeders. The high number of Porifera appears to be a common feature of eastern Mediterranean coralligenous assemblages, which is most likely because of the absence of alcyonarians and gorgonians (Pérès & Picard 1958). The "large animal builders" (sensu, Hong 1980) reported here include the Serpulidae Serpula vermicularis and Serpula concharum,

the Vermetidae Thylacodes arenarius, and the Anthozoa Leptopsammia pruvoti, Caryophyllia inornata, and Caryophyllia smithii. Cladocora caespitosa is rare on Italian outcrops, whereas it is an important builder in Slovenia (Orlando-Bonaca et al. 2012). On the Veneto outcrops, the fossil record testifies to the historical relevance of this bioconstructor (Ponti et al. 2008). The most common animals with "reduced builder activity" (sensu, Hong 1980) are the Serpulidae Hydroides spp. and the Verrucidae Verruca stroemia. Finally, the "agglomerative builders" (sensu, Hong 1980) include the Anthozoa Epizoanthus arenaceus and the Demospongia Geodia cydonium. Another characteristic feature of these northern Adriatic outcrops is the absence of large Bryozoa (i.e., Margaretta cereoides, Cellaria salicornioides, Pentapora fascialis, and Reteporella grimaldii), which are abundant in Mediterranean coralligenous environments.

In the bioconstruction buildup an important counterpart to the biological carbonate deposition is the bioeroders activity (Bianchi 2001). A total of 11 bioeroders were found, which include 4 Porifera, 1 Sipuncula, 4 Bivalvia, and 2 Polychaeta (Supplementary information, Checklist). Cliona viridis and Cliona celata are the more common taxa, whereas Cliona rhodensis and Cliona thoosina were only found by Ponti et al. (Ponti et al. 2011). Microborers (i.e., fungi and cyanobacteria) have not been considered, whereas among the macroborers, the most frequent were the Mollusca Hiatella arctica, Rocellaria dubia, Lithophaga lithophaga, and Petricola lithophaga.

The most frequent and widespread taxa found on the northern Adriatic calcareous bio-concretions are reported in Table 5.2.

Habitat classification: Habitat types

According to expert judgment, 3 dominant epibenthic assemblages have been distinguished (Fig 5.2).

The first group of reefs (Habitat A) is distinguished by opportunistic and tolerant macroalgal species that are resistant to mud and organic matter (i.e., turf-forming algae such as Cladophora sp., Antithamnion sp., and Pseudochlorodesmis furcellata); encrusting Porifera [i.e., Antho (Antho) inconstans, Dictyonella incisa and Mycale (Mycale) massa]; and bioeroders

(i.e., Cliona spp. and Rocellaria dubia). A second group of reefs (Habitat B) is dominated by massive Porifera (i.e., Chondrosia reniformis, Tedania anhelans, and Ircinia variabilis); erect Tunicata (Aplidium conicum and Aplidium tabarquensis); and non-calcareous encrusting algae (Peyssonnelia spp.). The third group of reefs (Habitat C) is located in deep offshore waters and is dominated by non-articulated calcareous macroalgae and, to a lesser extent, by the tunicate Polycitor adriaticus.

Macroalgae	*Aglaothamnion* spp.		*Suberites domuncula*
	Cladophora spp.		*Tedania (Tedania) anhelans*
	Cryptonemia lomation		*Tethya aurantium*
	Dasya spp.	**Anthozoa**	*Cereus pedunculatus*
	Dictyota dichotoma		*Cerianthus membranaceus*
	Gracilariopsis longissima		*Cornularia cornucopiae*
	Halymenia floresii		*Epizoanthus* spp.
	Halopteris filicina	**Mollusca**	*Arca noae*
	Lithophyllum spp.		*Bolma rugosa*
	Lithothamnion spp.		*Calliostoma zizyphinum*
	Mesophyllum macroblastum		*Haliotis tuberculata*
	Nitophyllum punctatum		*Hiatella arctica*
	Peyssonnelia spp.		*Ostrea edulis*
	Pseudochlorodesmis furcellata		*Rocellaria dubia*
	Rhodophyllis divaricata	**Crustacea**	*Dromia personata*
	Rhodymenia ardissonei		*Homarus gammarus*
	Scinaia complanata	**Echinodermata**	*Holothuria (Holothuria) tubulosa*
	Taonia atomaria		*Ocnus planci*
	Zanardinia typus		*Ophiothrix fragilis*
Porifera	*Antho (Antho) inconstans*		*Sphaerechinus granularis*
	Aplysina aerophoba	**Tunicata**	*Aplidium* spp.
	Axinella spp.		*Cystodytes dellechiajei*
	Chondrosia reniformis		*Microcosmus vulgaris*
	Cliona viridis		*Phallusia* spp.
	Dictyonella incisa		*Polycitor adriaticus*
	Dysidea spp.	**Polychaeta**	*Sabella spallanzanii*
	Geodia cydonium		*Serpula* spp.
	Ircinia variabilis		*Spirobranchus triqueter*
	Sarcotragus spinosulus		

doi:10.1371/journal.pone.0140931.t002

Table 5.2 Common and abundant taxa on northern Adriatic calcareous bio-concretions.

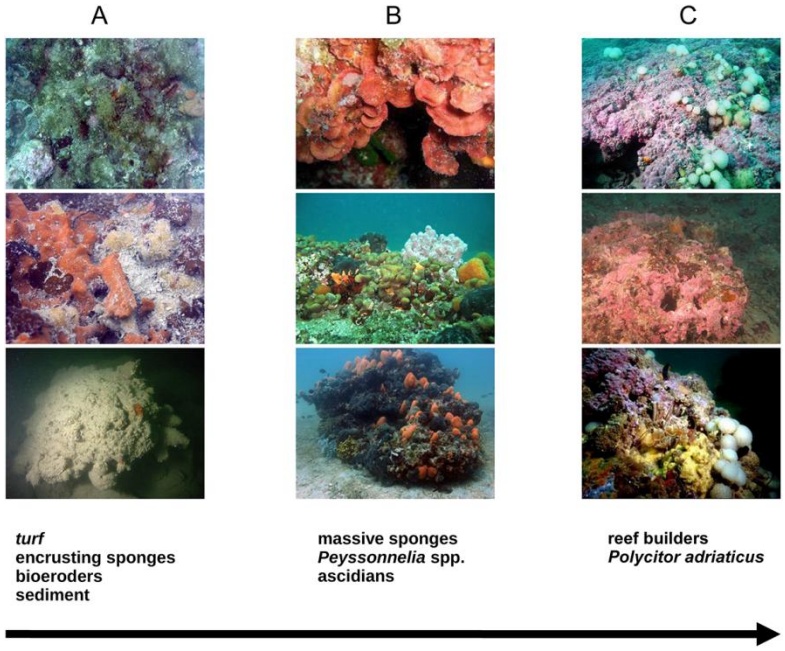

Fig. 5.2 Dominant epibenthic assemblages of calcareous bio-concretions (Habitat A, Habitat B, and Habitat C) (original copyright 2015).

Habitat classification: Fuzzy clustering

A comparison between the FKM results and the reef types based on expert knowledge is consistent (Table 5.3). Only 5 sites (ChioL2, Lastre, Corvine, Nordalti, and TR2-Pinnacoli) are assigned to a different type by the FKM cluster with the highest fuzzy membership. In all these cases, the expert type assignation is more "conservative" (Fig 5.2) compared with that of the FKM, i.e., the sites that were assigned by expert knowledge fell in the category immediately below the maximum membership category assigned by the FKM. Furthermore, two of these mismatches occur for sites that the FKM assigned high levels of fuzziness (ChioL2 and Nordalti). Thus, the three FKM clusters have been renamed according to the expert typology. High fuzziness levels, i.e., no membership >0.50, is observed in one-third of the studied sites. Among the remaining sites, 8 have FKM_A>0.50, 7 have FKM_B>0.50, and 8 have FKM_C>0.50. The FKM_B cluster shows the most restricted membership range (min 0.14 –max 0.60); however, both the FKM_A (0.07–0.70) and FKM_C (0.11–0.78) clusters clearly prevail at

certain sites, while they show low membership values at other sites. These results supports the interpretation of the FKM_A and FKM_C clusters as the extremes of a gradient that characterizes the epibenthic assemblages on the outcrops. There is also a difference in the mean depth of the reefs of each cluster; the FKM_A and FKM_B clusters are found in shallower waters (17.6 m and 18.0 m, respectively), whereas the FKM_C reefs are found in deeper areas (22.6 m).

STATION	Typ	FKM_A	FKM_B	FKM_C
ChioL1	C	0.13	0.39	0.48
ChioS1	A	0.61	0.25	0.14
ChioS3	A	0.49	0.30	0.21
ChioL2	**B**	0.24	0.32	0.44
ChioS2	A	0.41	0.35	0.24
ChioL3	C	0.20	0.33	0.46
TR12-Nicola	B	0.19	0.49	0.32
TR13	B	0.19	0.54	0.28
TR14-Misto	B	0.19	0.52	0.29
TR3-Spari	B	0.23	0.49	0.29
TR4	B	0.30	0.47	0.22
SanPietro	B	0.22	0.60	0.17
Menegh	A	0.70	0.19	0.11
Meneghel	A	0.70	0.19	0.11
Strucolo	C	0.10	0.21	0.69
Gubana	C	0.08	0.15	0.77
Colomba	C	0.07	0.14	0.78
Colomba2	C	0.11	0.20	0.69
Cerniotta	C	0.09	0.17	0.74
Lastre	**B**	0.18	0.32	0.51
Pivetta	C	0.16	0.29	0.55
Tartaruga	C	0.15	0.26	0.59
Amerigo	A	0.54	0.32	0.14
Corvine	**A**	0.37	0.50	0.13
NordAlti	**A**	0.40	0.44	0.16
Palo Largo	A	0.66	0.22	0.12
TR2-Pinnacoli	**A**	0.27	0.51	0.22
Salient	A	0.63	0.26	0.11
Saratoga	A	0.52	0.35	0.13
Dorsale	B	0.37	0.42	0.21
Aldebaran	B	0.25	0.55	0.20
La Longa	B	0.34	0.44	0.22
Bardelli	B	0.16	0.51	0.32

doi:10.1371/journal.pone.0140931.t003

Table 5.3 Results of the FKM membership grades (FKM_A, FKM_B, and FKM_C) and habitat typology (Typ) to which the outcrop has been assigned based on expert knowledge (Habitats A, B, and C). The mismatches between the expert typology and the FKM results are in bold.

Direct gradient analysis according to the RDA

The surface chemical-physical model constructed with 14 variables (the median and value ranges for the surface TEMP, SAL, DOX, NTRA, AMON, PHOS, DOX, and CPHL) had an adjusted R2 (Blanchet et al.

2008, Bianchi 2001) of 0.78 (0.63 on the first axis, 0.15 on the second axis, both $p<0.001$, 999 permutations). Many of the variables were not statistically significant because they presented high collinearity. The forward selection only retained four variables (PHOS, SAL, CPHL, and value range for CPHL) and had an adjusted $R2 = 0.67$ and first axis $R2 = 0.60$ (both axes $p<0.01$, 999 permutations) (Supplementary information, Fig).

The bottom chemical-physical RDA of 14 variables (the median and value ranges for the bottom TEMP, SAL, DOX, NTRA, AMON, PHOS, DOX, and CPHL) had an adjusted R2 of 0.58. The majority of the variance was explained by the first axis (0.49), although both axes were significant ($p<0.001$, 999 permutations). The forward selection only retained two variables (value ranges for TEMP and PHOS). The reduced model explained 0.58 of the variance on the first axis and 0.05 of the variance on the second axis (both axes $p<0.05$, 999 permutations) (Supplementary information, Fig).

The hydrodynamic model was built with all 4 hydrodynamic variables (Vmean and Vmax of the surface and bottom). The adjusted R2 was 0.23 on the only significant axis ($p<0.001$, 999 permutations). The forward selection retained only the two surface velocities, and the adjusted R2 was 0.26 on the only significant axis ($p<0.001$, 999 permutations) (Supplementary information, Fig).

The final RDA was built using the selected variables of the three RDA subsets: the median surface PHOS, SAL, and CPHL; value ranges for the surface CPHL; and value ranges for the bottom TEMP and PHOS, surface Vmean and Vmax, and depth. The entire model had an adjusted R2 of 0.79; 0.64 of the variance was explained by the first axis, and 0.14 of the variance was explained by the second axis, with both of these values highly significant ($p<0.001$, 999 permutations). This result was obtained using only 9 variables out of the initial 33. A further forward selection retained only 3 variables (range of phosphate at bottom, mean surface velocity, and surface phosphate), with an adjusted R2 of 0.74 on the two significant axes ($p<0.001$, 999 permutations). In the following, we discuss the final model with 9 partially redundant variables because many of them are of great ecological importance and might be available for comparison in other study areas. For the FKM_A cluster, 0.66 and 0.13 of the variance was explained

by the first and second axis, respectively, whereas for the FKM_B cluster, a greater amount of variance was explained by the second axis (0.55) relative to the first axis (0.15). For the FKM_C cluster, almost all of the variance was explained by the first axis (0.93). The high FKM_A and high FKM_C values were observed on opposite ends of the main gradient (Fig 5.3).

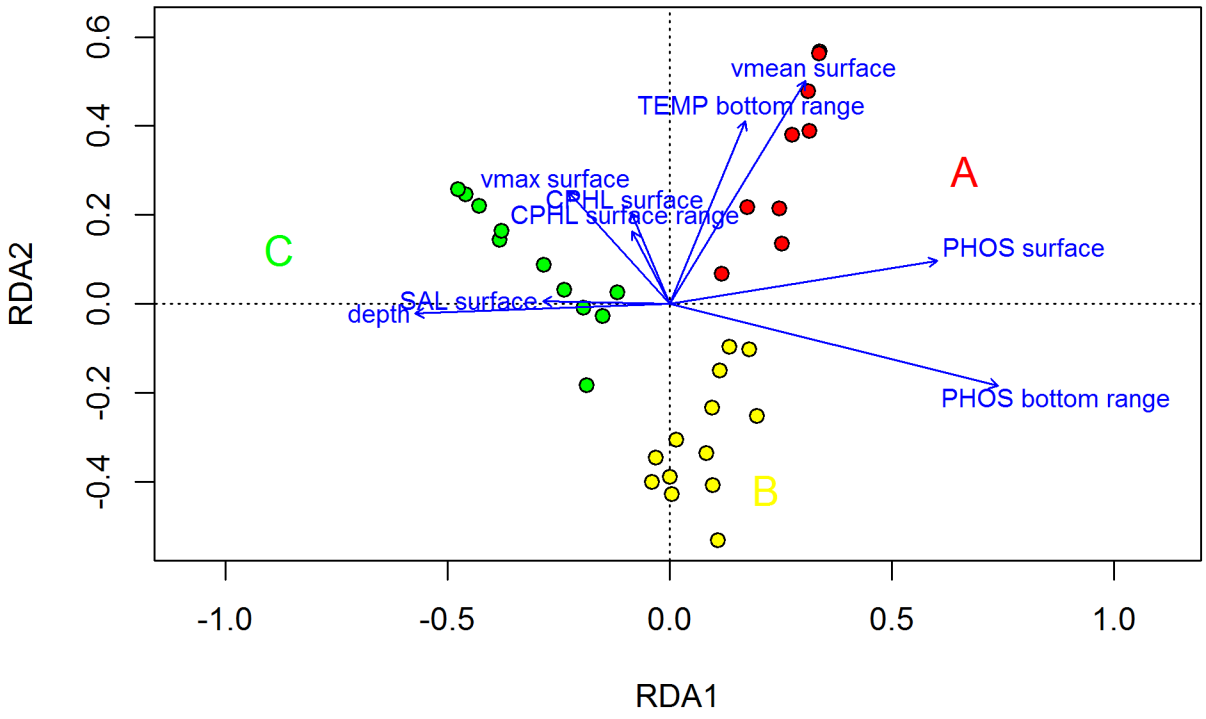

Fig. 5.3 Final RDA model. Entire model adjusted to R2 = 0.79, first axis adjusted R2 = 0.64, second axis adjusted R2 = 0.14. Both axes are significant at p<0.001 after 999 permutations (original copyright 2015).

This gradient was primarily from high median surface PHOS and high bottom PHOS range values, which are associated with high FKM_A values, toward high depth and high surface salinity values, which are associated with high FKM_C values. The FKM_C sites were positioned offshore at a distance from the effects of river inputs, whereas the FKM_A sites were those closest to the coastline and river inputs. The FKM_B sites were somewhat in the middle of this gradient, but only a rather small fraction of their variance was explained by this gradient.

The high range of PHOS may have been related to more shallow areas, where occasional inputs of high river flow can affect the entire water column. Moreover, the bottom sediments in the shallow areas may be easily

resuspended by vertical mixing and turbulence caused by waves and wind. The high concentrations of PHOS at depth, which is a signature of remineralization, have previously been described for the northern Adriatic Sea (Solidoro et al. 2007b, 2009).

The second axis gradient mainly included the surface Vmean and Vmax, the median surface CPHL, the surface CPHL range, and the bottom TEMP range, with high FKM_B membership grades associated with low values of these variables and FKM_A membership grades associated with high values of these variables. The sites with high FKM_B memberships presented more of an offshore distribution relative to the FKM_A sites; thus, they were less influenced by riverine waters, which cause strong fluctuations in primary production because of seasonal fluctuations in river flow.

A portion of the variance could not be explained by our model, especially for the FKM_B membership grades (Supplementary information, Table). The distribution of high FKM_B values (Fig 5.1) revealed that several sites showing high FKM_A and FKM_B are located close to each other and many are also in the same cell within the 2.5 x 2.5 km grid on which the model was applied. Our resolution was constrained by the scarcity of available data; thus, it could not explain the observed differences between these sites. Moreover, the sites that were poorly fit by our model were found at a distance from each other in different parts of the study domain. This result suggests that certain local factors (e.g., fishing, sedimentation regimes, and endogenous factors such as autocorrelations caused by the clumping/dispersion of organisms) might have contributed to the observed variance in the outcrops.

Our results show that the surface and bottom dynamics are not always decoupled because of the limited depth of the water column in the study area. Thus, appropriate surface or bottom environmental descriptors can provide nearly equivalent explanations of the observed gradients in the outcrops (Table 5.4) notwithstanding possible causal relationships, which are not accounted for by the RDA. The depth range of the study sites was between 12.4 and 26 m, and even the deepest layers of the water column can be influenced by surface dynamics. Moreover, the height of the outcrops ranged from 0.5 to 4.5 m, and biotic data were collected on horizontal surfaces on top of the outcrops, which further reduced the possible effects of depth on the assemblages. In the study area, surface heat

loss and wind-driven mixing in autumn and winter tend to homogenize the water column, but intense pulses of freshwater from rivers can induce relevant vertical stratification due to a layer of less saline water at surface. In spring and early summer, the vertical profile of temperature and salinity is strongly stratified with a noticeable thermocline; however, after strong wind events, the stratification can be broken and the mixed layer can reach the deepest parts of the water column. These wind events are less frequent in spring/summer than in autumn/winter.

The high correlation of depth with selected surface and bottom environmental descriptors (Table 5.4) reveals that coastal-related processes, such as river inflows, play an important role in structuring the assemblages of the outcrops, whereas other processes, such as coastal pollution and recreational and commercial fishing, might also have an important role. In particular, the outcrops are threatened by mechanical damage related to trawling, heavy bottom gear disturbances, and anchoring. These practices are particularly destructive because of their direct effects, and they also increase the turbidity and sedimentation rates, which negatively affect the structure and composition of the assemblages. Encrusting calcareous macroalgae and Polycitor adriaticus, which are species that characterize Habitat C, are negatively correlated with the mud content of sediment (Ponti et al. 2011, Naranjo et al. 1996). In particular, P. adriaticus is found in undisturbed environments, and its populations are reduced or disappear at increased stress rates. Other tunicates, such as Aplidium conicum, which characterize Habitat B, are adversely affected by excessive sediment deposition, which causes burial and clogging of the siphons and the branchial wall (Naranjo et al. 1996). Finally, the additive action of silting and high hydrodynamism has injurious consequences because the suspended inorganic particles have a mechanically abrasive effect on living organisms (Carballo & Garcia-Gomez 1994). However, turfs are dominant in areas with increased sedimentation rates (Curiel et al. 2012, Falcae et al. 2010, Balata et al. 2005). The abundance of encrusting sponges (i.e., Dictyonella incisa), which, together with turf algae, characterize Habitat A, increased with the mud and organicmatter content of nearby sediment, whereas it decreased with increasing distance from the coast and increasing longitude and salinity (Ponti et al. 2011).

GROUP OF VARIABLES	adjusted R^2	GROUP OF VARIABLES	adjusted R^2
Single groups		***Conditional on 1 group***	
Surface	0.67	Surface|Bottom	0.09
Bottom	0.63	Surface|Hydro	0.48
Hydro	0.29	Surface|Depth	0.38
Depth	0.33	Bottom|Surface	0.05
Combinations of 2 groups		Bottom|Hydro	0.39
Surface+Bottom	0.72	Bottom|Depth	0.30
Surface+Hydro	0.78	Hydro|Surface	0.11
Surface+Depth	0.71	Hydro|Bottom	0.06
Bottom+Hydro	0.68	Hydro|Depth	0.21
Bottom+Depth	0.63	Depth|Surface	0.04
Hydro+Depth	0.54	Depth|Bottom	0.00
Combinations of 3 groups		Depth|Hydro	0.25
Surface+Bottom+Hydro	0.79	***Conditional on 2 groups***	
Surface+Bottom+Depth	0.73	Surface|Hydro+Depth	0.23
Surface+Hydro+Depth	0.77	Surface|Bottom+Depth	0.10
Bottom+Hydro+Depth	0.70	Surface|Bottom+Hydro	0.11
All groups of variables		Bottom|Hydro+Depth	0.16
All	0.79	Bottom|Surface+Depth	0.03
Residuals (not explained)		Bottom|Surface+Hydro	0.02
Residuals	0.21	Hydro|Surface+Depth	0.06
Conditional on 3 groups		Hydro|Bottom+Depth	0.07
Surface|Bottom+Hydro+Depth	0.09	Hydro|Surface+Bottom	0.08
Bottom|Surface+Hydro+Depth	0.02	Depth|Bottom+Hydro	0.01
Hydro|Surface+Bottom+Depth	0.05	Depth|Surface+Hydro	-0.01
Depth|Surface+Bottom+Hydro	0.00	Depth|Surface+Bottom	0.02

Table 5.4 Portions of the variance explained by the three groups of variables (surface parsimonious model, bottom parsimonious model, and hydrodynamic parsimonious model) and depth. Only the effects of single groups, combinations of groups, and single groups conditioned to single groups and combinations of groups are shown. The (+) sign indicates that the variance is explained by that combination of variables. The (—) sign indicates that the variance explained by the group on the left is conditional on the variance explained by the group(s) on the right of the sign.

Hydrodynamism appears to play an important role that is not shared among any of the other groups of variables (Table 5.4), and this result might be related to water renewal, advection in nutrient rich waters, variations in organism dispersal, and physical constraints on species that can cling onto the substrate. The sites with high FKM_A memberships are found close to the coast; thus, they are strongly affected by coastal currents that flow westward and south-westward in the study area and are seasonally enhanced by surface river inputs and meteorological conditions (easterly winds). These shallower areas display more energetic hydrodynamics throughout the year, whereas the areas characterized by high FKM_C membership appear to be occasionally affected by strong surface velocities that most likely do not affect the bottom assemblages

because of the greater bottom depth. The FKM_B sites appear to be related to areas of weaker hydrodynamism; however, an inspection of the hydrodynamic subset RDA (Supplementary information Fig) revealed that the FKM_B variance explained by the hydrodynamic variableswas negligible. Thus, we can conclude that hydrodynamic variables do not play a role in differentiating FKM_B sites from the other two site clusters.

The onshore-offshore gradient is the most important gradient for explaining the variability of the assemblages growing over northern Adriatic biogenic outcrops because of the extent of coastal freshwater influence, which is the main driver of nutrient dynamics in the Northern Adriatic Sea, and the deepening of the water column in offshore sites, which lessens the sensitivity of the bottom population to certain surface dynamics (waves, surface) and is a proxy for the available light provided to the organisms growing on the outcrops. A less important gradient that is more difficult to explain according to the variables used in this study is confined to a coastal belt and differentiates two habitat types, FKM_B and FKM_A, with FKM_A experiencing greater exposure to environmental variability.

Predictive model

The final RDA model that was produced with 9 variables was used to predict the fuzzy membership grades of the three clusters over the entire study domain. The high predicted values for each fuzzy membership grade were generally consistent among the areas where they were observed (Figs 5.4, 5.5 and 5.6).

High FKM_A memberships are predicted along the coast, particularly in the north-western and south-western study area (Fig 5.4). The coastal belt in front of the Venice Lagoon and the Grado-Marano Lagoon are predicted to be less suitable for habitats in FKM_A. A few cells with high predicted FKM_A values are positioned in the Gulf of Trieste close to the mouth of the Isonzo River. In general, high FKM_A memberships appear to favor areas close to freshwater sources and areas at shallow bottom depths.

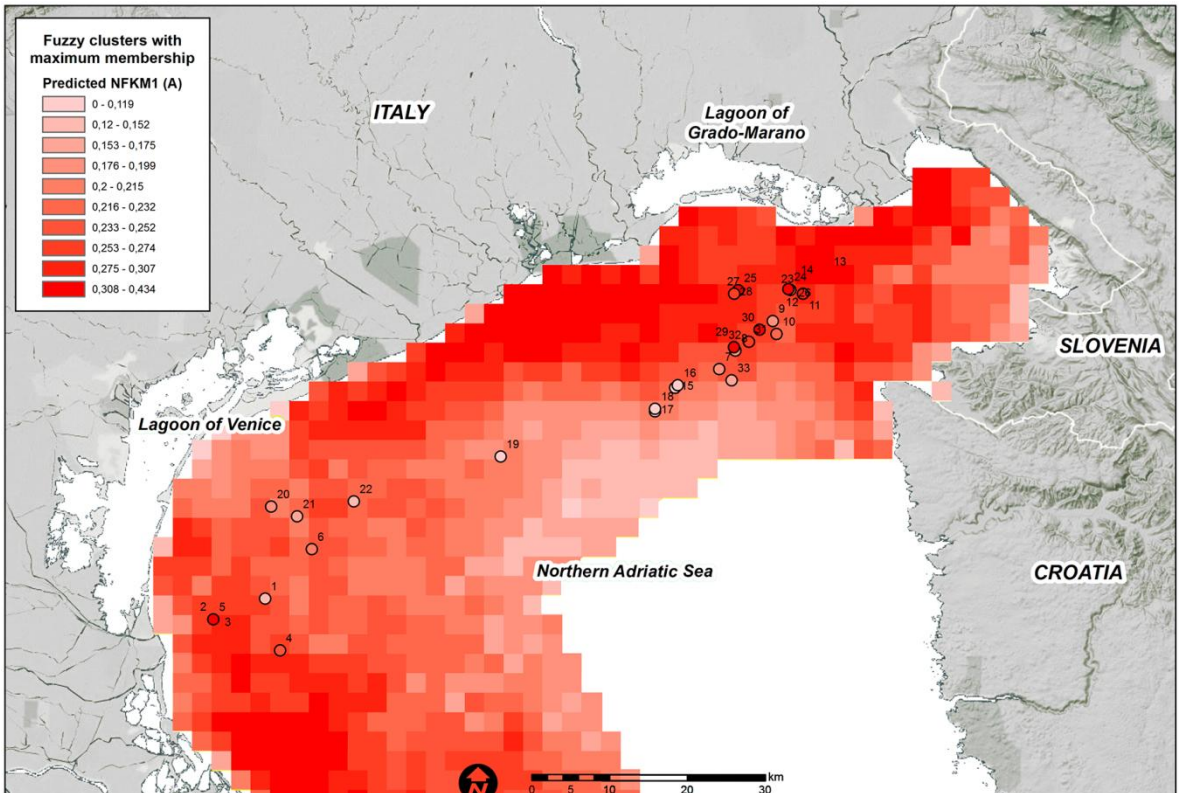

Fig. 5.4 Predicted FKM_A memberships over the entire study area. Points show the sampling sites used in the present study. White = low membership and dark red = high membership.

High FKM_C values are predicted offshore, at far distances from rivers and in deeper areas (Fig 5.5). In addition, the majority of the Gulf of Trieste as well as the coastal belt in front of the Venice Lagoon appear to be suitable for this cluster. The higher suitability of FKM_C compared with FKM_A in front of the Venice Lagoon might be a result of the buffer effect of the lagoon, which acts as a filter for high-nutrient loads transported to the lagoon from freshwater and from industrial and residential wastes (Solidoro et al. 2004, 2007a).

FKM_B is predicted to occur close to the areas where this cluster has been observed, particularly in front of the Grado-Marano Lagoon (Fig 5.1). Nevertheless, the "intermediate" characteristics of the macrobenthic populations on the reefs of this cluster and its lower fit in the final RDA model compared with that of the other two clusters increase its likelihood

in areas of the study domain where FKM_A or FKM_C (or both) are not predicted at high values (Fig 5.6).

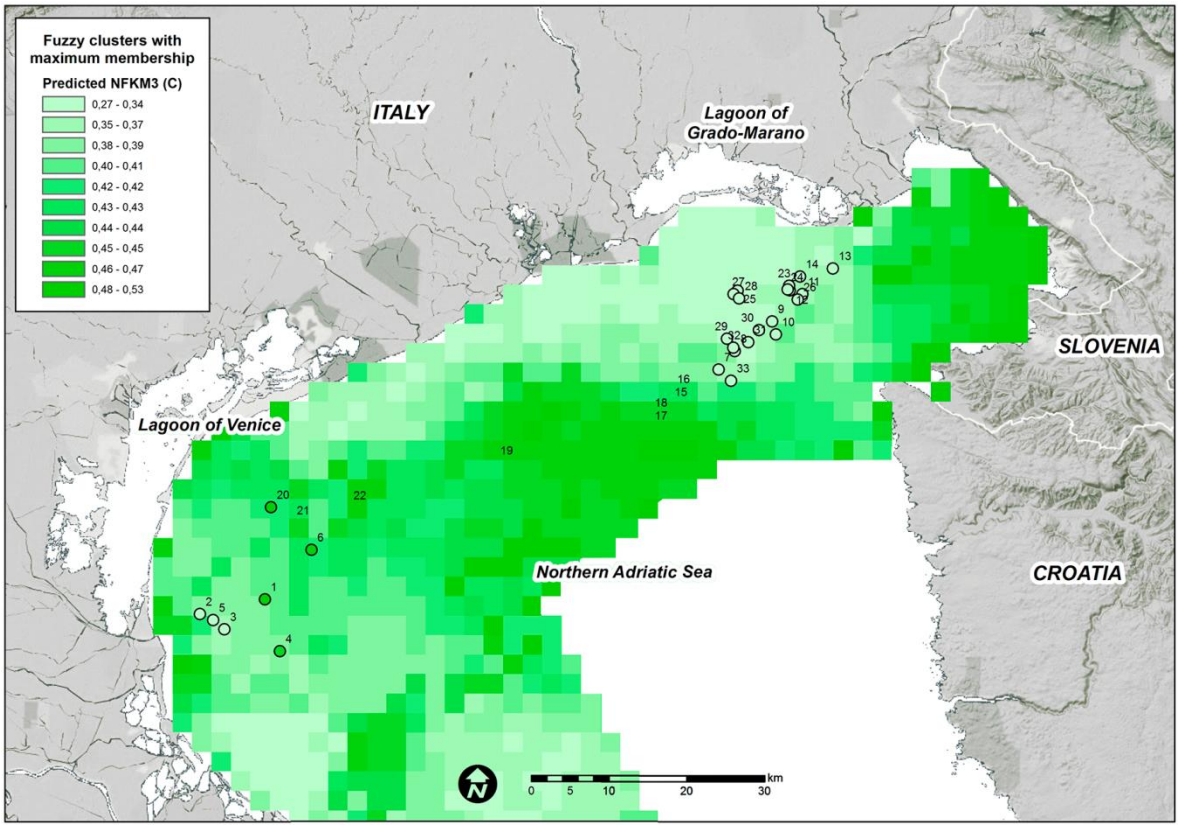

Fig. 5.5 Predicted FKM_C memberships over the entire study area. Points show the sampling sites used in the present study. White = low membership and dark green = high membership.

Areas of transition are a natural feature of the marine environment and may include a mixture of habitats and species.

The proposed model, that applies to the Italian side of the Northern Adriatic, and the actual occurrence of Habitat A, B, or C in the areas predicted by the model should be assessed with new samplings. Nevertheless, a major constraint that was not included in the model is the presence of a hard substrate. The presence or absence of a hard substrate is critical for the development of epibenthic communities; however, a complete cartography of substrate types in the study area is not available. Thus, our results might be helpful for defining areas worthy of exploration in further research projects.

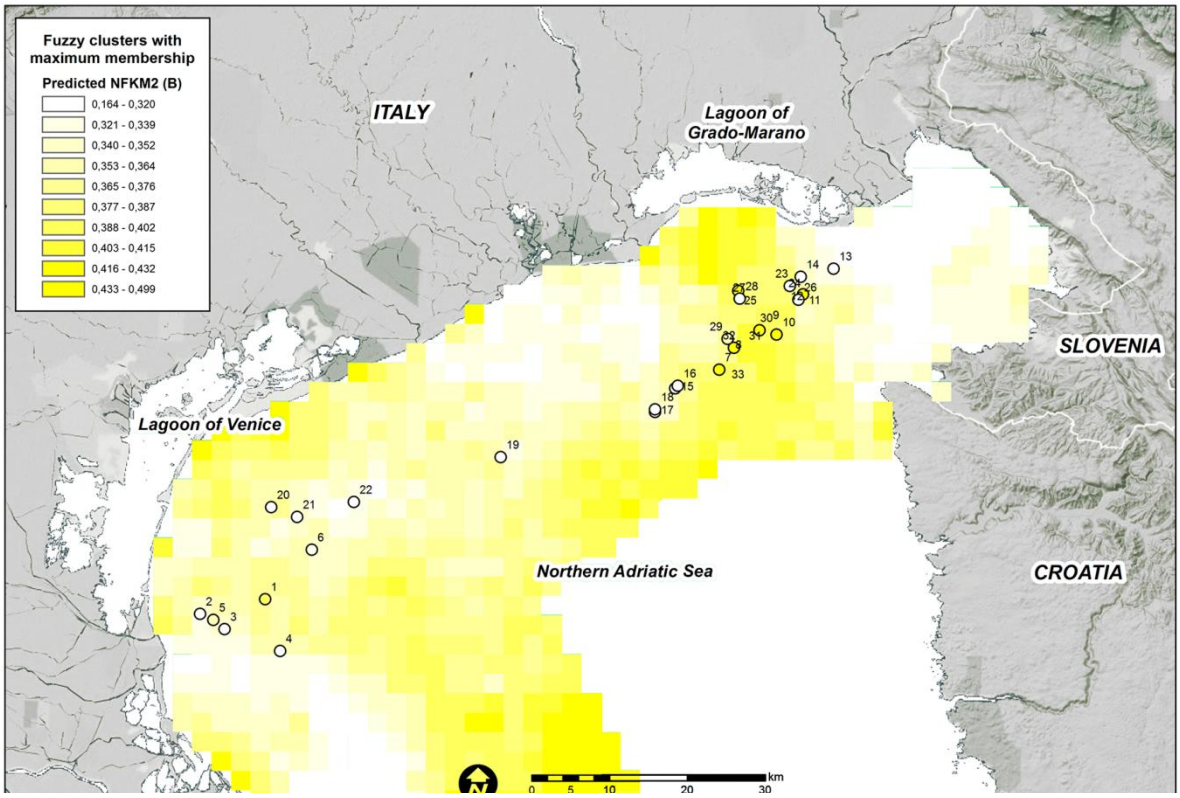

Fig. 5.6 Predicted FKM_B memberships over the entire study area. Points show the sampling sites used in the present study. White = low membership and jellow = high membership.

Because mapping and comparing habitats across geographic regions is a key component of the classification process (Costello 2001, 2005), the habitats derived from this study may be suitable for application in studies focused on other geographic areas. The Apulia continental shelf coralligenous outcrops fall into the "bank" category, which is similar to those in the northern Adriatic, and both contain the same features: isolated blocks randomly scattered on the soft bottom and clusters of blocks or ridges with several meters of lateral continuity. These features could represent distinct phases of morphological development (Bracchi et al. 2015). Outcrops with columnar shapes resembling small patch reefs also characterize the bottom off southeast Sicily (Di Geronimo et al. 2002). If we consider the biotic component, the Apulian outcrops are colonized by coralline algae associated with organisms that also characterize the proposed habitats of the northern Adriatic; however, some of these outcrops show an additional "erect ramified" animal layer, thus representing a fourth complex habitat. The absence of larger bryozoans and gorgonians in the studied area is most

likely related to the increased sediment resuspension, the reduced surface of colonization, and the high water turbidity.

Information on marine habitats must play a major role in ecosystem-based management promoted at national and international levels (Connor et al. 2002, DEFRA 2002). The three habitats proposed here are easy to identify in the field, and we have related these habitats to different environmental features (i.e., geography, nutrients, salinity, and temperature). We have also developed a predictive model based on environmental features, thus providing a large-scale probabilistic model of the presence of these different habitats in the northern Adriatic basin.

Supporting Information

Available at:
http://journals.plos.org/plosone/article?id=10.1371/journal.pone.0140931#sec015

5.4 References

ARPAV–Fondazione Musei Civici Venezia. 2010. Le tegnùe dell'Alto Adriatico: valorizzazione della risorsa marina attraverso lo studio di aree di pregio ambientale. Venice: Stamperia Cedit S.r.l.

Artegiani, A., Bregant, D., Paschini, E., Pinardi, N., Raicich, F., Russo, A. 1997. The Adriatic Sea general circulation. Part II: baroclinic circulation structure. J Phys Oceanogr. 27: 1515–1532.

Balata, D., Piazzi, L., Cecchi, E., Cinelli, F. 2005. Variability of Mediterranean coralligenous assemblages subject to local variation in sediment deposition. Mar Environ Res. 60: 403–421. PMID: 15924991

Ballesteros, E. 1992. Els vegetals i la zonació litoral: espècies, comunitats i factors que influeixen en la seva distribució. Arxius Secció Ciències 101, 1–616. Barcelona: Institut d'Estudis Catalans.

Ballesteros, E., 2006. Mediterranean coralligenous assemblages: a synthesis of present knowledge. Oceanogr Mar Biol Annu Rev. 44: 123–195.

Bandelj, V., Solidoro, C., Curiel, D., Cossarini, G., Melaku Canu, D., Rismondo, A. 2012. Fuzziness and heterogeneity of benthic metacommunities in a complex transitional system. PLoS One. 7: e52395. doi: 10.1371/journal.pone.0052395 PMID: 23285023

Bezdek, J.C. 1981. Pattern recognition with fuzzy objective function algorithms. New York: Plenum Press.

Bianchi, C.N. 2001. La biocostruzione negli ecosistemi marini e la biologia marina italiana. Biol. Mar. Mediterr. 8 (1): 112–130.

Blanchet, F.G., Legendre, P., Borcard, D. 2008. Forward selection of explanatory variables. Ecology. 89: 2623–2632. PMID: 18831183

Borcard, D., Legendre, P., Drapeau, P. 1992. Partialling out the spatial component of ecological variation. Ecology. 73: 1045–1055.

Borg, J.A., Schembri, P.J. 2002. Alignment of marine habitat data of the Maltese Islands to conform to the requirements of the EU habitats directive (Council Directive 92/43/EEC). [Report Commissioned by the Malta Environment and Planning Authority]. Malta: Independent Consultants; 136pp + Figs 1- 23Sarà M. 1969. Il coralligeno pugliese e I suoi rapporti con l'ittiofauna. Bollett. Mus. Istit. Biol. Univ. Genova 37: 27–33.

Bosence, D.W.J., 1983. Coralline algal reef frameworks. J Geol Soc Lond. 140: 365–376.

Bosence, D.W.J., 1985. The "coralligène" of the Mediterranean —a recent

analogue for tertiary coralline algal limestones. In: Toomey DF, Nicketi MH, editors. Paleoalgology: contemporary research and applications. Heidelberg: Springer-Verlag; pp. 216–225.

Bracchi, V., Savini, A., Marchese, F., Palamara, S., Basso, D., Corselli, C. 2015. Coralligenous habitat in the Mediterranean Sea: a geomorphological description from remote data. Ital J Geosci. 134.

Braga, G., Stefanon, A. 1969. Beachrock e Alto Adriatico: aspetti paleogeografici, climatici, morfologici ed ecologici del problema. Atti Istit Ven.Sci, Lett Art, Class Sci Mat Nat. 77: 351–361.

Boudouresque, C.F. 1973. Recherches de bionomie analytique, structurale et expérimentale sur les peuplements benthiques sciaphiles de Méditerranée Occidentale (fraction algale). Les peuplements sciaphiles de mode relativement calme sur substrats durs. Bulletin du Muséum d'Histoire Naturelle de Marseille. 33: 147–225.

Burba, N., Cabrini, M., Del Negro, P., Fonda Umani, S., Dilani, L. 1994. Variazioni stagionali del rapporto N/P nel Golfo di Trieste. In: Albertelli G, Cataneo-Vietti R, Picazzo M, editors. Atti X Congresso Associazione Italiana Oceanologia Limnologia, Alassio. p. 333–344.

Canals, M., Ballesteros, E. 1997. Production of carbonate sediments by phytobenthic communities in the Mallorca-Minorca Shelf, northwestern Mediterranean Sea. Deep Sea Res Part II. 44: 611–629.

Carballo, J.L., Garcia-Gomez, J.C. 1994. The northeastern Atlantic species Mycale micracanthoxea Buiser & Van Soest 1977 (Porifera, Poccilosclerida) in the Strait of Gibraltar (southern Spain). Beaufortia. 44: 11–16.

Casellato, S., Sichirollo, E., Cristofoli, A., Masiero, L., Soresi, S. 2005. Biodiversita'delle "tegnùe" di Chioggia, zona di tutela biologica del Nord Adriatico. Biologia Marina Mediterranea. 12: 69–77.

Casellato, S., Masiero, L., Sichirollo, E., Soresi, S. 2007. Hidden secrets of the Northern Adriatic: "Tegnùe", peculiar reefs. Cent Eur J Biol. 2: 122–136.

Casellato, S., Stefanon, A. 2008. Coralligenous habitat in the northern Adriatic Sea: an overview. Mar Ecol. 29: 321–341.

Colantoni, P., Gabbianelli, G., Ceffa, L., Ceccolini, C. 1998. Bottom features and gas seepages in the Adriatic Sea. In: Proceedings Vth International Conference on Gas in Marine Sediments, Bologna, 9–12 September 1997 p. 28–31.

Connor, D.W., Breen, J., Champion, A., Gilliland, P.M., Huggett, D., Johnston, C., et al. 2002. Rationale and criteria for the identification of nationally important marine nature conservation features and areas in the UK. Version 02.11. Peterborough: Joint Nature Conservation Committee (on behalf of the statutory nature conservation agencies and Wildlife and Countryside Link) for the Defra Working Group on the Review of Marine Nature Conservation.

Conti, A., Stefanon, A., Zuppi, G.M. 2002. Gas seeps and rock formation in the northern Adriatic Sea. Cont Shelf Res. 22: 2333–2344.

Costello, M. J. 2001. To know, research, manage, and conserve marine biodiversity. Oceanis. 24: 25–49.

Costello, M.J., Emblow, C.A. 2005. classification of inshore marine biotopes. In: Wilson JG, editor. The intertidal ecosystem: the value of Ireland's shores. Dublin: Royal Irish Academy; 25–35.

Curiel, D., Bellemo, G., Marzocchi, M., Iuri, M., Scattolin, M. 1999. Benthic marine algae of the inlets of the lagoon of Venice (Northern Adriatic Sea —Italy) concerning environmental conditions. Acta Adriat. 40: 111–121.

Curiel, D., Orel, G., Marzocchi, M. 2001. Prime indagini sui popolamenti algali degli affioramenti rocciosi del Nord Adriatico. Boll Soc Adriat Sci. 80: 3–16.

Curiel, D., Miotti, C., Marzocchi, M. 2009. Distribuzione quali-quantitativa delle macroalghe dei moli foranei della Laguna di Venezia. Boll Mus Civ Stor Nat Ven. 59: 3–18.

Curiel, D., Molin, E. 2010. Comunità fitobentoniche di substrato solido. In: Agenzia Regionale per la Prevenzione e protezione Ambientale del Veneto ARPAV (eds.) Le tegnùe dell' Alto Adriatico: valorizzazione della risorsa marina attraverso lo studio di aree di pregio ambientale. Venice: ARPAV; 2010. p. 62–79.

Curiel, D., Rismondo, A., Miotti, C., Checchin, E., Dri, C., Cecconi, G., et al. 2010a. Le macroalghe degli affioramenti rocciosi (tegnùe) del litorale veneto. Lavori Soc Ven Sc Nat. 35: 39–55.

Curiel, D., Checchin, E., Dri, C., Miotti, C., Rismondo, A., Mizzan, L., et al. 2010b. Le macroalghe degli affioramenti rocciosi (tegnùe) antistanti le bocche di porto della Laguna di Venezia. Boll Mus Civ St. Nat Venezia. 61: 5–20.

Curiel, D., Falace, A., Bandelj, V., Kaleb, S., Solidoro, C., Ballesteros, E. 2012. Spatial variability of macroalgal coralligenous assemblages on biogenic reefs in the northern Adriatic Sea Bot Mar. 55: 625–638.

Davies, C.E., Moss, D. 1999. EUNIS habitat classification. Final report to the European Topic Center on Nature Conservation. Copenhagen: European Environment Agency.

Davies, A.J., Guinotte, J.M. 2011. Global habitat suitability for framework-forming cold-water corals. PLoS ONE. 6: e18483. doi: 10.1371/journal.pone.0018483 PMID: 21525990

DEFRA. 2002. Safeguarding our seas. A strategy for the conservation and sustainable development of our marine environment. London: Department for Environment, Food and Rural Affairs.

Diaz, R.J., Solan, M., Valente, R.M. 2004. A review of approaches for classifying benthic habitats and evaluating habitat quality. J Environ Manag. 73: 165–181.

Di Geronimo, I., Di Geronimo, R., Rosso, A., Sanfilippo, R. 2001a. Structural and taphonomic analysis of a columnar coralline algal build-up from SE Sicily. Geobios Mem Spec. 35: 86–95.

Di Geronimo, I., Di Geronimo, R., Improta, S., Rosso, A., Sanfilippo, R. 2001b. Preliminary observation on a columnar coralline build-up from off SE Sicily. Biologia Marina Mediterranea. 8: 229–237.

Di Geronimo, I., Di Geronimo, R., Rosso, A., Sanfilippo, R. 2002. Structural and taphonomic analyses of a columnar coralline algal build-up from SE Sicily. Geobios. 24: 86–95.

Dray, S., Dufour, A.B. 2007. The ade4 package: implementing the duality diagram for ecologists. J Stat Software. 22: 1–20.

Dray, S. 2013. spacemakeR: Spatial modelling. R package version 0.0-5/r113. Available: http://RForge.R-project.org/projects/sedar/. Accessed:
http://www.gebco.net/data_and_products/gridded_bathymetry_data/gebco_30_second_grid/ British Oceanographic Data Center, Liverpool, U.K.

Elith, J., Phillips, S.J., Hastie, T., Dudık, M., Chee, Y., Yates, C.J. 2011. A statistical explanation of MaxEnt for ecologists. Divers Distrib. 17: 43–57.

Ezekiel, M. 1930. Methods of correlation analysis. New York: Wiley; 1930.

Falace, A., Kaleb, S., Curiel, D. 2009a. Implementazione dei S.I.C. marini italiani. Biologia Marina Mediterranea. 16: 82–83.

Falace, A., Curiel, D., Sfriso, A. 2009b. Study of the macrophyte assemblages and application of phytobenthic indices to assess the ecological status of the Marano-Grado Lagoon (Italy). Mar Ecol. 30: 480– 494.

Falace, A., Alongi, G., Cormaci, M., Furnari, G., Curiel, D., Ester, C., Petrocelli, A. 2010. Changes in the benthic algae along the Adriatic Sea in the last three decades. Chem Ecol. 26: 77–90.

Faresi, L. 2010. Macrozoobenthos. In: Ciriaco S, Gordini E, editors. Trezze o "Grebeni ": biotopi e geotopi dell'Alto Adriatico. Trieste: ArtGroup Trieste; 2010. p. 69–71.

Ferraro, M.B., Giordani, P.A. 2015. Toolbox for fuzzy clustering using the R programming language. Fuzzy Sets and Systems; In press, doi: 10.1016/j.fss.2015.05.001

Franklin, J., Miller, J. 2009. Statistical methods —modern regression. In: Franklin J, editor. Spatial inference and prediction with biogeographical data. Cambridge: Cambridge University Press; p. 113–153.

Gabriele, M., Bellot, A., Gallotti, D., Brunetti, R. 1999. Sublittoral hard substrate communities of the northern Adriatic Sea. Cah Biol Mar. 40: 65–76.

Giakoumi, S., Sini, M., Gerovasileiou, V., Mazor, T., Beher, J., Possingham, H.P., et al. 2013. Ecoregion-based conservation planning in the Mediterranean: dealing with large-scale heterogeneity. PLoS One. 8: e76449. doi: 10.1371/journal.pone.0076449 PMID: 24155901

Gordini, E., Marocco, R., Tunis, G., Ramella, R. 2004. The cemented deposits of the Trieste Gulf (Northern Adriatic Sea): areal distribution, geomorphologic characteristics and high resolution seismic survey. J Quat Sci. 2004; 17: 555–563.

Gordini, E., Falace, A., Kaleb, S., Donda, F., Marocco, R., Tunis, G. 2012. Methane-related carbonate cementation of marine sediments and related macroalgal coralligenous assemblages in the Northern Adriatic Sea. In: Harris PT, Baker EK, editors. Seafloor geomorphology as benthic habitat: geohab atlas of seafloor geomorphic features and benthic habitats. Amsterdam: Elsevier; p. 185–200.

Guisan, A., Zimmermann, N.E. 2000. Predictive habitat distribution models in ecology. Ecol Model. 135: 147–186.

Hong, J.S. 1980 Étude faunistique d'un fond de concrétionnement de type coralligène soumis à un gradient de pollution en Méditerranée nord-occidentale (Golfe de Fos). Doctoral Thesis, Université d'Aix-Marseille II.

Kipson, S., Fourt, M., Teixidó, N., Cebrian, E., Casas, E., Ballesteros, M., et al. 2011. Rapid biodiversity assessment and monitoring method for highly diverse benthic communities: a case study of Mediterranean coralligenous outcrops. PLoS One. 6: e27103. doi: 10.1371/journal.pone.0027103 PMID: 22073264

Laborel, J. 1987. Marine biogenic constructions in the Mediterranean. Scientific Reports of Port-Cros National Park. 13: 97–126.

Legendre, P., Gallagher, E.D. 2001. Ecologically meaningful transformations for ordination of species data. Oecologia. 129: 271–280.

Legendre, P., Legendre, L. 2012. Numerical ecology, 3rd ed. Developments in environmental modelling. Amsterdam: Elsevier.

Magistrato Alle Acque di Venezia–Corila-SELC. 2006. Studio B.6.72 B/I. Attività di rilevamento per il monitoraggio degli effetti prodotti dalla costruzione delle opere alle bocche lagunari. Rapporto variabilità attesa. Area: Ecosistemi di Pregio. Macroattività: Affioramenti rocciosi, Tegnùe. Available: http://pub.corila.it/DocumentiPubblici/Monitoraggio/13_MAVeCVN/RapportiValutazione/RapportoVariabilita00/ Tegnue-RapportoVariabilita.pdf

Martin, C.S., Giannoulaki, M., De Leo, F., Scardi, M., Salomidi, M., Knitweiss, L., et al. 2014. Coralligenous and maerl habitats: predictive modelling to identify their spatial distributions across the Mediterranean Sea. Sci Rep. 4: 5073.

McCune, B. 1997. Influence of noisy environmental data on canonical correspondence analysis. Ecology. 78: 2617–2623.

Mizzan, L. 1992. Malacocenosi e faune associate in due stazioni altoadriatiche a substrati solidi. Boll Mus Civ Stor Nat Ven. 41: 7–54.

Moss, D., Wyatt, B.K. 1994. The CORINE biotopes project: a database for conservation of nature and wildlife in the European community. Appl Geogr. 14: 327–349.

Naranjo, S.A., Carballo, J.L., Garcia-Gomez, J.C. 1996. Effects of environmental stress on ascidian populations in Algeciras Bay (southern Spain). Possible marine bioindicators? Mar Ecol Prog Ser. 144: 119–131.

Newton, R., Stefanon, A. 1975. The 'Tegnue de Ciosa' area: patch reefs in the Northern Adriatic Sea. Mar Geol. 8: 27–33.

Oksanen, J., Guillaume Blanchet, F., Kindt, R., Legendre, P., Minchin, P. R., O'Hara, R.B., et al. 2015. vegan: community ecology package. R package version 2.2–1. Available: http://CRAN.R-project.org/package= vegan.

Orlando-Bonaca, M., Lipej, L., Malej, A., Francé, J., Čermelj, B., Bajt, O., et al. 2012. Začetna presoja stanja slovenskega morja. Poročilo za člen 8 Okvirne direktive o morski strategiji (Initial assessment of Slovenian marine waters. Report for Article 8 of the MSFD). Report 140. Piran,

Slovenia: Marine Biology Station, National Institute of Biology.

Pérès, J., Picard, J.M. 1964 Nouveau manuel de bionomie benthique de la mer Méditerranée. Recueil des Travaux de la Station Marine d'Endoume. 31: 1–131.

Peres-Neto, P.R., Legendre, P., Dray, S., Borcard, D. 2006. Variation partitioning of species data matrices: estimation and comparison of fractions. Ecology. 87: 2614–2625. PMID: 17089669

Ponti, M., Mescalchin, P. 2008. Meraviglie sommerse delle "Tegnùe". Guida alla scoperta degli organismi marini. Associazione "Tegnùe di Chioggia" —onlus. Imola: Editrice La Mandragora.

Ponti, M., Fava, F., Abbiati, M. 2011. Spatial-temporal variability of epibenthic assemblages on subtidal biogenic reefs in the northern Adriatic Sea. Mar Biol. 158: 1447–1459.

Ponti, M., Falace, A., Rindi, F., Fava, F., Kaleb, S. 2014. Beta diversity pattern in Northern Adriatic Coralligenous outcrops. In: Proceedings of the Second Mediterranean Symposium on the Conservation of Coralligenous and Other Calcareous Bio-concretions; 2014. p. 147–152.

QGIS Development Team. 2015. QGIS geographic information system. Open Source Geospatial Foundation Project. Available: http://qgis.osgeo.org.

Querin, S., Cossarini, G., Solidoro, C. 2013. Simulating the formation and fate of dense water in a mid latitude marginal sea during normal and warm winter conditions. J Geophys Res Oceans. 118: 885–900.

Pérès, J., Picard, J.M. 1958. Recherches sur les peuplements benthiques de la Méditerranée nord-orientale. Annales de l'Institut Océanographique de Monaco. 34: 213–291.

Rao, C.R. 1964. The use and interpretation of principal component analysis in applied research. Sankhyaá, Ser A. 26: 329–358.

Russo, A., Artegiani, A. 1996. Adriatic Sea hydrography. Sci Mar. 60: 33–43.

Salomidi, M., Katsanevakis, S., Borja, A., Braeckman, D., Damalas, D., Galparsoro, I., et al. 2012. Assessment of goods and services, vulnerability, and conservation status of European seabed biotopes: a stepping stone towards ecosystem-based marine spatial management. Mediterr Mar Sci. 13: 49–88.

Sfriso, A., Curiel, D. 2007. Check-list of marine seaweeds recorded in the last 20 years in the Venice lagoon and comparison with the previous records. Bot Mar. 50: 22–58.

Sfriso, F., Curiel, D., Rismondo, A. 2009. The lagoon of Venice. In: Cecere E, Petrocelli A, Izzo G, Sfriso A, editors. Flora and vegetation of the Italian transitional water systems. Spinea: Ed. CORILA, Multigraf; p. 17–80.

Solazzi, A., Tolomio, C. 1981. Alghe bentoniche delle "tegnue de Ciosa". Adriatico Nord-occidentale. Stud Trent Sci Nat. 58: 463–470.

Solidoro, C., Pastres, R., Cossarini, G., Ciavatta, S. 2004. Seasonal and spatial variability of water quality parameters in the lagoon of Venice. J Mar Syst. 51: 7–18.

Solidoro, C., Bandelj, V., Cossarini, G., Melaku Canu, D., Trevisani, S., Bastianini, M. 2007a. Biogeochemical properties in the coastal area of the northwestern Adriatic Sea. In: Campostrini P, editor. Scientific research and safeguarding of Venice 2007 Corila Research Programme 2004–2006 volume VI 2006 results. Venice: Corila; 2007. p. 371–384.

Solidoro, C., Bandelj, V., Barbieri, P., Cossarini, G., Fonda Umani, S. 2007b. Understanding dynamic of biogeochemical properties in the northern Adriatic Sea by using self-organizing maps and k-means clustering. J Geophys Res. 2007; 112: C07S90.

Solidoro, C., Bastianini, M., Bandelj, V., Codermatz, R., Cossarini, G., Melaku Canu, D., Ravagnan, E., et al. 2009. Current state, scales of variability, and trends of biogeochemical properties in the northern Adriatic Sea. J Geophys Res. 114: C07S91.

Stefanon, A. 1967. Formazioni rocciose del bacino dell'Alto Adriatico. Atti Istit Ven Sci Lett Arti. 125: 79– 89.

Stefanon, A. 1970. The role of beachrock in the study of the evolution of the North Adriatic Sea. Mem Biogeogr Adriat. 8: 79–99.

Stefanon, A., Zuppi, G.M. 2000. Recent carbonate rock formation in the Northern Adriatic Sea. Hydrogeologie. 4: 3–10.

UNEP-MAP-RAC/SPA. 2008. Action plan for the conservation of the coralligenous and other calcareous bioconcretions in the Mediterranean Sea. Tunis: RAC/SPA.

van den Wollenberg, A.L. 1977. Redundancy analysis. An alternative for canonical correlation analysis. Psychometrika. 42: 207–219.

Zore-Armanda, M. 1969. Water exchange between the Adriatic Sea and Eastern Mediterranean. Deep Sea Res. 16: 171–178.

Aknowledgements

This work of course wouldn't have been possible without so many persons other than myself, whom I'd like to thank, but since I'm a shy person, I'll keep it short. My family, first of all, for supporting me all along, my supervisor Cosimo for picking me up in the first place and for guiding me trough all of this, when the pipeline allows, all the ECHO people, we are a big clan, you're just too many to mention but I love you all, and the rest of OGS also, ça va sans dire. Thanks also to all the people around the Mediterranean with whom I got to work with, if you were not diving or in the lab picking up those data all of this work would never have existed. My friends from Trieste that made me feel at home in this place ever since I moved in, and my friends from elsewhere also, for making me feel at home wherever I go, including the most expected places, like Bassano del Grappa of course, and the most unexpected also, like remote villages in southern France. The Murena diving club people for giving me the chance to see some hard-substrate-benthic-ecosystems in real life also. Thanks to Chiara and to Gloria. Thanks also to Alberto Barausse and Luca Palmeri from Padova University for introducing me to ecological modelling and guiding me while I was moving my first steps into this, I still am, I guess. Thanks also to all the scientists that came before me and that understood something that later I used, and also to those that didn't, for leaving me something to discover. Thanks to the anonymous person that wrote on the backboard that everybody believes an experimental result except the experimentalist, nobody believes a model's result except the modeller himself, maybe, it made my day. And, last but not least, thanks to Aurora, among other things for admiring what I do, one day I hope I'll be able to explain you what exactly it is.